CHOLINE PHOSPHATE: AN IMPROVED SYNTHESIS AND APPLICATIONS IN RED CELL AND PLATELET BINDING

by

Youping Li

B.Sc., McMaster University, 2016

A THESIS SUBMITTED IN PARTIAL FULFILLMENT OF

THE REQUIREMENTS FOR THE DEGREE OF

MASTER OF SCIENCE

in

THE FACULTY OF GRADUATE AND POSTDOCTORAL STUDIES

(Chemistry)

THE UNIVERSITY OF BRITISH COLUMBIA

(Vancouver)

April 2019

The following individuals certify that they have read, and recommend to the Faculty of Graduate and Postdoctoral Studies for acceptance, a thesis/dissertation entitled:

Choline phosphate: an improved synthesis and applications in red cell and platelet binding

submitted by Youping Li in partial fulfillment of the requirements for

The degree of Master of Science

in Chemistry

Examining Committee:

Prof. Donald E Brooks, Chemistry and Pathology

Supervisor

Prof. Suzana K Straus, Chemistry

Supervisory Committee Member

Prof. Zachary Hudson, Chemistry

Supervisory Committee Member

Prof. Keith A R Mitchell, Chemistry

Supervisory Committee Chair

Abstract

Biomembrane adhesive materials that are effective in aqueous media have gained attention in the past decade owing to their broad uses such as tissue sealants and localized drug delivery agents. Here we demonstrate that hyperbranched polyglycerols (HPG) surface-modified with choline phosphate (CP) in a multivalent fashion are able to bind to eukaryotic cell membranes containing phosphatidyl choline (PC), which is structurally in a reverse orientation compared to CP. This work is dependent on a new synthesis of the CP reagent which allows an efficient production of HPG-CP. In the experimental design section, the preparation and characterization of a library of HPG molecules decorated with different densities of zwitterionic CP ligands is described. A post-polymerization pathway was followed that employs azido moieties on an HPG core for the conjugation of triple bond attached functional groups through "click" reaction, providing the desired HPG-CP macromolecule. The proportions of CP moieties were controlled by adjusting the monomer concentration. It was demonstrated that polymer conjugates carrying over 10% zwitterionic CP groups induced significant hemagglutination without causing red blood cell lysis or any cytotoxic effect. As the CP density was increased on the carrier HPG, cellular adhesion and aggregation became stronger as the intercellular contact area became maximized. The polymer conjugates, including HPG (20 kDa) decorated with 30 and 80 CP groups, were also found to be capable of activating platelets to a significant level while, interestingly, platelet aggregation tests demonstrated negative results. Future studies will investigate the mechanism of this unusual result, perhaps due to HPG-CP interacting with ADP which is intimately involved in platelet aggregation *in vivo.* DSC results showed that each CP ligand bound more than 37 water molecules on average, compared to each hydroxyl unit on the native HPG binding ~7, primarily owing to the dual-ion structure of CP and the multiple oxygens on the group. It is believed that the

hydration ability contributed by the unique zwitterionic construct contributes to a barrier to resist biofouling on the polymer surface. These properties together render HPG-CPs potentially able to participate in various bio- or pharmaceutical- related applications with outstanding biocompatibility.

Lay Summary

This project has focused on creating a novel bioadhesive material that is able to universally bind to membranes of all types of cells through electrostatic interaction. A library of choline phosphate (CP) decorated hyperbranched polyglycerol (HPG) molecules was developed by varying the amount of CP ligands being added coupled to the core HPG. The binding of these HPG derivatives to human red blood cells was investigated, and the results show that polymer bearing different densities of CP groups exhibited different aggregation effects. Followed by a series of biocompatibility tests, it was concluded that these synthesized polymer conjugates displayed binding affinity yet do not cause any cytotoxicity issues, suggesting their future use as hemostatic agents, and potential bioadhesive applications in fields such as tissue sealants and drug delivery.

Preface

The work presented in this thesis was conducted by Youping Li under the supervision of Professor Donald E. Brooks at the UBC Centre for Blood Research. Design of reaction pathways, chemical synthesis and characterization experiments described in Chapter 2 were all performed and completed by the author. Dr. Narges Hadjesfandiari assisted with the interpretation of results. Chapter 3 includes a series of physical and *in vitro* biological tests to analyze the surface properties, bioactivity and biocompatibility of the synthesized polymers. The experiments solely conducted by the author include: hydration test, zeta potential measurement, hemagglutination, hemolysis and platelet aggregation tests. Lily Takeuchi helped with the cytotoxicity experiments and I interpreted the data. The platelet activation tests were performed by mad and Dr. Narges Hadjesfandiari together. Dr. Srinivas Abbina provided assistance and advice for the performance and the result analysis of the hydration tests. Dr. Don Brooks, along with Dr. Narges Hadjesfandiari participated in project discussions and editing of the writing. Ethics approval was received for studies conducted with human blood: UBC Ethics approval number H07-02067.

Table of Contents

List of Tables

List of Figures

List of Schemes

List of Symbols and Abbreviations

υ	Stretching vibration in IR spectroscopy
ζ	Zeta (potential)
Đ	Polydispersity index
ACN	Acetonitrile
ADP	Adenosine diphosphate
API	Atmospheric pressure ionization
aPTT	Activated partial thromboplastin time
$CDCl_3$	Deuterated chloroform
CP	Choline phosphate
CuAAC	$Copper^{I}$-catalyzed azide/alkyne cycloaddition
DCM	Dichloromethane
DIC	Diisopropylcarbodiimide
DMAP	4-(dimethylamino)pyridine
DMSO	Dimethyl sulfoxide
DSC	Differential scanning calorimetry
ES	electrospray
FT-IR	Fourier-transform infrared spectroscopy
GPC	Gel permeation chromatography
h	Hour
HUVEC	Human umbilical vein endothelial cell
HPG	Hyperbranched polyglycerol

IgG	Immunoglobulin G
kDa	Kilo Dalton
LC	Liquid chromatography
LT	Light transmittance
MALLS	Multi-angle laser light scattering
MeOD	Deuterated methanol
min	Minute
M_n	Number average molecular weight
M_w	Weight average molecular weight
MPC	2-methacryloyloxyethyl phosphorycholine
MS	Mass spectrometry
MW	Molecular weight
MWCO	Molecular weight cut-off
NMR	Nuclear magnetic resonance
P2Y1	Purinergic receptor (subclass: P2Y)
PBS	Phosphate buffered saline
PC	Phosphatidyl choline
PDI	Polydispersity index
PEG	Poly(ethylene glycol)
PI	Propidium iodide
PPP	Platelet poor plasma
PRP	Platelet rich plasma

PT	Prothrombin time
QA	Quaternary amine
QELS	Quasi-elastic light scattering
RBC	Red blood cell
RCF	Relative centrifuge force
Rh	Hydrodynamic radius
ROMP	Ring-opening multi-branching polymerization
RPM	Revolution per minute
SB	Sulfate betaine
SD	Standard deviation
TLC	Thin-layer chromatography
TMP	1,1,1-tris(hydroxylmethyl)propane
UV	Ultraviolet
WBC	White blood cell

Acknowledgements

I would like to take this opportunity to express my heartfelt thanks to my supervisor, Dr. Donald Brooks, for letting me in the gate of biomaterial science while I was hanging around at the beginning of my graduate study. During the past two and half years, he guided me through lots of challenges not only in research, but also in life. Those fascinating life experiences, philosophic talks and time-honored research stories that he never hesitated to share with me, will become the most beautiful memories when I look back to my graduate life. For Don, I sincerely appreciate all his consideration, support and encouragement in this winding journey.

I also owe particular thanks to Dr. Narges Hadjesfandiari, whose rejoining to the lab lightened up the darkest hours in my research life, making me stand up again to conquer the barriers existed in this project. Narges offered me tremendous helps in spectrum interpretation, polishing the synthetic methods, showing me strategies of performing experiments, as well as editing the thesis. It was extremely fortunate to work with such a caring, dedicated and sagacious scientist during my graduate study, and without her helps and encouragement, I would not walk this far.

In addition, a thank you to everyone in Brooks/Kizhakkedathu Lab, who have always been so eager to help me overcome each desperate plight, which makes me feel that I am not alone. It is my honour to work with people in this professional and united group, past and present, including Dr. Srinivas Abbina, Dr. Manu Thomas Kalathottukaren, Dr. Kai Yu, Dr. Erika Siren, Chu Liu, Iren Constantinescu, Irina Chafeev, Usama Abbasi, Lily Takeuchi, Arshdeep Gill, Haisle Moon, Sreeparna Vappala, Hossein Yazdani, Chanel La and Daniel Luo.

Besides, I am eternally grateful to my friends, Melody, Kelly and Haiyan in Department of Chemistry, for generously offering me helps when I was stuck at the bottleneck of research. Melody

also urged me a lot to keep up the hard work during thesis writing when I was not motivated, and Kelly always encouraged me throughout my graduate life.

I would also like to show my appreciation to the staff at UBC who trained or discussed research questions with me, especially to Dr. Paul Xia (Dept. of Chemistry), Dr. Lawrence Amankwa (cdrd) and Benjamin Herring (Dept. of Chemistry). In the meanwhile, it was fortunate for me to work as a member in Centre for Blood Research (CBR, UBC), who offered me a lot of opportunities to go to symposiums and absorb fresh knowledge from the weekly talks.

Finally, I would like to acknowledge with gratitude, the massive support and understanding of my beloved family - my parents, Shujuan and Yi, as well as my husband, Peiwen (Jason). Without receiving the financial support from my parents since high school, I wouldn't pursue my study in Canada as an international student. For my husband, I am extremely grateful to have him accompany around in these years, for scarifying his own plan of staying in Toronto to fulfill my dream of studying at UBC. I will embalm their love forever.

Dedication

To my husband, for the motivation and happiness he intangibly brought to my graduate life.

Chapter 1: Introduction

1.1 Phospholipids on cell membrane

As the boundary of cells, biomembranes are composed of a double layer structure containing phospholipids in which protein macromolecules are embedded in different forms. The lipids being well arranged in a double layer possess amphiphilic properties, where the hydrophobic tails face each other in the interior of the bilayer matrix, and the polar hydrophilic portions orient to the outer space in an aqueous medium.[1] Glycerophospholipids which bear glycerol as a backbone are considered as the main phospholipids in eukaryotic cells. The difference in head group, the chain length and saturation degree of hydrophobic tail tails, as well as the type of bonds connecting aliphatic groups and backbone together, classify the chemical structures of glycerophospholipids.[2] Among different classes of phospholipids, phosphatidylcholines (PC) are the major composition of biological membranes, which is formed either by incorporating choline with phosphatidylethanolamine functionalized by phosphatidyletha-nolamine N-methyltransferase (PMET)[3,4] in liver, or via the condensation reaction carried out by the diacylglycerol cholinephosphtransferase enzyme acting on diacylglycerol (DAG) and citicoline.[5] Phosphatidylcholines are found in membrane of eukaryotic cells including all plants and animals, while being absent from archaea and some of the bacteria.[6,7] The widespread distribution of PC headgroups on lipid bilayers is capable of stabilizing the human immune system by not binding to the positively charged peptides in the cellular medium due to zwitterionic property of PC.[8-10] As a vital substance formed in massive amounts among phospholipid headgroups, PC plays a key role in supporting biological events such as cell signaling and activating other enzymes.[11] The schematic model in Figure 1.1 illustrates phospholipid with a PC headgroup bonding to both saturated and unsaturated alkyl chains.

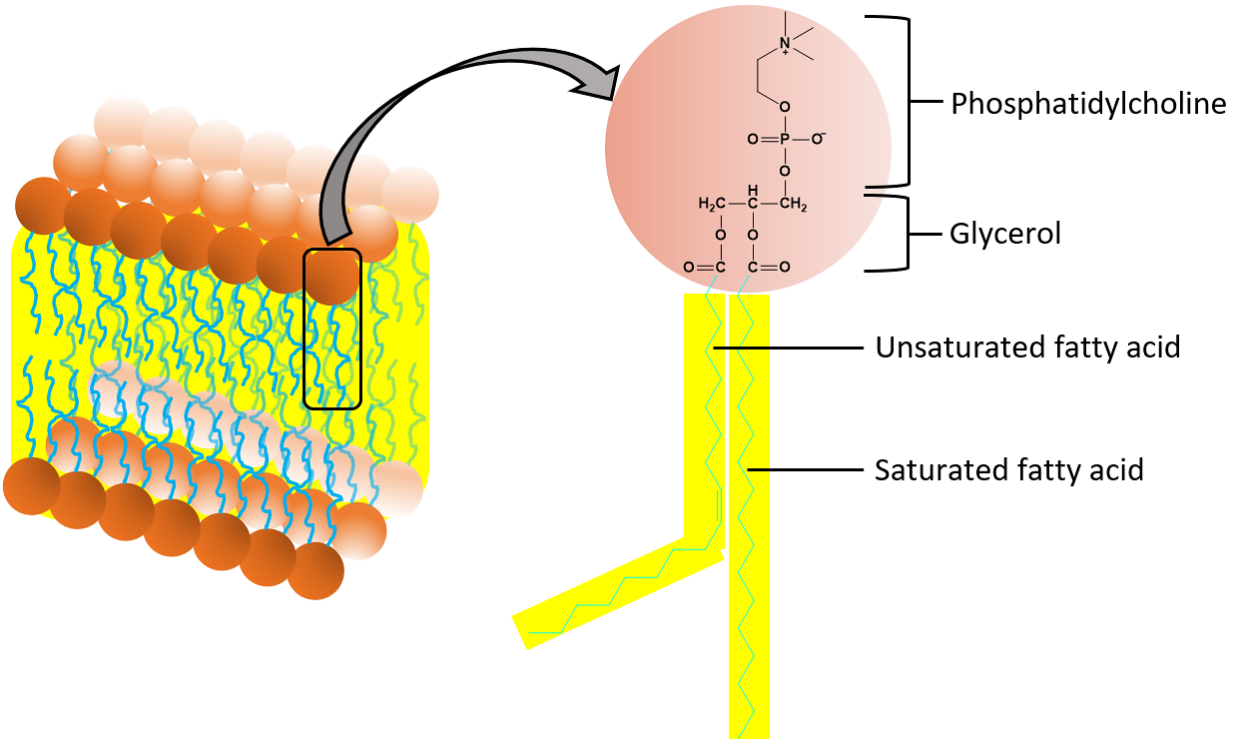

Figure 1.1 Phospholipid bilayer containing phosphatidyl choline (PC) as head group accompanied with both saturated and unsaturated fatty acid as hydrophobic tails.

1.2 Blood study

To elucidate the molecular architecture of cell membranes, human blood cells are commonly chosen as the objective for research due to their rapid availability, relative homogeneity and medicine-related properties.[12] Different components of blood can be easily isolated through performing simple protocols, providing convenience in blood-representative cell studies. In order to study a universal bioadhesive material capable of interacting with eukaryotic cell membranes, it is convenient to use the formation of blood cell aggregations as a measure of binding of macromolecules to adjacent membranes in a bridging conformation. Such reactions are also

relevant to biomaterials that can also act as hemostatic agents that is capable of controlling or preventing hemorrhage.

1.2.1 Blood basics

In the human body, blood makes up 7-8 % of the weight, which equates to 4.5~6 L of body fluid for an adult. As an essential circulating fluid, blood possess many functions to maintain biological activities, including oxygen and nutrition transportation, forming blood clots for bleeding control, fighting with infection, delivering wastes to kidney and liver, as well as body temperature regulation. Blood mainly contains four components, namely, plasma, platelets, red blood cells (RBCs) and white blood cells (WBCs), as shown in Figure 1.2.

Among all the blood constituents, about 55% of the blood's volume is plasma, which is a relatively transparent, yellow colored liquid consisting of over 92% of water, sugar, salt, fat and protein macromolecules. Plasma is basically in charge of transporting blood cells, as well as the essential elements such as nutrients, metabolic wastes, regulating hormones, antibodies, and clotting factors inside the human body. RBCs, also known as erythrocytes, are the most common blood cell, which take up about 40~45% of the blood volume. RBCs participate in delivering oxygen generated by gas exchange in the lung to different body tissues and returning CO_2 to the lungs for release. For healthy humans, mature RBCs exist in a biconcave-disk shape flattened in the mid, which resembles the look of a donut. White blood cells (WBCs), accounting for only 1% of blood volume with a size larger than RBCs, are well known for fighting against infections as cells belonging to the immune system. One type of WBCs that people are familiar with is the stem cell - generated neutrophil, which occupies 55~70% of the WBC family and commonly known as the "first responder" to inflammation.[13] The last major blood component, platelets, also known as

thrombocytes, are considered as pseudo cells due to the absence of a nucleus. Platelets are the smallest among all blood cells, with the mean diameter between 1 to 2 μm and exist in the form of biconvex disc. Platelets play important role in coagulation process, as will be introduced below. In our study, the characteristics of RBCs and platelets were stressed due to their potential interactions with the developed materials.

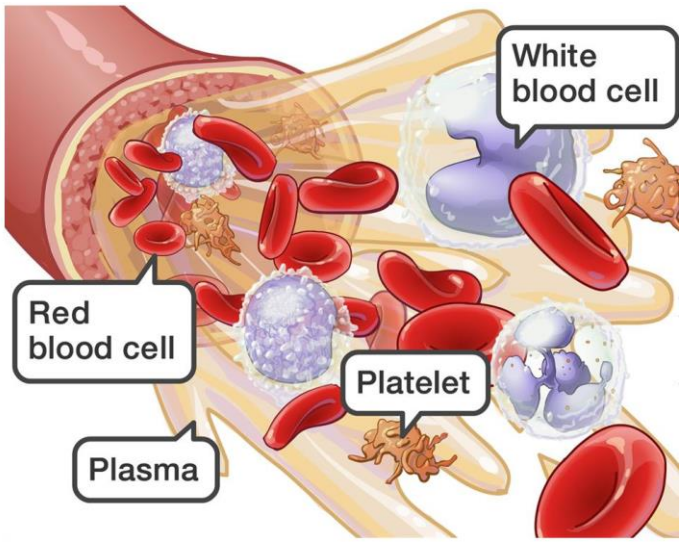

Figure 1.2 Cartoon illustrating components of flowing blood inside of vessel. (© AboutKidsHealth.ca, by permission).

1.2.2 Surface composition of RBC membranes

As an abundant component in human blood, study of RBCs is necessary and representative when testing a novel material to be introduced to the blood medium. Most of the human cells are nucleated and are much bigger than a typical human RBC, of which the diameter is usually between 6.2-8.2 μm[14] with a surface area about 135 μm^2. The membranes of normal human RBC are made up of lipids (40% w/w), carbohydrate (0~10%) and the rest is a variety of proteins. RBCs

are able to bear reversible structural deformations up to 250% with respect to the linear extension, while maintaining surface area unchanged. This unique behavior exhibited due to the high elasticity, rapid adaptation to fluidic pressure change, as well as the structural barrier provided by RBC membranes.

Like a normal eukaryotic cell, the RBC membranes behave according to a fluid mosaic model, and is composed of a phospholipid double layer with transmembrane protein molecules embedded in it. The lipid bilayer contains equal amounts of cholesterol and phospholipids by weight, where cholesterol is equally distributed between the two leaflets, while phospholipids are unequally arranged. Among the 4 major phospholipids, phosphatidylcholine (PC) and sphingomyelin are mainly disposed in the outer monolayer, while phosphatidylethanolamine and phosphatidylserine basically face towards the interior of the layer. Phospholipid asymmetry is maintained and generated by transport proteins which operate dependent or independent of energy. On the other hand, RBCs also contain more than 50 types of transmembrane proteins, defining various antigens of blood groups.[15] It is believed that membrane proteins bridged with skeletal proteins through protein linkages play an important role in maintaining the surface area of RBCs via regulating the strength of cohesion between the membrane skeleton and the phospholipid bilayer, where the skeletal proteins are a 2-dimentional elastic network composed of various spectrins. One example showing naturally occurring RBC deformation is rouleaux. Rouleaux form when RBCs stack or aggregate together when the plasma proteins, especially globulins and fibrinogen are high in concentration and thus contribute to this face-to-face morphology of RBCs as shown in Figure 1.3. The proposed mechanism of rouleau formation is the “bridging” hypothesis, which describes the situation where plasma proteins are adsorbed onto the surfaces of RBCs that join two adjacent cells together.[16]

(a) (b)

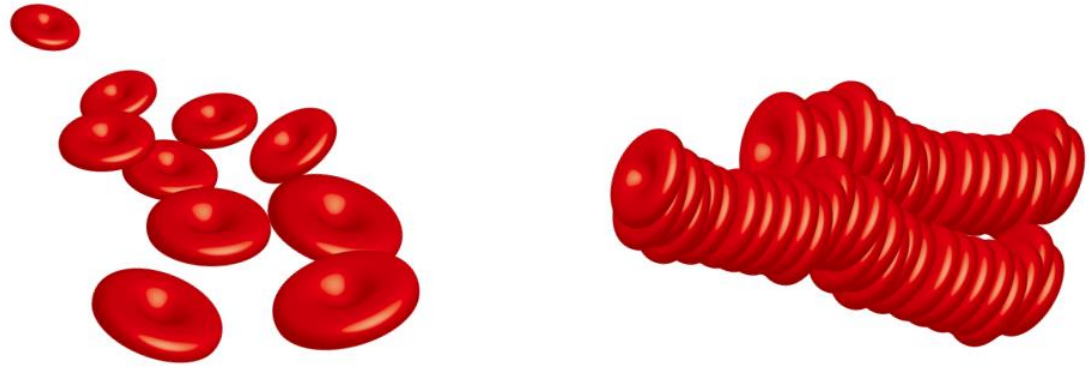

Figure 1.3 Typical human red blood cells. (a) freely flowing erythrocytes; (b) forming rouleaux.

1.2.3 Functionalities of platelets in hemostasis

Another factor participating in the hemostatic process is related to platelets, which are small disc-shaped cells circulating in human blood with an 8~12-day half-life. Although RBCs play a crucial role in controlling hemorrhage when being presented to a physical hemostatic material, the driving mechanism can be either explained as the surface adhesion between RBC membranes and the introduced agents, or it could be the platelets being activated that induces the coagulation process (Figure 1.4).

After platelets are exposed and adhered to a damaged vessel, change in platelet shape is induced, which in turn causes granule secretion to occur supplying active compounds such as adenosine diphosphate (ADP) to attract more platelets and hold them to the von Willebrand factor (VWF) on subendothelial tissue. These "sticky" platelets are then prone to bind quickly onto the collagen exposed at the damaged site of the vessel wall, forming a stable platelet plug, as illustrated in Figure 1.5 (A), (B) and (C). This cohesive function of platelets is considered as the primary hemostasis event.[17,18] Meanwhile, the second event is taking place where the coagulation process

is activated during platelets' exposure to a phospholipidic surface. After the coagulation cascade is initiated by clotting factors and tissue factor (VIIa), which are activated through surface contact and tissue damage separately, thrombin forms in the blood vessel. The presence of thrombin awakens the intrinsic blood clotting factor, fibrinogen and turns it into highly cross-linked fibrin. The insoluble net-shape fibrins hold the aggregated platelets tightly, adding bulk to the developing clot[19], as illustrated in figure 1.5 (D). Platelet aggregation and blood coagulation are regarded as two parallel but complementary processes in functioning hemostasis (Figure 1.4).

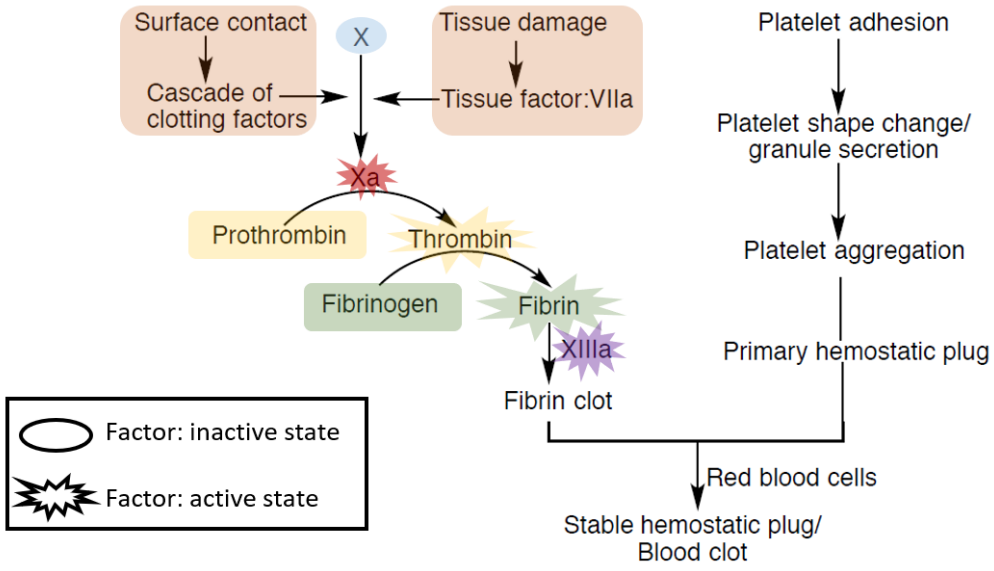

Figure 1.4 Blood clot synthesis cascade in simplified version, modified from a previously submitted thesis.[20]

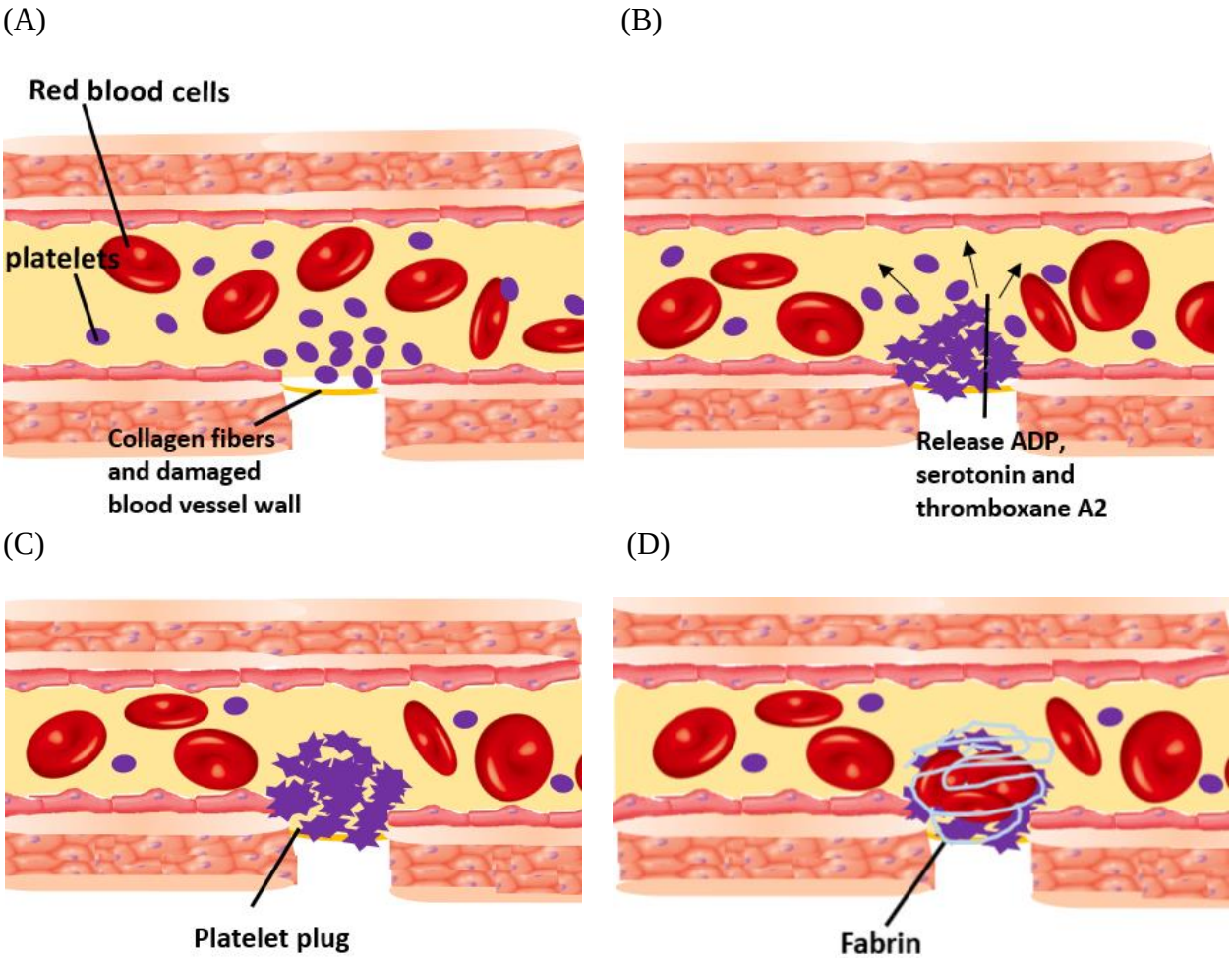

Figure 1.5 Cartoon illustration of platelet's role during hemostatic process. (A) platelets exposed to collagen at the damaged vessel are activated. (B) Platelets adhere to the subendothelial components and release active molecules such as ADP to recruit more platelets. (C) Platelets aggregate at the injury site, forming a platelet plug which shows hemostatic effect. (D) Fibrin forms a net that entraps platelets and some RBCs.

1.3 Polymer materials applied in biomedical fields

1.3.1 Development of drug delivery material

Biomaterials play a critical role in delivering pharmaceuticals and biomolecules. The ultimate goal of developing drug delivery agents is to provide a formulation that can sustainably act on the targeted biological events, resulting in increased drug efficacy. Conjugating the effective drug to a biomaterial is commonly applied in controlled-release formulations, such materials typically include glycol- or glycerol-based macromolecules, which are able to stabilize body proteins by not interacting with them. As widely used nanoparticles in drug delivery systems, polymers have provided a versatile matrix for carrying drugs or biomolecules as shown in figure 1.6 (A). The pharmaceutical agents can be wrapped within microparticles, microcapsules, polymer fibers or conjugated to polymer chains. To address the materials to specific cells, cell-targeting surface modification is commonly implemented.[21]

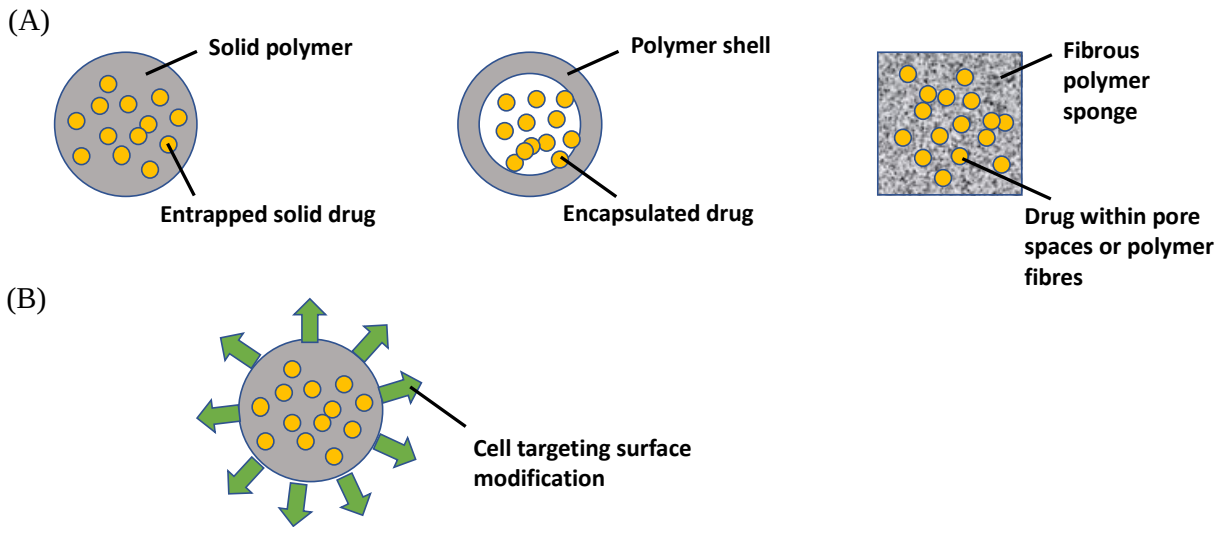

Figure 1.6 (A) Drugs carried by various types of polymers. (B) Drug delivery polymer modified with cell-specific ligands on surface.

Among various surface modification approaches, bioadhesive polymers are regarded as a novel tool in drug delivery systems. Bioadhesion means attaching the drug carrier system to different biological site, and can be further classified broadly into two groups: nonspecific and specific.[22] According to their purposes, specific bioadhesive polymer materials have the ability to bind with designated chemical groups belonging to that biological molecule while the nonspecific adhesion represents polymers that are able to attach to both the cell surfaces and mucosal layer. A number of studies have demonstrated that bioadhesive polymer carriers can not only improve the local therapeutic activity, but also maintain long-term function at the application site through increasing the residence time of drugs.[23]

1.3.2 Biocompatibility and hemocompatibility

Biocompatibility is an important concept to consider when developing a novel biomaterial for medical applications. This means that the agents making contacts with biological molecules must be well accepted without causing abnormal responses in the cell system. However, as a whole complex system, living organisms hardly stay inert when facing the intervention of a new material, thus some uncontrolled biological activities may occur to respond to the altered system environment. So far, no strict or unified definition of biocompatibility has been released due to the diverse applications of the designed drugs, and only narrowed explanation can be given with respect to specific applications. Conceptually, however, within the past three decades "biocompatibility" has been commonly deemed as "the ability of a material to perform with an appropriate host response in a specific situation".[24] The three criteria implied from this definition are that this material has to properly perform its desired function instead of merely presenting in any tissues, that the induced series of reactions have to be proper and under control for the intended

application, and that the response of a biological system to a particular material and its suitability may not be applied in a different context.[25] Figure 1.7 adequately demonstrates the relationship between the three dogma, where host, materials and applications all required to be considered when referring to the biocompatibility.

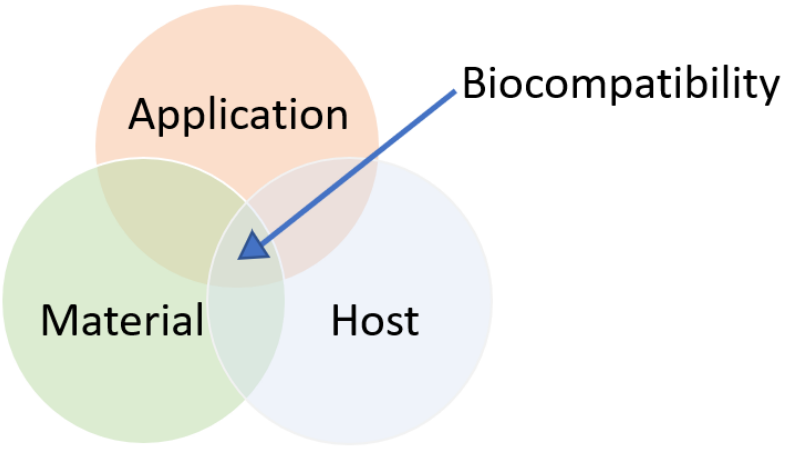

Figure 1.7 Diagram illustrating the principles of biocompatibility.

Hemocompatibility refers to the benign existence of a biomaterial which presents in the blood environment. It is always challenging for a material to achieve a non-toxic effect given the harsh electrolytic medium of the human vascular system. As in defining "biocompatibility", there has always been much debate about what hemocompatibility actually expresses, and as a result, the evaluation is usually adjusted to the specific functions of the material.[26] For example, in terms of this project, the final objective was manufacturing a cell-adhesive macromolecule that is compatible with biological systems. Thus, achieving red blood cell aggregation and adhesion is a desired material response, at the same time avoid the inducing any hemolysis or accumulating protein fouling.

1.3.3 Biocompatible material: hyperbranched polyglycerol (HPG)

Developing biocompatible materials is the base point for achieving many applications in biomedical sciences. Based on the observation that most of the structural tissues in living organisms are made up of naturally occurring polymers, biomacromolecules produced by modifying biosynthetically produced materials usually overweigh the artificial polymers in many aspects, such as biodegradability, bioactivity and biocompatibility, etc. However, problems related to low reproducibility and ways of increasing the scale of production are difficult to overcome when dealing with natural materials[27], therefore, synthetic polymers with benign properties are of interest due to their flexibility in structure modification and synthesis design.

Among various classes of polymeric material, dendrimers are relatively modern and well known for their extensively branched three-dimensional structure that leaves much space for versatile surface and interior modification. The sharp rise of dendrimer applications in the biological field cannot be separated from their unique properties such as uniform size, high degree of branching, hydrating function, polyvalence, narrowed polydispersity (Đ) and constructible internal space.[28] As a carrier for drug and gene delivery, all these properties enable dendrimers to behave as a core that either encapsulate the bioactive agents or having them chemically attached onto the periphery of the branched polymer[29,30], as shown in Figure 1.8. In addition, dendrimers have to satisfy certain biological criteria in order to be considered safe or biocompatible when put into use as biological agents. These demands include: freedom from toxicity and immunogenicity; ability to cross biobarriers; being able to stay present in the circulation system for the time required to show a desired effect; and accurately targeting to specific biological components.[28]

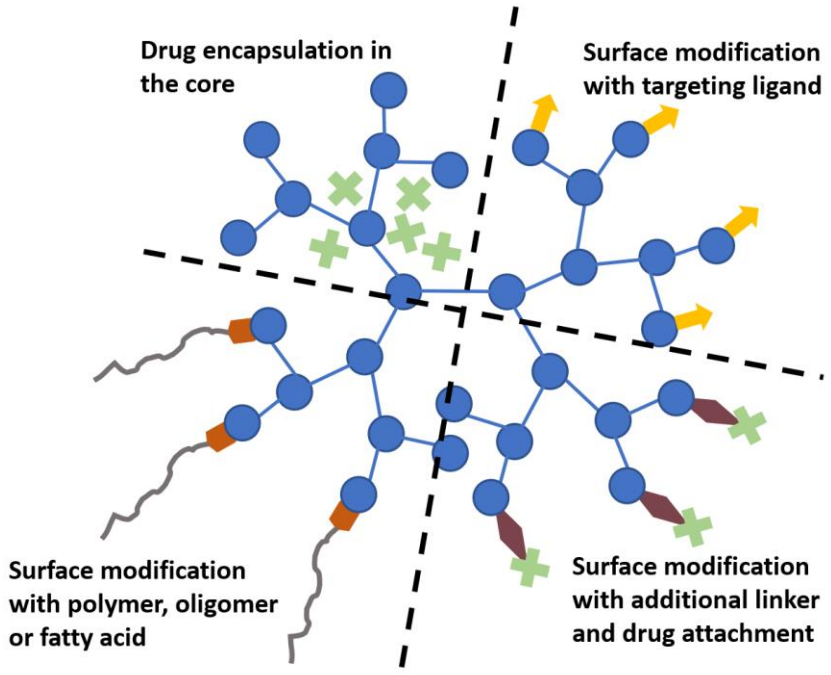

Figure 1.8 Diagram illustrating approaches for design of dendrimer-based drug delivery system. Modified from work published by Duncan and Izzo.[30]

Although dendrimers have been attractive due to their structural aesthetics of controllable repetition, the complicated stepwise synthetic pathways required for producing dendrimers limit their broad application. In comparison, as an alternative, syntheses of hyperbranched polymers through one-pot reactions from AB_x monomers are of increasing interest in terms of technology level.[31,32] Figure 1.9 shows examples of typical dendrimer and hyperbranched polymers, both of which belong to the dendritic family.

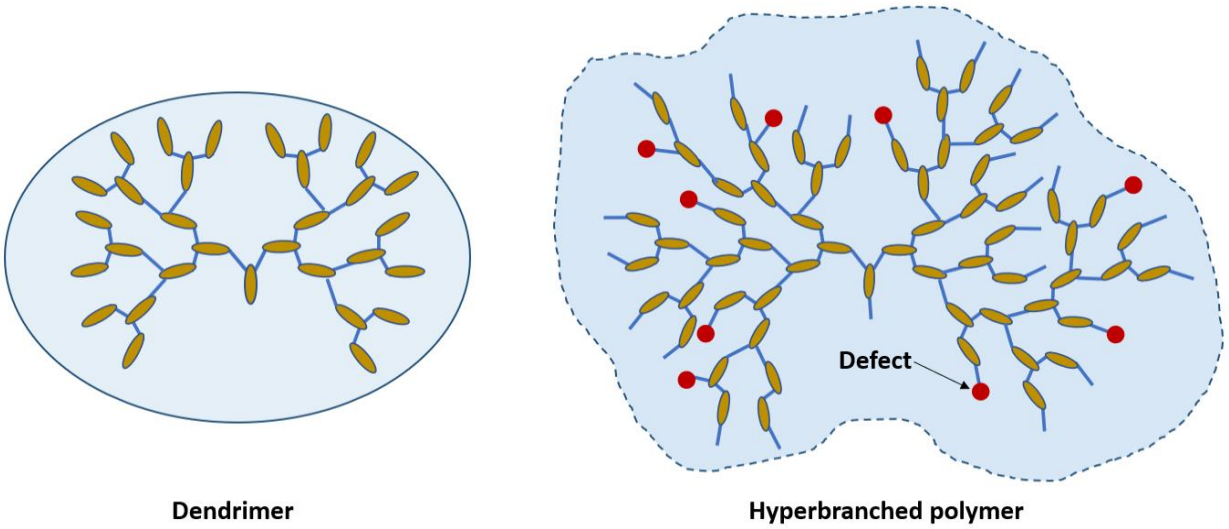

Figure 1.9 Structural difference between dendrimer and hyperbranched polymer. Both belong to dendronized family.

As a hyperbranched polymer, hyperbranched polyglycerol (HPG) is a highly compact, branched and hydrophilic polymer manufactured by a single-step ring-opening multi-branching polymerization (ROMP) via slowly adding glycidol as the reaction monomer.[33] Our group has been working on HPG syntheses and modification for over two decades, and with strict control in protocol, we have successfully produced HPGs with a wide range of molecular weights spanning from 3 to 100 kDa. The water solubility of HPG is over 400 mg/mL, with a low intrinsic viscosity which is between 4-7 ml/g, and thus make HPG highly soluble in water and polar organic solvents[34]. The hydration ability stems from the large number of hydroxyl groups per molecule, and this also enables HPG to exist under physiological pH aqueous condition.[34] Experimental studies performed previously have demonstrated that HPG and its derivatives are blood-compatible (by not causing platelet activation or coagulation), free of immunogenicity and toxicity.[35-38] Compared to another polyether compound, polyethylene glycol (PEG), which is

widely used in areas from industrial manufacturing to medicine, HPG and its derivatives have demonstrated much improved chemical stability in the oxygen environment or during the exposure to oxidative transition metal ions.[39] Both HPG and PEG show non-fouling properties by energetically resisting protein approach, and recent studies have agreed that it is the hydration ability of both macromolecules that lead to this particular biological phenomenon.[40,41]

Based on all these outstanding properties, such as relatively low polydispersity (Đ) after polymerization, high water solubility, considerable biocompatibility, chemically and thermally stable structure, as well as flexibility in structural design, HPG-based polymers have gradually become promising candidates participating in various fields of modern biological applications, including plasma protein substitutes, hemostatic material, antidotes for anticoagulants, osmotic agent in peritoneal dialysis, and antibacterial peptide.[42-45]

1.3.4 Zwitterionic compounds

Zwitterionic compounds are a family of polar materials that contain equal numbers of both cationic and anionic moieties, which results in an overall neutral charge. The unique structural properties of zwitterionic materials have led to applications in many new emerging biomedical fields, attributes contributing to their biocompatible merits including resistance to nonspecific protein adsorbance[46], increased stability and bioactivity of enzymes[47], as well as lack of induction of immunological response in the blood circulation.[48] After being discovered that zwitterionic 2-methacryloyloxyethyl phosphorylcholine (MPC) polymers could perform impressively in protein-adsorbance-resistance functioning task[49], in 2005, Chen and his colleagues first demonstrated that the hydration layer induced by strong electrostatic force of zwitterionic surface (Figure 1.10) was the key factor in reducing protein adsorption.[50] Other than the hydration properties, according to

the model proposed by De Gennes *et al*., as the protein molecules approach to the surface of branched material, the chains being compressed during the process lead to a loss in entropy and an increase of Gibb's free energy of the system, which makes the proteins' diffusion into the chains less favorable as well.[51] These two results are in accordance with the earlier findings on PEG studies, where the materials also manifested strong resistance to protein adsorption owing to their hydration ability contributed by the intermolecular hydrogen bonds formed between PEG molecules.[52]

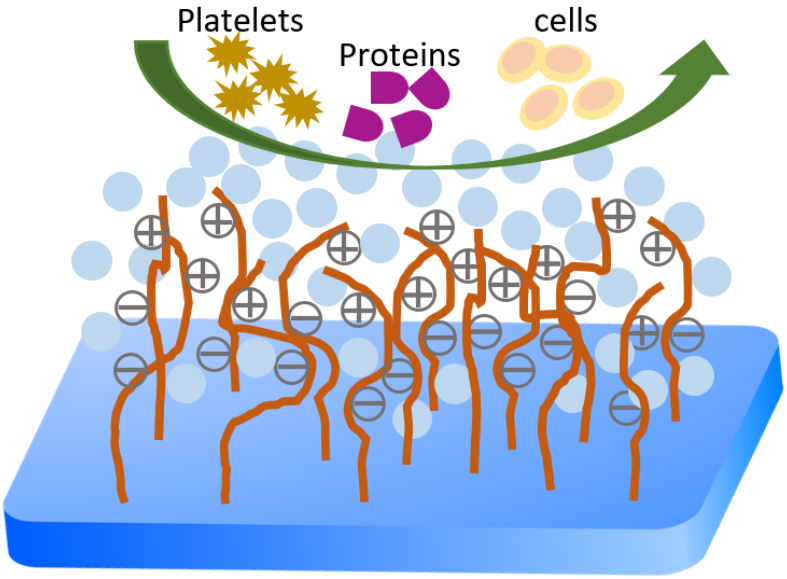

Figure 1.10 Illustration of a surface modified with zwitterionic materials demonstrate non-fouling properties due to the presence of hydration layer.

Among all the cases applying zwitterionic moieties to polymer surface modification, sulfobetaines, carboxybetains and phosphorylcholine betaines, as shown in Figure 1.11, are the prominent examples as exhibiting outstanding performance during biological contact. The non-

fouling functions of Sulfobetaines (SB) and carboxybetaines (CB) were discovered in early studies by conducting the tests in protein solutions and undiluted blood plasma. After this early-stage success was laid, CB and SB moieties-involved biomedical applications have sprung up massively in the past 15 years, mostly including developments in biosensors and drug delivery vehicles.[53-55] Another popular zwitterionic moiety is considered to be phosphorylcholine betaine, which is bio-inspired by the phosphorylcholine (PC) groups on cell membranes. Polymers bearing PC effective ligands have proven successful as a critical ingredient of implant materials[56] owing to their non-fouling and biocompatible features. Specifically referring to the polymer constructs, the PC functionalized methacrylate macromolecule has opened the gate for marching into the living polymerization[57,58] and bioconjugation fields.[59]

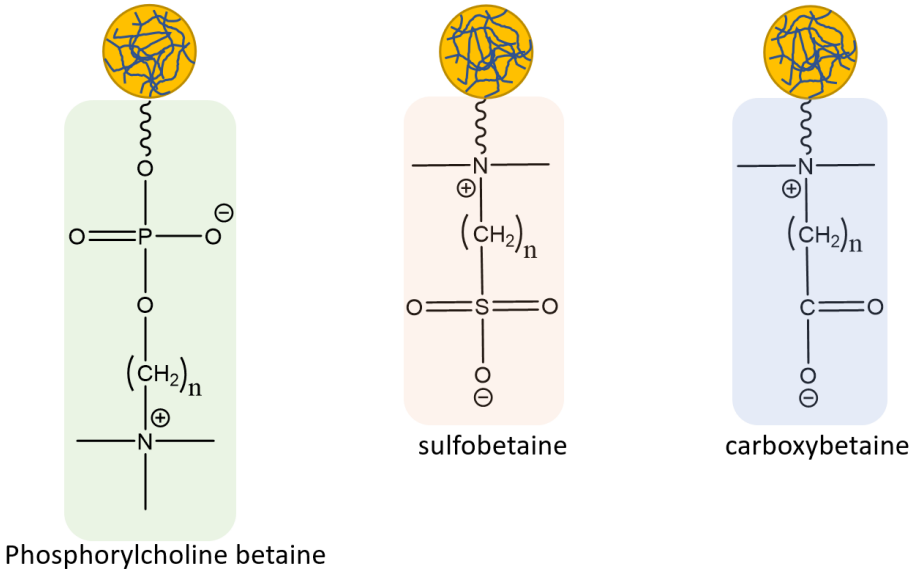

Figure 1.11 Polymers underwent surface modification with phosphorylcholine betaine, sulfobetaine, and carboxybetaine.

1.3.5 Choline phosphate

As a novel zwitterionic design possessing PC-reversed structure, choline phosphates (CPs) have caught deep-seated interests in recent years as being able to demonstrate stronger structural viability as well as more tunable solution properties than other zwitterionic ligands. CP is also electrically neutral, as illustrated in Figure 1.12, it is virtually identical to phosphatidyl choline (PC) headgroup but only in inverse orientation. It is believed that the structural area of CP is similar to that of PC when present in aqueous media, and therefore could in principle stabilize the phospholipid bilayers. Even though CP resembles PC unassailably in terms of the molecular construct, CP synthesis does not occur naturally, which sharply contrasts with PC manufactured abundantly by biological cells. In 2012, our group reported a critical finding that HPG decorated with CP was capable of producing strong binding to the cell surfaces functioned by the unique "PC-CP" electrostatic interaction (Figure 1.12), which was proved to induce aggregation of red blood cells (RBCs). It has also been concluded that increasing CP density on HPG resulted in higher binding affinity, while further increasing both CP derivatization and molecular weight of HPG core could only result in a small increase in adhesion ability. Thus, performing modification on HPGs of molecular weights Mn = 20,000 kDa provided the optimized binding efficiency.[60] Interestingly, it has also been found that the alkyl group R of CP in Figure 1.12 could affect CP-PC adhesion to a great extent, where the phosphate ester bearing only a methyl group would result in RBC aggregation while a longer carbon-chain substituent did not induce any cell binding effect.[61] This result limited certain synthetic routes and required more trouble-shooting strategies during material development, making the chemistry work non-trivial and exciting.

Our group believed this work is able to illustrate the general understanding of CP-PC interaction applicable to all eukaryotic cells containing phosphatidyl choline headgroups on the

surface. This universal mechanism potentially opens up new fields in bio-related applications, such as tissue engineering, tissue sealants and local drug delivery.

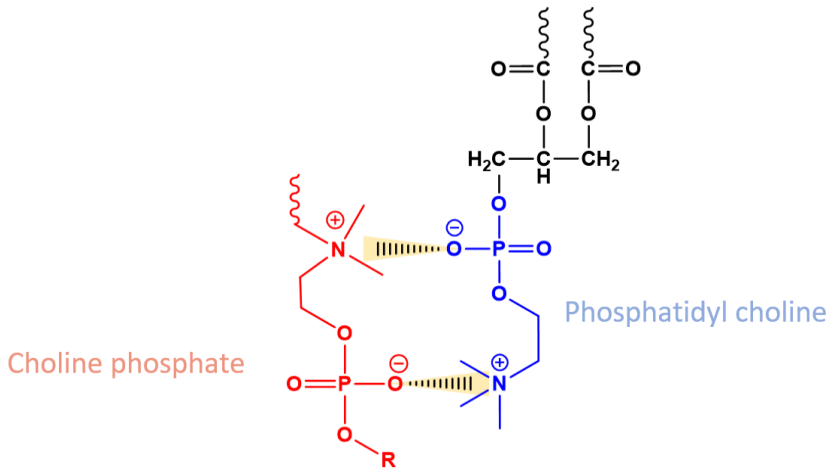

Figure 1.12 Illustration of electrostatic interaction between choline phosphate (CP) and phosphatidyl choline headgroup on cell membrane.

1.4 Thesis objectives and layout

The primary aim of this project is to develop a polyvalent HPG-based material that is readily synthesized and is capable of binding to cell surface without causing biofouling or cytotoxicity. The mechanism behind the desired material is based on the electrostatic interaction between phosphatidyl choline (PC) headgroups on a membrane bilayer and the designed zwitterionic moieties, choline phosphate (CP), which possess a "PC-reverse" chemical structure. Human blood was chosen as the object of study, where the structural components, namely an HPG backbone and neutrally charged CP are expected to function synergistically to induce aggregation of red blood cells (RBCs) by adsorbing in a bridging conformation. These polymer conjugates are

believed to impart hemocompatibility and attenuate protein adsorption by the strong hydration property of both HPG core and multivalent CP.

To obtain the desired structure, in Chapter 2, a new synthetic route for multivalent HPG-CP was developed. The synthetic steps are shown and the structures of each synthesized material are also given as determined through various characterization methods. Briefly, HPG was prepared via one-pot ring-opening multi-branching polymerization (ROMP), followed by attaching an azido linker to it through an esterification reaction. Lastly, CP functional groups were coupled onto HPG-N_3 through Cu^I-catalyzed azide/alkyne cycloaddition (CuAAC) to achieve the target product. The chemical properties and structural information were provided by nuclear magnetic resonance (NMR), gel permeation chromatography (GPC), dynamic light scattering (DLS), liquid chromatography-mass spectrometry (LC-MS) and Fourier-transform infrared spectroscopy (FT-IR). The results are given and discussed in the following chapter.

In Chapter 3, the synthesized HPG conjugates were further tested to understand their physical and biological properties. Physical tests were aimed at examining the net charge on the polymer periphery, as well as quantifying the hydration ability of the material. Biological tests were conducted to discover how the novel HPG-based zwitterionic conjugates behave *in vitro* with regard to blood aggregation performance, hemocompatibility and toxicity.

The final part of this thesis, Chapter 4, concludes the significant findings of the entire project. Future directions are considered and proposed as a continuation of this project.

Chapter 2: Synthesis and characterization of polyvalent hyperbranched polyglycerols (HPGs)

2.1 Background and synopsis

In this chapter, hyperbranched polyglycerols (HPGs), synthesized by ring opening multi-branching anionic polymerization, were used as starting material to be modified by 5-azidovaleric acid to introduce azide-terminated structures which replace a controlled fraction of the original hydroxyl groups. The linker-carrying HPGs were further coupled with different amounts of triple bond moieties on choline phosphate (CP) via Cu^{I}-catalyzed azide/alkyne cycloaddition (CuAAC) to obtain HPG-CPs (structure shown in Figure 2.1).

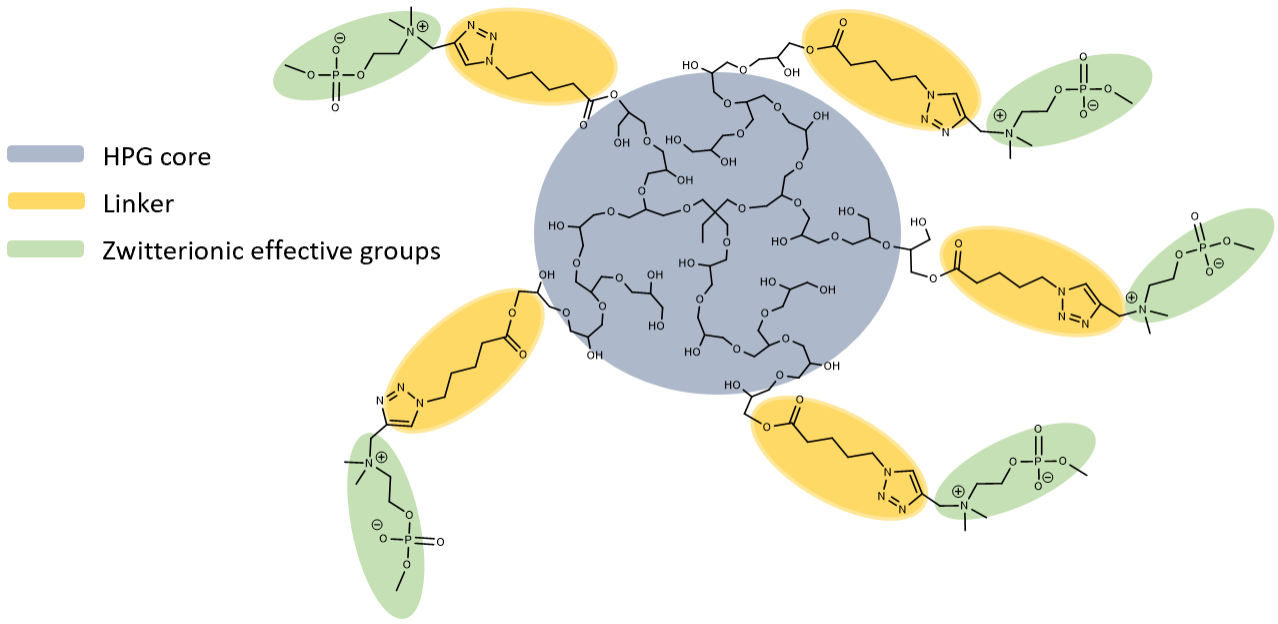

Figure 2.1. The structure of partially modified HPG-CP designed in this project.

In comparison with previous methods, this novel reaction pathway for preparing CP focuses on improving yield via attenuating the occurrence of side reactions. As shown in Scheme

2.1, the traditional synthetic protocol of manufacturing methyl decorated CP through employing cyclic phosphate ester as a starting substrate[59] could lead the reaction to proceed by two pathways. It has been reported that the exocyclic side reaction causes the undesired phosphonate salt to form as the major product, which in turn results in a yield much less than 10%.[60] Introducing dimethyl chlorophosphate to react directly with hydroxyl-carrying quaternary ammonium salt can avoid the nucleophilic attack of the tertiary amine towards the methoxy on phosphate, as shown in Scheme 2.1 (c). In this way, the competing side product salt will be absent from the product mixture.

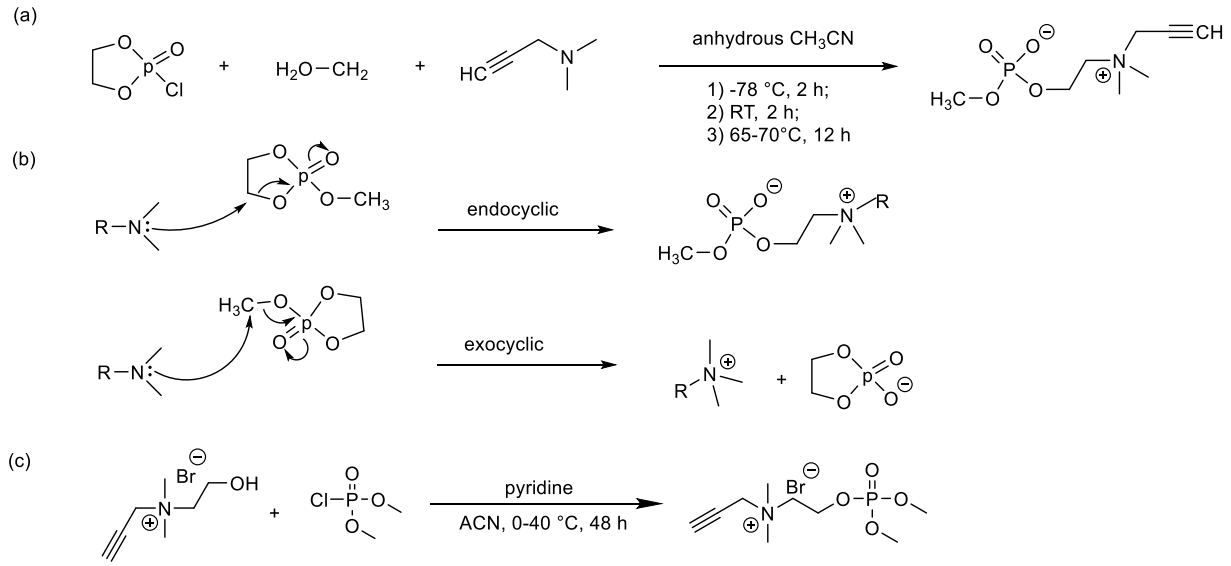

Scheme 2.1. Previously reported reaction routes of CP synthesis. (a) The traditional synthetic scheme for prop-2-ynyle choline phosphate (CP). (b) Proved competing exocyclic and endocyclic pathways. (c) The reaction pathway for CP synthesis developed in this project.

To attach CP groups onto the HPG core modified with azido linkers, the idea of a "click" reaction was utilized to realize this efficient "one-pot" conjugation. In 2001, the concept of "click" chemistry was first introduced by Kolb, Finn and Sharpless, describing a type of reactions which

take place selectively and facilely under ambient and mild conditions which is able to obtain high yield with few or no by-products.[62] The most commonly applied "click" reaction by far is the Cu^{I}-catalyzed azide/alkyne cycloaddition (CuAAC), which is considered as an improved version of a non-catalyzed Huisgen reaction in which only 1,4-disubstituted triazoles form as the product due to the selectivity of the terminal alkyne.[63] Although ligands are not necessary to participate in CuAAC, it has been reported that the reaction rate can be enhanced with the presence of polydentate nitrogen donors. Therefore, CuBr/PMDETA, which is probably the most popularly employed system, was chosen to catalyze the surface modification of HPGs in an efficient manner[64] (Scheme 2.2).

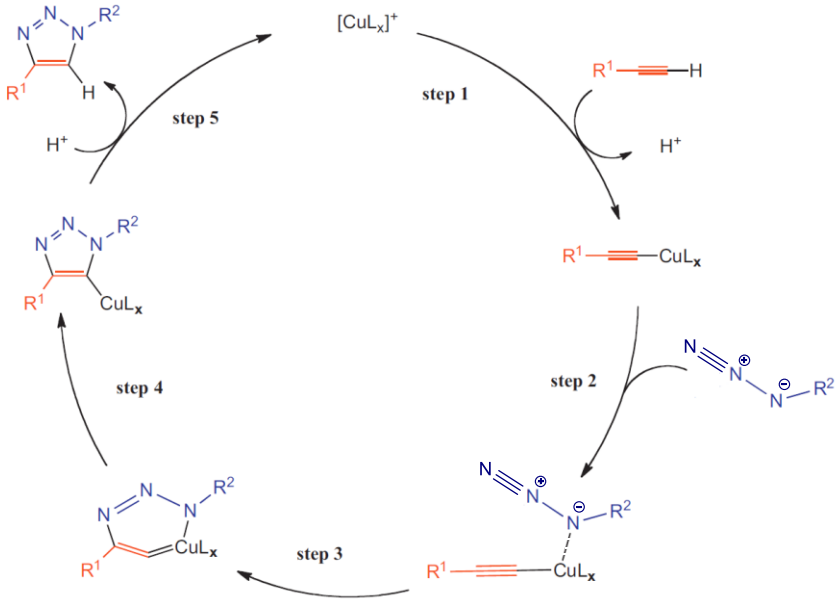

Scheme 2.2. Mechanism of CuAAC "click" reaction proposed by Fokin and Finn. The catalytic cycle was modified from a review by Liang *et al.*[65]

2.2 Experimental section

2.2.1 Materials and methods

All reagents and solvents were ACS reagent grade and purchased from Sigma-Aldrich and Fisher Scientific (ON, CA), except for glycidol (96%) and dimethyl chlorophosphate (95%) that were purified by fractional distillation under reduced pressure; all the other chemicals received were directly used without further purification. Molecular weight cut-off (MWCO) dialysis tubing made of regenerated cellulose was obtained from Spectrum Laboratories, Inc. (CA, US). The analytical thin-layer chromatography (TLC) plates containing Silica Gel 60 as sorbent were produced by MilliporeSigma (MA, US). ^{1}H, ^{13}C, ^{31}P and ^{1}H-^{31}P HMBC NMR spectra were all generated by Brucker AV300 NMR instrument. Chemical shifts are expressed in parts per million (ppm) by frequency, relative to the residual peak of deuterated solvent. Number average molecular weight (Mn) and polydispersity index (Đ) of HPG polymers were determined by gel permeation chromatography (GPC) equipped with a multi-angle laser light scattering (MALLS) detector and a refractive index (RI) detector purchased from Wyatt Technology Corporation (CA, US), with aqueous $NaNO_3$ buffered at pH = 7 applied as loading solvent. The dn/dc value used for the molecular weight calculation of polymer was 0.12 mL/g.

2.2.2 Synthesis of hyperbranched polyglycerol (HPG)

HPG was synthesized following the published methods[66] as shown in Scheme 2.3. Briefly, a 250 mL three-necked round bottom flask (RBF) equipped with a magnetic stir bar was flame dried to remove moisture by switching between vacuum and argon for three cycles. Under the argon condition, the initiator 1,1,1-tris(hydroxymethyl)propane (TMP) (16.3 mg, 1.22 mmol) was first transferred into the RBF at 81 °C. After the TMP was fully melted into a viscous liquid,

potassium methylate methanol solution (0.10 mL, 25 wt % in methanol) was added to partially (10%) deprotonate the initiator. The excess methanol was removed under vacuum for 4 hours until the mixture turned into dry white solid. Then, the flask was equipped with a mechanical stirrer and glycidol (24 mL, 0.37 mol) was added dropwise via syringe pump over 12 h at 95 °C, followed by stirring for another 6 h. The reaction was quenched by adding methanol (50 mL) to fully dissolve the mixture, and then neutralized using 1 M aqueous HCl solution. The weight-average molecular weight (Mw) of crude product was determined by the GPC-MALLS system equipped with Waters ultrahydrogel columns using 0.1 N $NaNO_3$ solution as running eluent. Then, fractional precipitation was performed by introducing acetone to get rid of the polymer with undesired molecular weights to lower the polydispersity (Đ). The collected portion was then concentrated under vacuum and dissolved in water for further purification by dialyzing against water for 3 days using a regenerated cellulose membrane (MWCO = 1000 Da). The final aqueous product was lyophilized on a freeze dryer to obtain the targeted 20 kDa HPG as viscous colorless liquid with the yield of 65% (15.5 g).

The final Mw and Đ were determined by GPC-MALLs, and structure of HPG was determined by ^{1}H and ^{13}C NMRs

^{1}H NMR (δ: ppm, 300 MHz, D_2O) 3.99-3.52 (m, -OC***H***$_2$C***H***-, -C***H***$_2$OH, 5H).

^{13}C NMR (δ: ppm, 75 MHz, D_2O) 79.6 (-CH_2***C***HOR-), 78.1 (-CH_2***C***HOR-), 72.3 (-RO***C***H-$_2$CHOH), 70.9 (-RO***C***H_2CH-), 70.6 (-CH_2***C***HOH-), 69.4 (-RO***C***H_2CH-), 69.1 (-CH_2***C***HOH-), 62.7 (OHCH***C***H_2OH), 60.9 (-ROCH***C***H_2OH).

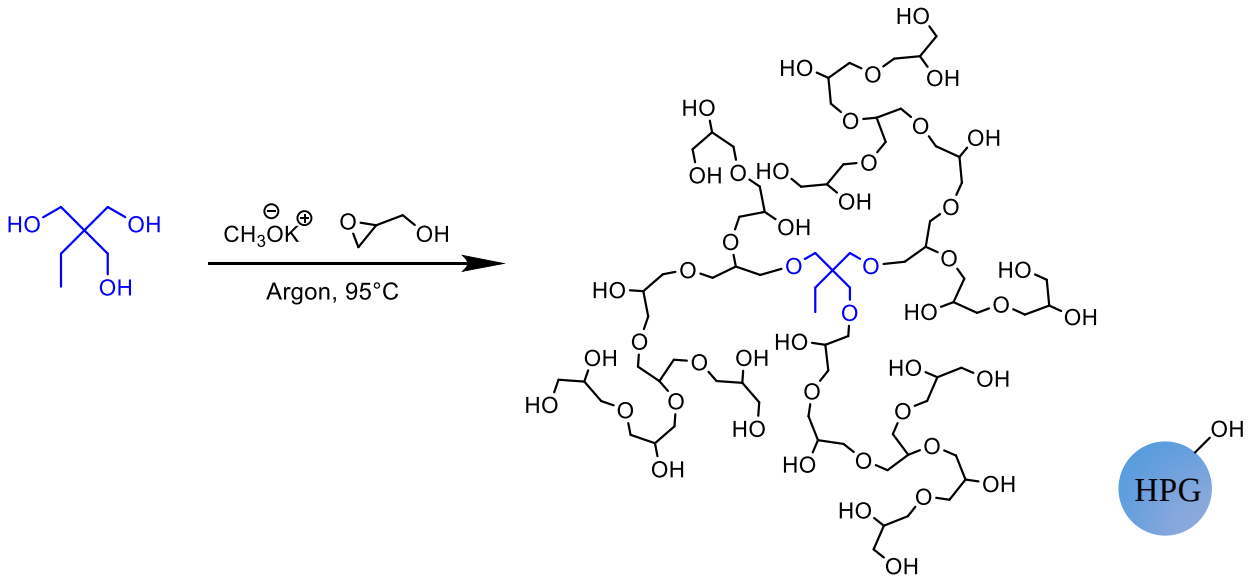

Scheme 2.3. The synthetic route for HPG.

2.2.3 Synthesis of 5-azidovaleric acid

The HPG linker 5-azidovaleric acid was synthesized following Scheme 2.4. Ethyl 5-bromopentanoate (4.78 g, 0.022 mol), sodium azide (2.96 g, 0.044 mol) and an acetone/water mixture (40 mL, acetone: water = 3:1, v/v) were transferred to a 250 mL one-neck round bottom flask equipped with a tap water-cooled condenser. The mixture was heated to 75 °C and kept under stirring and reflux for 12 h. After the resulting mixture was cooled down to room temperature, acetone was expected to evaporate during the reaction and the aqueous layer was treated with DCM extraction three times. The organic phase was then collected, washed with brine and water each twice separately. Finally, the extract was dried over $MgSO_4$, and concentrated by evaporating DCM under vacuum to obtain ethyl 5-zaido pentanoate.

The synthesized ethyl 5-azido pentanoate, sodium hydroxide (1.76 g, 0.044 mol) and methanol/water (60 mL, methanol: water = 2:1) were together added to a 250 mL one-neck RBF

equipped with a magnetic stir bar. The mixture was kept stirring at room temperature for 18 h for a complete reaction. The resulting product was cooled in a 0 °C mixed water/ice bath and acidified by introducing aqueous HCl solution (1 N) added dropwise to adjust the pH to 1. DCM was then used for liquid-liquid extraction and the organic phase was combined and, dried over Na_2SO_4. Finally, 5-azidovaleric acid was obtained as a colorless liquid after removal of DCM under vacuum. The yield was 96%.

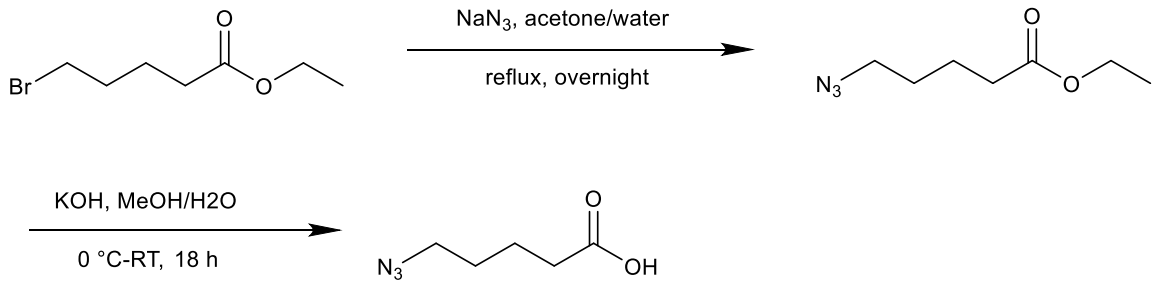

Scheme 2.4. The synthetic scheme for 5-azidovaleric acid.

^{1}H NMR (δ: ppm, 300 MHz, $CDCl_3$) 11.74 (s, -O***H***, 1H), 3.25 (t, $N_3C\boldsymbol{H}_2$-, *J* = 6.45 Hz, 2H), 2.35 (t, -C***H***$_2$C=O, *J* = 6.99 Hz, 2H), 1.63 (ddddd, -C***H***$_2$C***H***$_2$-, *J* = 2.61, 5.28, 7.77, 9.68, 17.02 Hz, 4H).

^{13}C NMR (δ: ppm, 75 MHz, $CDCl_3$) 179.9 (-$CH_2\boldsymbol{C}$=O), 51.1 ($N_3\boldsymbol{C}H_2$-), 33.5 (O=C***C***H_2-), 28.3 ($N_3CH_2\boldsymbol{C}H_2$-), 21.9 (O=$CCH_2\boldsymbol{C}H_2$-).

2.2.4 Preparation of azido functionalized hyperbranched polyglycerol (HPG-$(N_3)_X$)

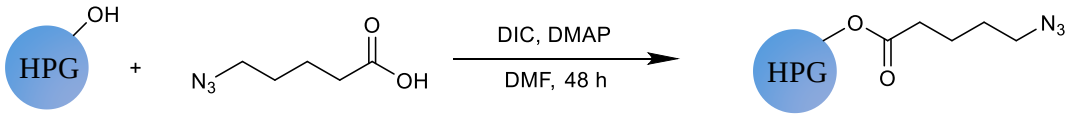

Scheme 2.5. The synthesis for azido functionalized HPG.

As shown in Scheme 2.5, HPG-$(N_3)_x$ was prepared by esterification of hydroxyls on HPG with 5-azidovaleric acid. For a representative reaction conducted on 20kDa HPG, 5-azido valeric acid (0.51g, 3.55 mmol), HPG (Mn = 20 K, 0.70 g, 9.5 mmol hydroxyl groups), N,N'-diisopropylcarbodiimide (DIC, 0.54g, 3.55 mmol), 4-(dimethylamino) pyridine (DMAP, 0.52 g, 3.55 mmol) and DMF (7 mL) were transferred to a 25 mL one-neck RBF equipped with a magnetic stir bar. The reaction was conducted over 48 h under room temperature. Precipitates formed during reaction were filtered off, and the resulting crude azido functionalized HPG was further purified by dialysis in cellulose membrane tubing (MWCO 1000) against DMF/water (2:1) mixture for 3 days with two times daily changes in DMF/water solution. The pure azido functionalized HPG was recovered by removal of DMF under vacuum first and then freeze-drying for 2 days. The final product, dry (20K)HPG-$(N_3)_{80}$ was achieved as a light yellow viscous liquid; both ^{1}H-NMR and ^{13}C-NMR analysis were run to characterize the structure of azido functionalized HPG.

By applying the same procedure, HPG with different molecular weights linked by different percent composition of azido groups were also prepared via varying the ratio of 5-azido valeric acid being added. The number of azido linkers attached on HPG was calculated from ^{1}H-NMR integration values.

^{1}H NMR (δ: ppm, 300 MHz, D_2O) 3.99−3.55 (m, C***H***$_2$ and -O***H*** of HPG), 3.36 (s, N_3C***H***$_2$, 1H), 2.48 (s, -C***H***$_2$C=O, 1H), 1.67 (s, N_3CH_2C***H***$_2C$***H***$_2$-, 1H).

^{13}C NMR (δ: ppm, 75 MHz, MeOD) 78.6-63.2 (-O***C***H_2- of HPG), 50.9 (N_3***C***H_2-), 33.1 (O=C***C***H_2-), 28.1 (N_3CH_2***C***H_2-), 21.9 (O=CCH_2***C***H_2-).

FT-IR (KBr): $\nu_{(O-H)}$ = 3451.3 cm^{-1}, $\nu_{(N=N)}$ = 2101.2 cm^{-1}, $\nu_{(C=O)}$ = 1733.3 cm^{-1}.

2.2.5 Synthesis of CP (N-(2-((dimethoxyphosphoryl)oxy)ethyl)-N,N-dimethylprop-2-yn-1-aminium bromide)

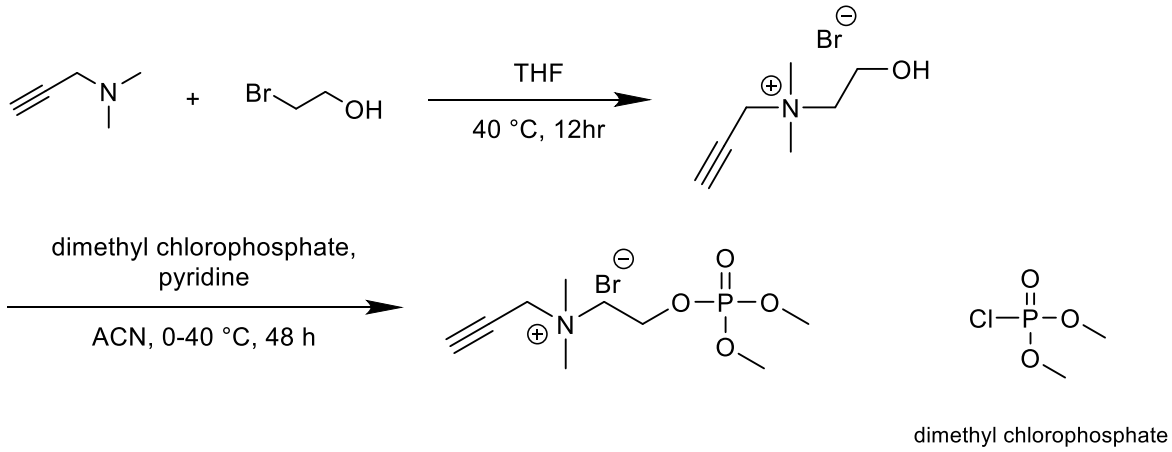

Scheme 2.6. The synthesis scheme for CP.

Scheme 2.6 shows the synthetic route for CP. All glassware was flame-dried and protected by argon. 3-Dimethylamino-1-propyne (5.00 g, 0.06 mol), 2-bromoethanol (7.53 g, 0.06 mol) and tetrahydrofuran (THF, 10 mL) were added to a 100 mL Schlenk flask equipped with a magnetic stir bar, heated to 40 °C in an oil bath and stirred for 12 h. A viscous layer containing product

formed during the reaction, which was then separated from the THF layer and dissolved in 5 mL methanol. The methanol-soluble crude product was then divided into two portions and transferred into two 50 mL conical centrifuge tubes filled with 45 mL cold THF. The mixture was centrifuged at 2200 rpm for 15 minutes three times along with the top phase being discarded and replaced with clean THF after each cycle. The bottom layer was finally obtained by evaporation under vacuum, gaining dried intermediate choline bromide as a white solid (10.9 g, 87%).

^{1}H NMR (δ: ppm, 300 MHz, ACN) 4.81 (q, -O***H***, *J* = 5.11, 1H), 4.53 (t, CH≡CC***H***$_2$-, *J* = 2.5 Hz, 3H), 3.98 (q, -C***H***$_2$OH, *J* = 4.9 Hz, 2H), 3.63-3.60 (m, -C***H***$_2$N-, 2H), 3.30 (t, C***H***≡C-, *J* = 2.5 Hz, 1H), 3.15 (s, C***H***$_3$NC***H***$_3$, 6H).

^{13}C NMR (δ: ppm, 75 MHz, CD_3CN) 81.6 (CH≡***C***-), 71.7 (***C***H≡C-), 65.6 (-***C***H_2CH_2OH), 55.4 (-CH_2***C***H_2OH), 55.3 (-N***C***H_3-), 51.4(***C***H_3N***C***H_3).

To a flame-dried 200 mL round bottom Schlenk flask equipped with a magnetic stir bar, choline bromide (4.50 g, 0.022 mol), freshly distilled dimethyl chlorophosphate (3.75 g, 0.026 mol) and anhydrous acetonitrile (70 mL) were added together at 0 °C. The reaction was continued in the 0 °C ice/water bath for 1 h. To this cooled mixture, anhydrous pyridine (2.1 mL, 0.026 mol) was transferred dropwise using a syringe pump over a period of 0.5 h. The reaction was allowed to warm to room temperature first and then heated up to 40 °C, stirring for 48 h. The bottom layer formed was washed with acetonitrile three times and dried under vacuum. The solid collected as crude CP was a yellow viscous solid, which was used directly for the next−step "click" reaction without further purification. The formation of positively charged CP in the product mixture was detected by gradient LC-MS system, with the eluent used starting from 95% water/methanol to

60% water/methanol over a period of 10 min. The yield determined based on area percentage calculated by LC-MS detection was about 40%.

API-ES (Positive scan), m/z: 236.2 (Mw of CP with one + charge)

FT-IR (KBr): $\nu_{(P=O)}$ = 1640.2 cm^{-1}, $\nu_{(C\equiv C)}$ = 2130.4 cm^{-1}

2.2.6 Polymer functionalization: CuAAC "click" reaction

The functionalization of HPG-N_3 was explored using a Cu(I)Br/PMDETA catalyst-system azide-alkyne cycloaddition reaction given in Scheme 2.7. For a typical reaction, azido functionalized hyperbranched polyglycerol (210 mg, (20K)HPG-$N_{3(80)}$), crude CP (500 mg), and mixed solvent (7 mL, DMF : methanol = 5 : 2) were transferred into a 50 mL Schlenk flask. Freeze-pump-thaw degassing was performed on the mixture for three cycles until no bubbles were observed as the solution thawed. The Schlenk flask containing reagents was then transferred into a glove box, from where copper(I) bromide (81 mg) and N,N,N',N'',N''-pentamethyldiethylenetriamine (PMDETA, 98 mg) were premixed in a 20 mL scintillation vial and added into the Schlenk flask under oxygen-free conditions. The mixture was then transferred out from the glove box and placed into an oil bath preheated to 40 °C, continually being stirred for 48 h under argon. Ten milliliter of acetate buffer (0.1 M, pH 5.0) was added to the reaction mixture and stirred for another 4 h. For the following 3 days, dialysis against EDTA/water (0.15%wt) in regenerated cellulose membrane (MWCO = 1000) was applied to remove catalyst and any unreacted material. After freeze drying, the conjugated HPG was collected and the molecular weight was determined by calculating integration from ^{1}H NMR, as well as obtaining results from GPC-MALLS system as a reference.

For synthesis of other functionalized HPGs, similar conditions were applied with varying the number density of CP zwitterions conjugated onto HPG-$N_{3(x)}$ (x is number of azido groups attached on HPG).

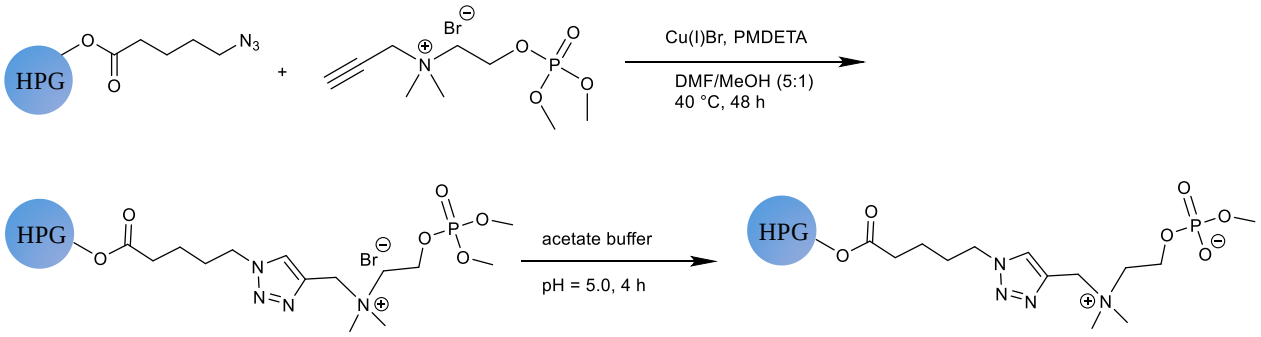

Scheme 2.7. The synthesis scheme of CuAAC "click" reaction.

^{1}H NMR (δ: ppm, 300 MHz, D_2O) 8.38 (s, -NC=C***H***-, 1H), 4.48 (s, -OC***H***$_2$-, 2H), 4.10 (s, -OCH$_2$C***H***$_2$N-, 2H), 4.04-3.50 (-C***H***$_2$-, -C***H***- of HPG), 3.14 (s, C***H***$_3$NC***H***$_3$, 2H), 2.43 (s, -C***H***$_2$C=O, 2H), 1.93 (s, -NC***H***$_2$C***H***$_2$-, 2H) 1.56 (s, -C***H***2CH$_2$C=O, 2H).

^{13}C NMR (δ: ppm, 75 MHz, D_2O) 129.4 (-***C***H from 1,2,3-triazole), 80.0-68.3, 63.1 (-O***C***H$_2$- of HPG back bone), 65.6 (-N***C***H$_2$CH$_2$-), 59.6 (-N***C***H$_2$C=), 55.9 (-O***C***H$_2$CH$_2$-), 53.8-53.5 (-P***C***H$_3$-), 51.3 (***C***H$_3$N***C***H$_3$), 50.7 (-N=NN***C***H$_2$-), 33.3 (-***C***H$_2$C=O), 29.1 (-***C***H$_2$CH$_2$CH$_2$C=O), 21.6 (-***C***H$_2$CH$_2$C=O).

^{31}P NMR (δ: ppm, 300 MHz, D_2O) 0.04 (s).

^{1}H-^{31}P HMBC: ^{31}P NMR (δ: ppm, 162 MHz, D_2O) 1.18, –9.48, 1.18. ^{1}H NMR (δ: ppm, 400 MHz, D_2O) 4.46, 3.65, 3.65.

FT-IR (KBr): $\nu_{(O-H)}$ = 3451.3 cm^{-1}, $\nu_{(C=O)}$= 1745.1 cm^{-1}, $\nu_{(P=O)}$=1640.2 cm^{-1}.

2.3 Results and discussions

2.3.1 Synthesis and characterization of HPG

HPGs were synthesized through anionic ring opening polymerization of glycidol in the presence of alkoxides as described in Figure 2.2. According to the third and fourth steps of the mechanism, after the ring-opening propagation, intra- as well as intermolecular transfer steps result in the formation of primary alkoxides, which activates the propagation step in a new cycle. This polymerization manner leads to the final branching structure. Specifically, 1,1,1-Tris(hydroxylmethyl) propane (TMP) holding three -OH groups were used as an initiator and partially deprotonated (10%) with potassium methoxide. This is essential to control the concentration of active sites on the initiator, enabling the chain ends to grow simultaneously and thus achieve the desired molecular weight (Mn = 20,000) and considerably quite narrow Đ (1.25) as shown in Figure 2.3. In the consequent propagation step the monomer glycidol was added dropwise over a period of 12 h using syringe pump to achieve homogeneous and moderate polymerization. The relatively slow monomer addition condition leads to the control of the number-average molecular weight as well as low dispersity. In addition, according to Sunder *et al*., the use of 10% deprotonated TMP is able to minimize undesired cyclization within the polymer. The controlled polymerization process enables the growing macromolecule to exclusively react with the monomer, resulting in a colorless hyperbranched glycerol. Methanol was eventually added to quench the “living” growth of HPG, followed by water dialysis to remove any low Mw fraction, achieving a lowered polydispersity.

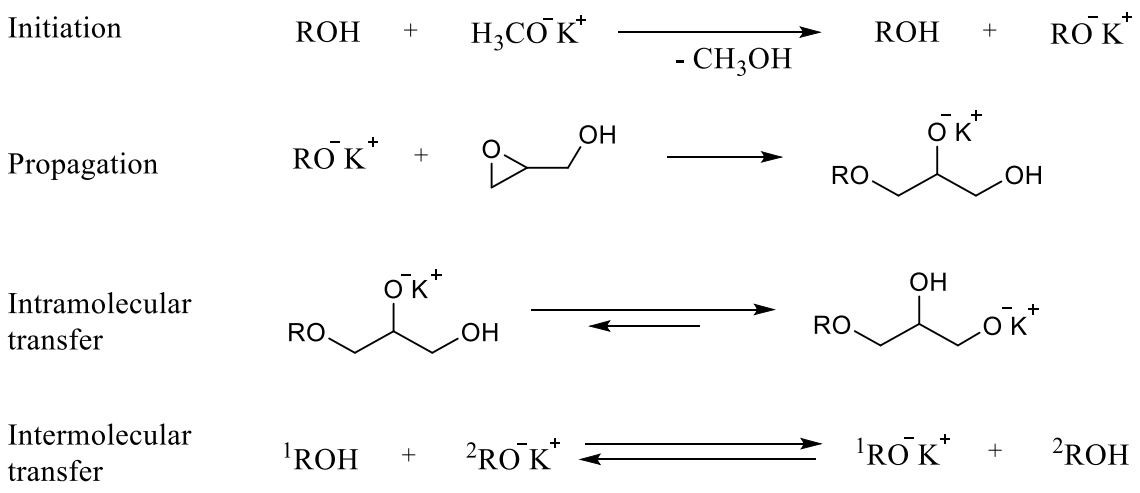

Figure 2.2. Mechanism of ring opening multibranching polymerization (ROMP).

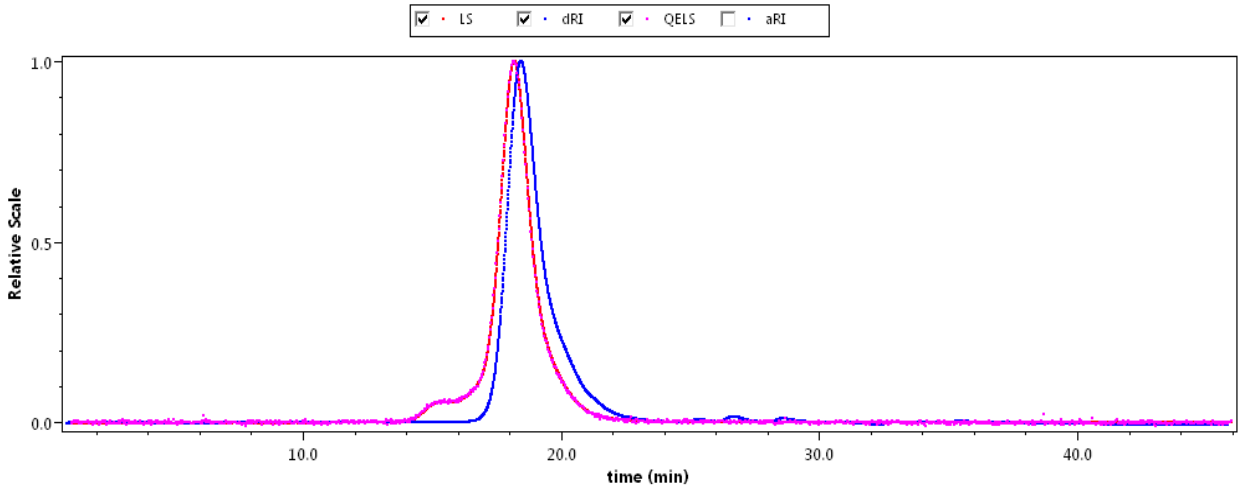

Figure 2.3. GPC of representative HPG macromolecule (Mn = 2.0 × 10^4 Da, Đ = 1.2). Signal intensity in red was measured by light scattering (LS) at 90 degree, which is in combination with concentration sensitive refractive index detection dRI in blue to determine molecular weight.

The resulting structure of the branched polyglycerol possesses three types of methylene and methine units: dendritic, linear and terminal, which are reflected in the ^{13}C NMR (Figure 2.5). Seven peaks were well-resolved and assigned between 60-80 ppm in accordance with different

positions in the polymeric structure. Compared to ^{13}C NMR, ^{1}H NMR spectra (Figure 2.4) provides less information. The four types of methylene and one methine protons of HPG present as a broad peak ranging from 3.5 to 4.0 ppm. The hydrogens of hydroxyl groups undergo proton exchange with the deuterium in D_2O, therefore are not shown on the spectrum.

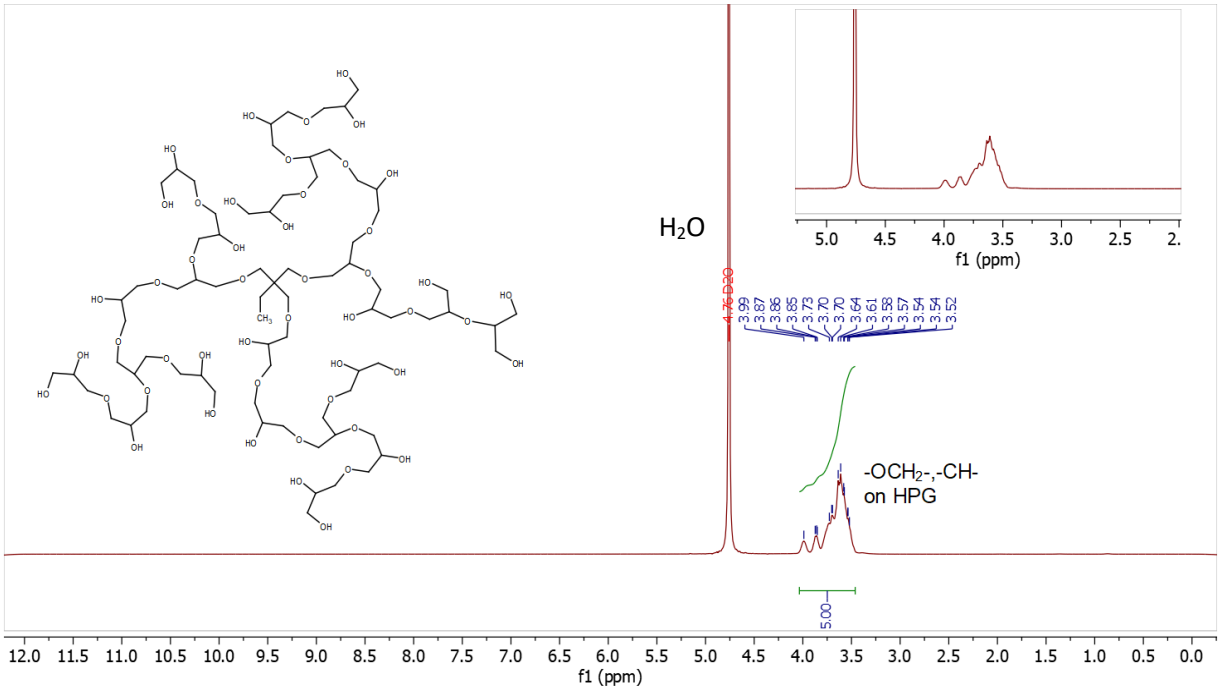

Figure 2.4. ^{1}H NMR spectrum of HPG in D_2O.

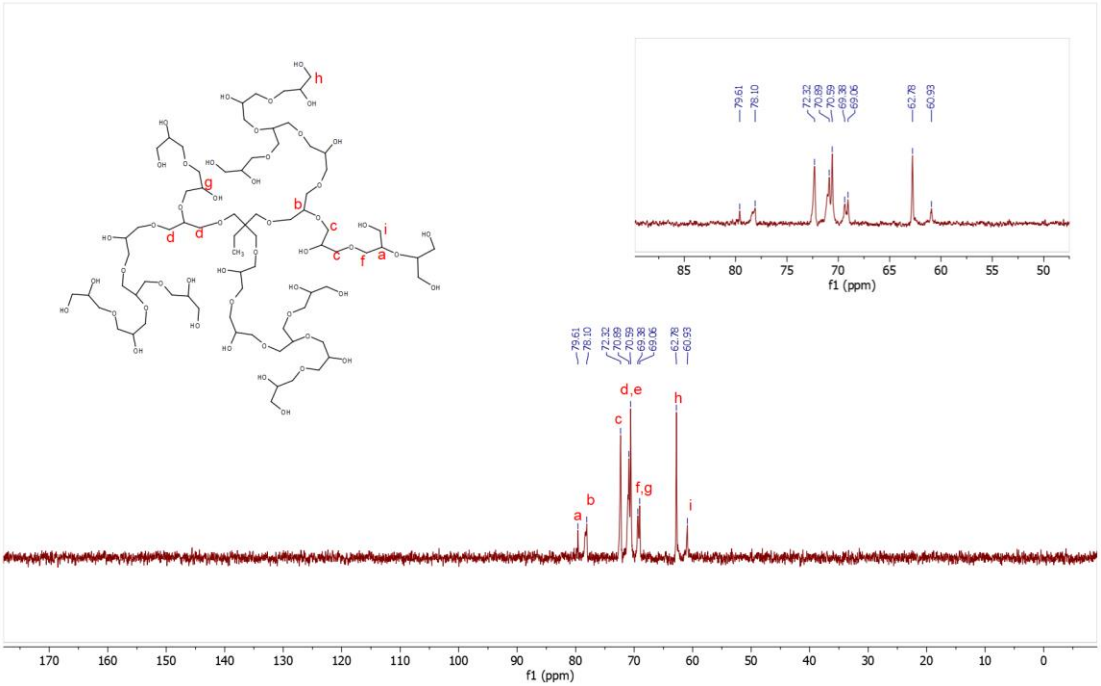

Figure 2.5. ^{13}C NMR spectrum of HPG in D_2O.

2.3.2 Synthesis and characterization of 5-azidovaleric acid

The linker, 5-azidovoleric acid, bridging HPG and CP was generated from the bromic ester followed by hydrolysis in a basic medium. The primary alkyl halide of ethyl 5- bromovalerate was displaced by N_3^- with the presence of the azide salt, NaN_3, via an effective SN_2 nucleophilic reaction. The mixture of acetone/water (3:1) applied as reaction solvent, is mainly considered as a polar aprotic solvent that enables a SN_2 reaction to be carried out properly. The resulting intermediate, ethyl 5-azidovalerate was extracted, dried and then dissolved in MeOH/H_2O mixture to continue on hydrolysis of ethoxy group. The hydroxide source is provided by NaOH. Dilute HCl solution was added at the end to offer protons in excess to avoid the formation of the carboxylate salt containing sodium. The whole process was carried out efficiently, quickly and

without significant side reactions, resulting in a final yield of 96%. Figure 2.6 and Figure 2.7 present the ^{1}H NMR spectrum and ^{13}C spectrum respectively.

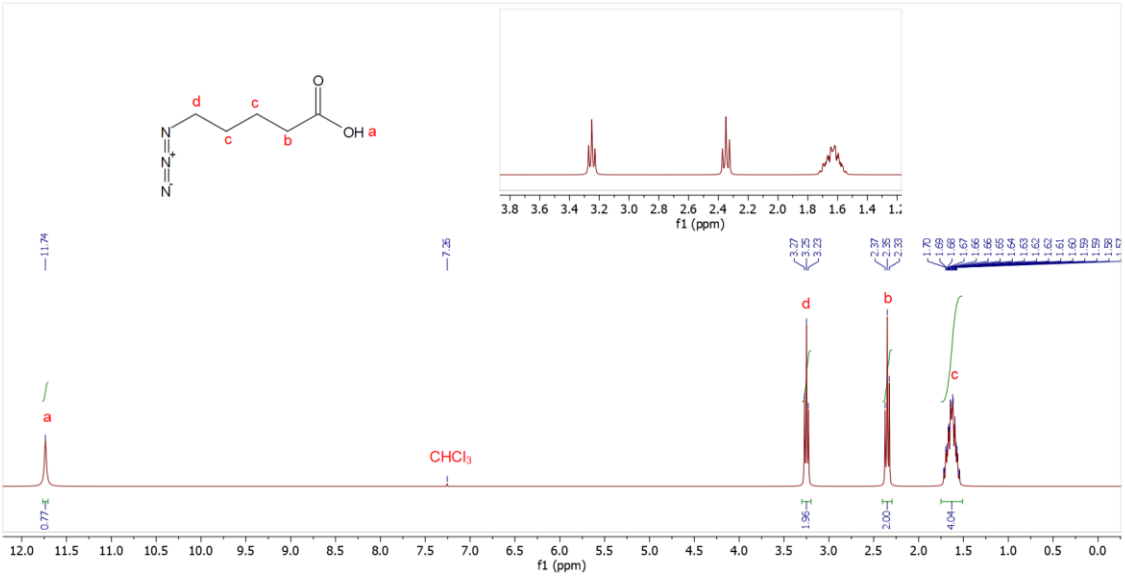

Figure 2.6. ^{1}H NMR spectrum of 5-azidovaleric acid in $CDCl_3$.

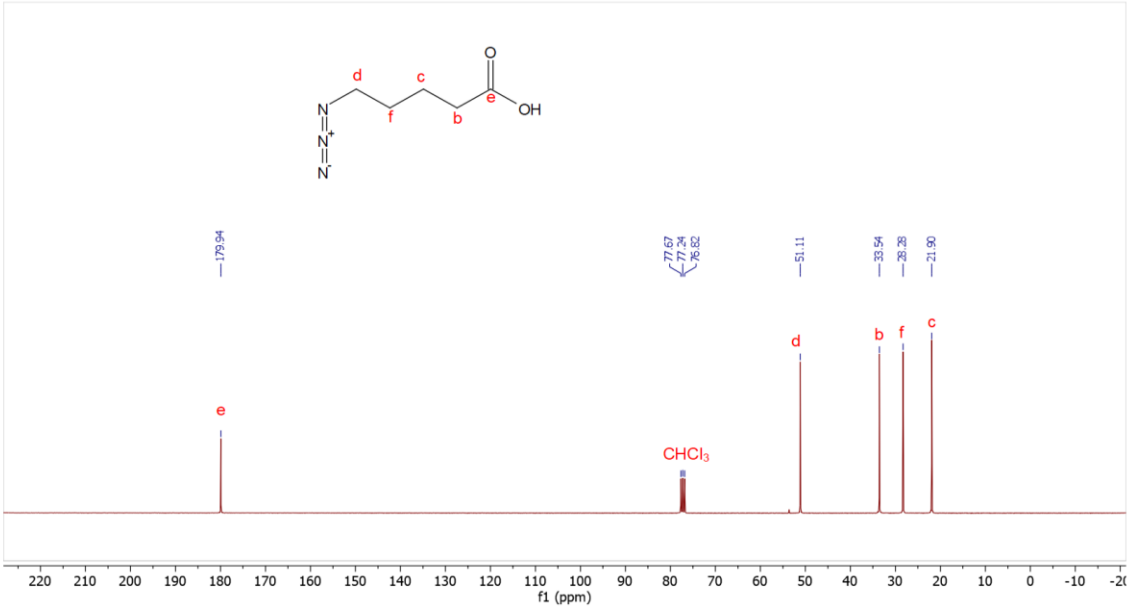

Figure 2.7. ^{1}C NMR spectrum of 5-azidovaleric acid in $CDCl_3$.

2.3.3 Synthesis and characterization of HPG-$N_{3(x)}$

The azido functionalized HPG was manufactured through esterification of hydroxyl groups by 5-azidovaleric acid prepared from the previous step. In order to carry out the Steglich esterification (R`OH + RCOOH = RCOOR`), a DIC/DMAP/DMF (solvent) system was employed as a common synthetic condition. DIC (N,N'-diisopropylcarbodiimide) and carboxylic acid together form an O-acylisourea intermediate, and then HPGs carrying -OH groups meet the activated 5-azidovaleric acid therefore forming the stable dipropylurea (DPU) and the desired ester. The addition of DMAP in excess is essential for the esterification to occur efficiently.[67]

In Figure 2.8, the chemical shifts (in ppm) corresponding to protons on HPG(20K)-$N_{3(15)}$ are all clearly assigned. Protons from the four-carbon azido spacer group demonstrate similar signal distribution compared to the original 5-azidovaleric acid, and the broad peak between 3.3 to 4.0 ppm is assigned to the protons from HPG backbone. The percentage of esterification was calculated based on comparing the integration of the protons at position b (Figure 2.8) and the protons on backbone of HPG. For instance, if every single hydroxy group undergoes functionalization with an azido linker, then the conversion will be 100% and the integration of HPG backbone and peak b should manifest a ratio of 5:2. Therefore by analyzing the ^{1}H NMR in Figure 2.8 specifically, around 7% -OH groups have been attached the linker after reaction, resulting in ~15 terminal azido groups.

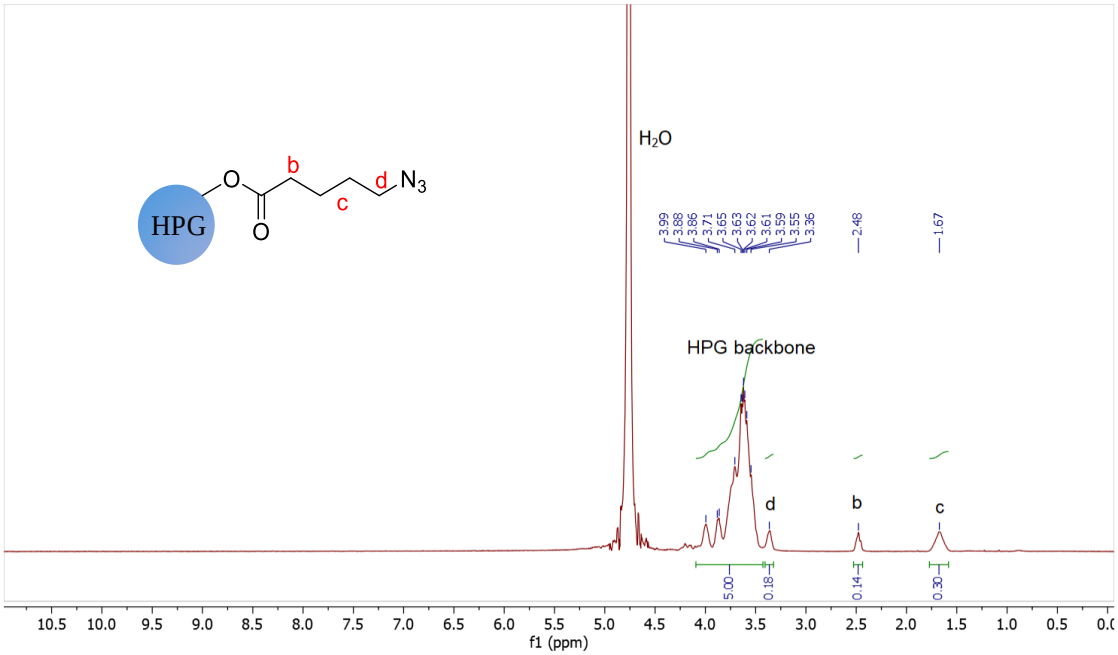

Figure 2.8. Representative ^{1}H NMR spectrum of HPG-$N_{3(x)}$ in D_2O. Ratio of the peak at 2.48 ppm, representing the protons at -C*H*$_2$C=O (indicated by *Italic H*), to protons on the HPG backbone is used to determine the percentage of functionalization.

As shown in Figure 2.9, ^{13}C NMR of azido functionalized HPG was obtained as well to confirm the structure. The septet around 48 ppm represents the solvent residual signals of deuterated methanol. Peaks located between 63 and 79 ppm correspond to the carbons on the HPG backbone. The rest of the carbon signals from 21 to 51 ppm distribute around in the manner similar to the ^{13}C NMR of 5-azidovaleric acid and are clearly assigned in the spectrum.

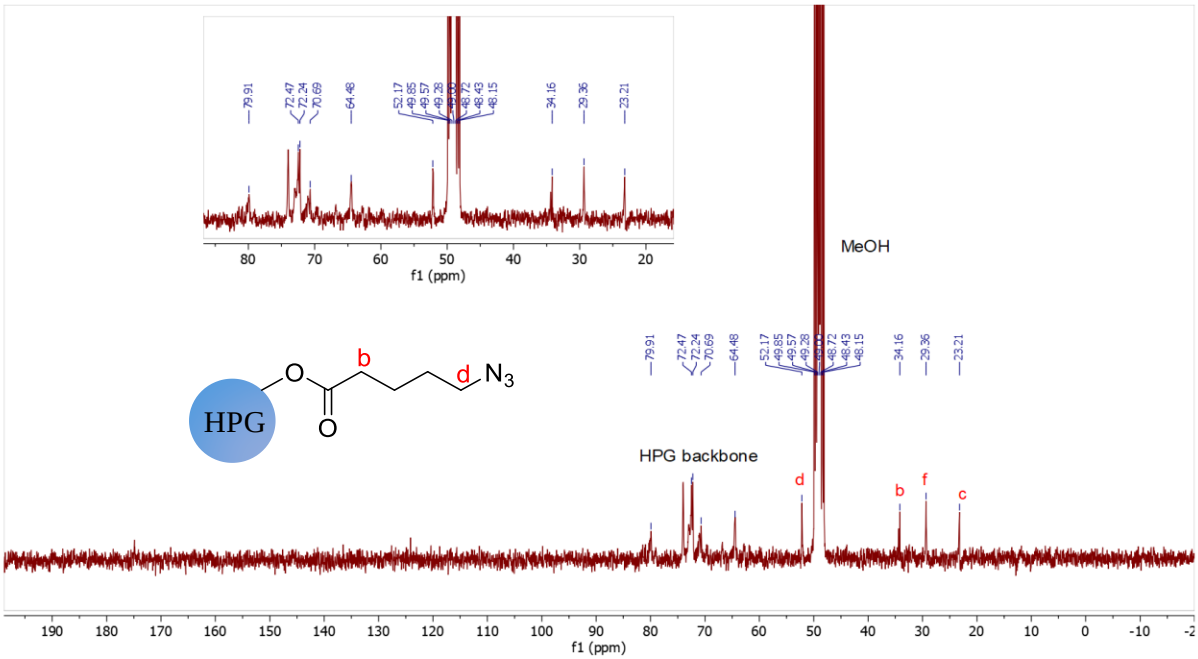

Figure 2.9. Representative ^{13}C NMR of HPG-$N_{3(x)}$ conjugate in MeOH-d_4.

2.3.4 Preparation and characterization of cationic headgroup: choline phosphate (CP)

The choline phosphate was prepared through a two-step synthetic pathway. In part I, the quaternary ammonium salt, 2-hydroxyethyl-N,N-dimethylprop-2-yn-1-aminium bromide was produced via the alkylation of 3-dimethylamino-1-propyne (a tertiary amine) by 2-bromoethanol. Here, the amine N from the tertiary ammonium starting material acts as the nucleophile and attacks the electrophilic C on 2-bromoethanol, forming the new C–N bond and bromide counterion. The polarity of the formed quaternary ammonium salt is quite high compared to the starting materials, which can precipitate out in THF and be easily collected, resulting in relatively high yield (87%) of product. ^{1}H NMR spectra and ^{13}C NMR spectra are shown in Figure 2.10 and Figure 2.11 respectively.

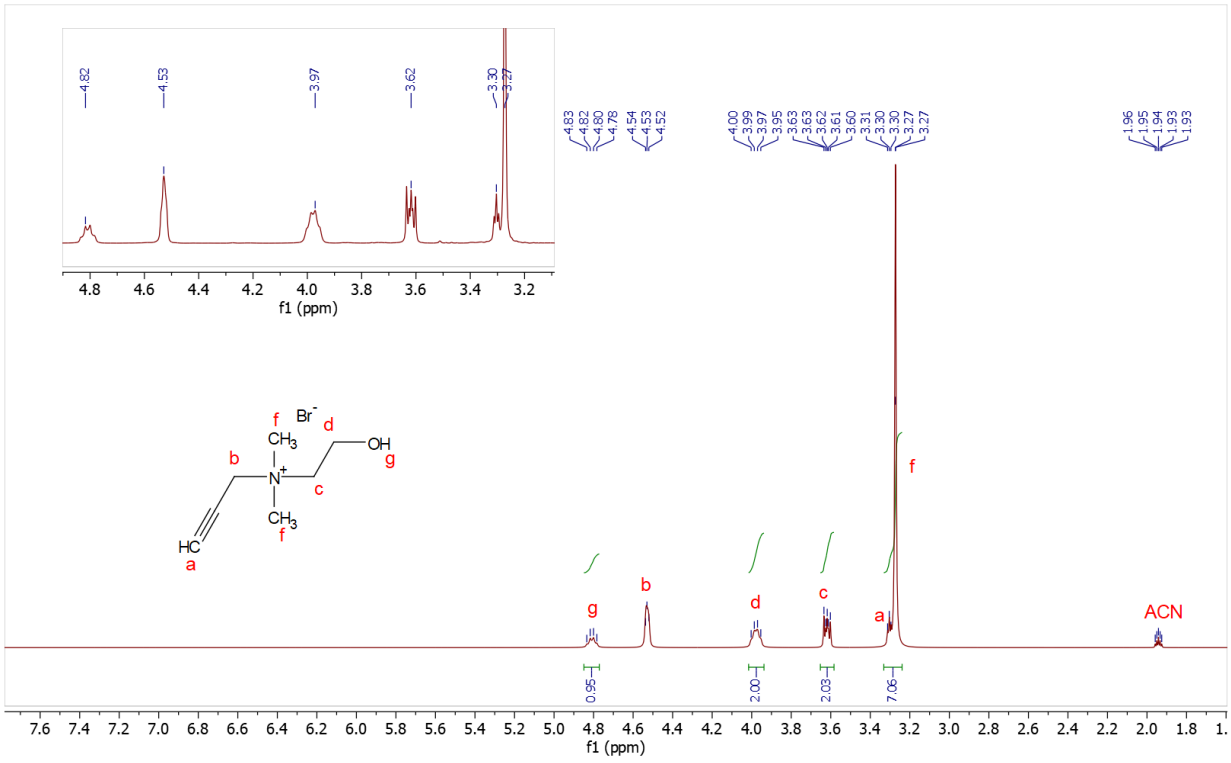

Figure 2.10. ^{1}H NMR of N-(2-hydroxyethyl)-N,N-dimethylprop-2-yn-1-aminium bromide in acetonitrile-d$_3$.

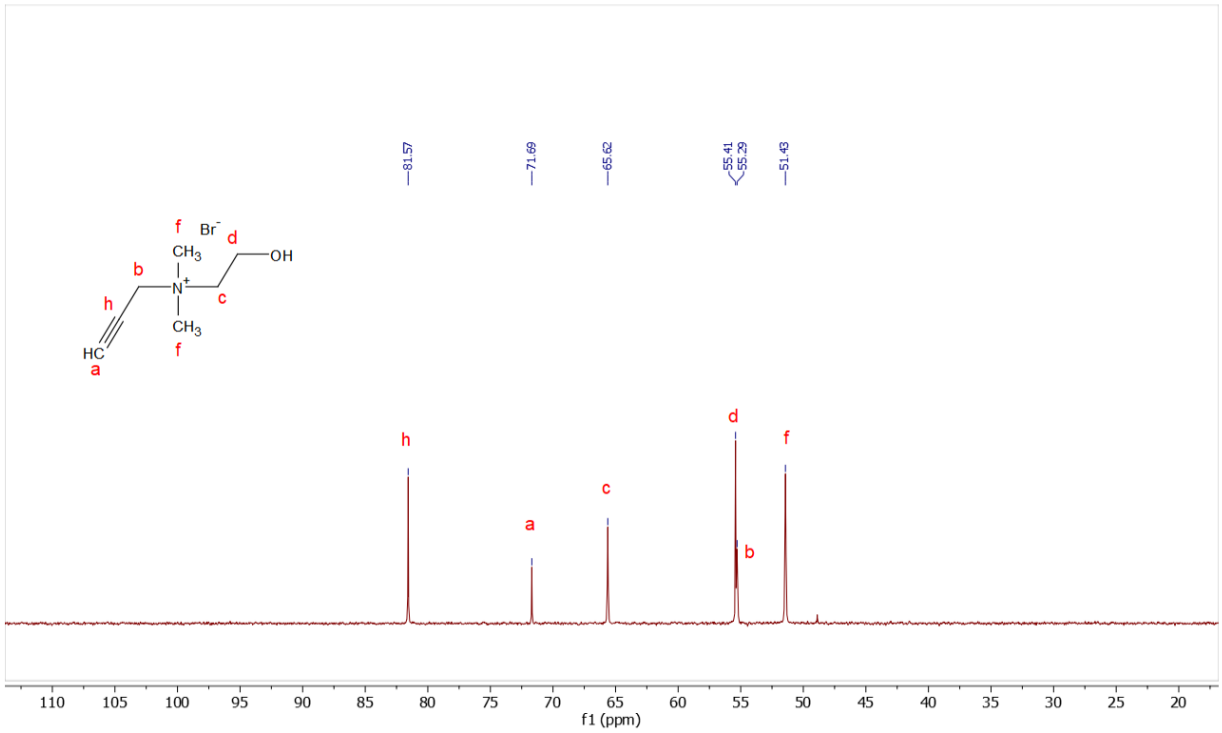

Figure 2.11. ^{13}C NMR of N-(2-hydroxyethyl)-N,N-dimethylprop-2-yn-1-aminium bromide in acetonitrile-d$_3$.

In the second step of CP preparation, acetonitrile was chosen as the reaction solvent according to the solubility difference between the quaternary ammonium salt formed after part I and CP. Pyridine was employed as the organic base to attract the free HCl produced due to the SN2 nucleophilic attack to neutralize the reaction. TLC analysis was utilized to monitor throughout the reaction to detect if a complete conversion was achieved. The bottom layer containing CP and pyridinium chloride was separated and washed to get rid of any unreacted starting materials, with a minimum exposure to moisture in case of any hydrolysis. The successful formation of CP was confirmed by running LC-MS. As shown in Figure 2.13, the peak fragmentation observed at 236 (m/z) manifests the existence of the positively charged CP, and the mass percentage was estimated by automatically integrating peaks on LC chromatogram spectra obtained in full scan mode (LC ES-API, Pos, Frag: 70). The ^{1}H NMR of the product mixture is given in Figure 2.12, where the desired CP compound and side products were both briefly defined on the spectrum. The product was used without further purification due to inefficient separation between the charged salts with similar polarity. However, the impurities did not participate in the following-step reaction, and could be easily removed by dialysis.

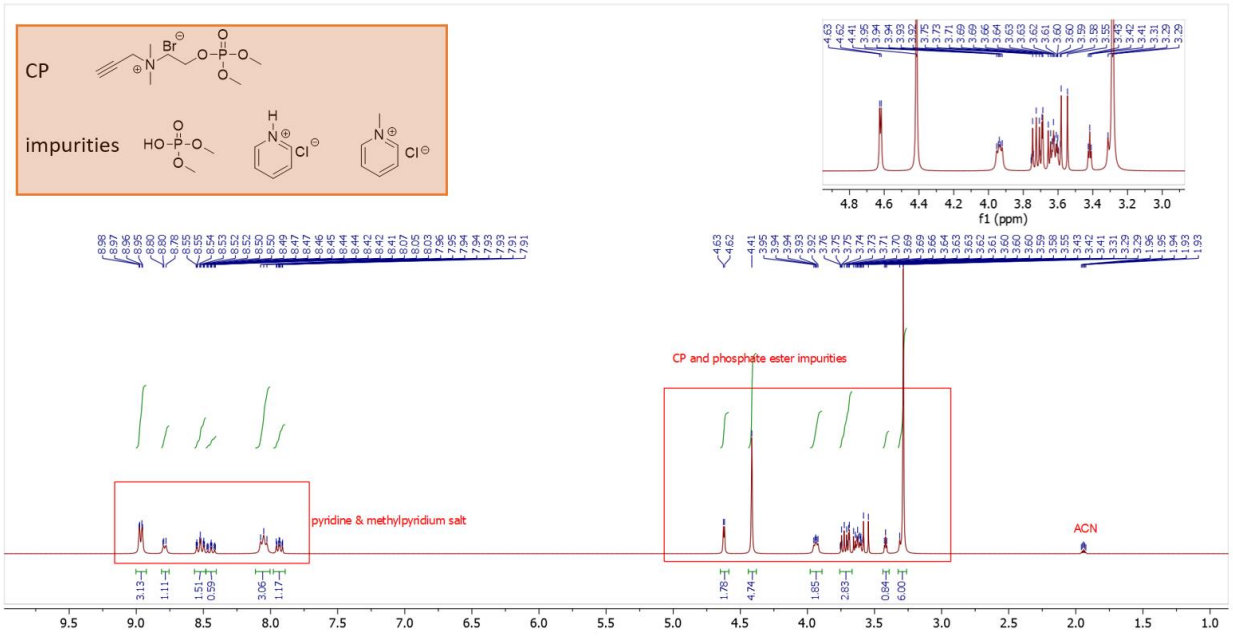

Figure 2.12 ^{1}H NMR of synthesized CP and side products in acetonitrile-d3.

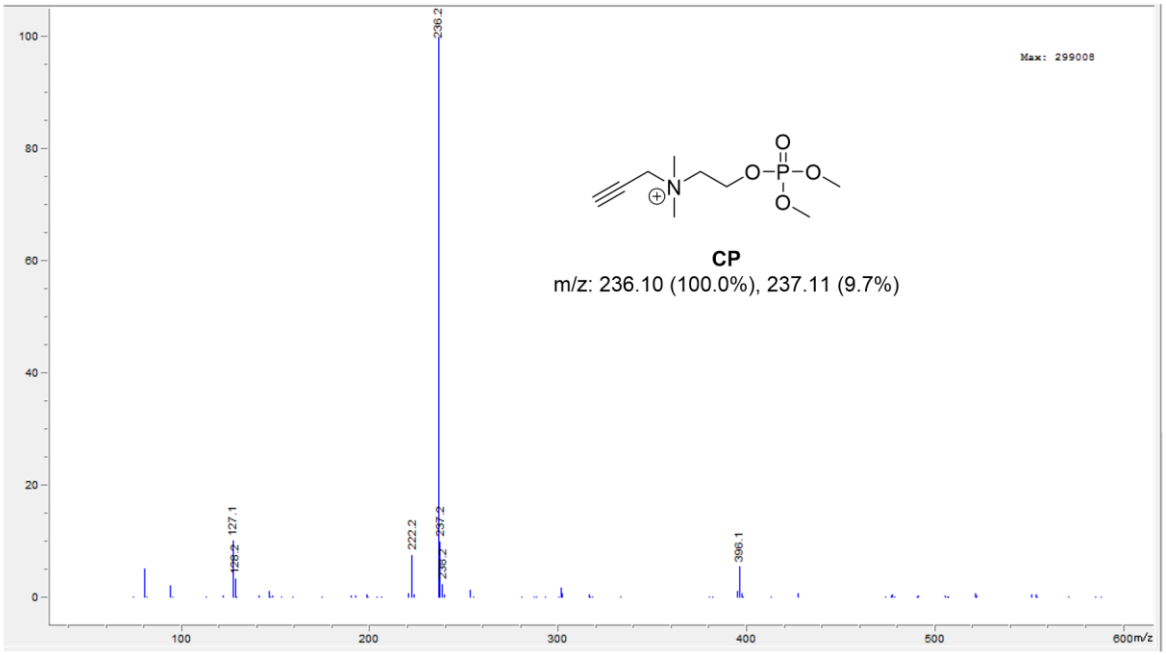

Figure 2.13. ES-API evidence of formation of CP in the product mixture. The literature m/z value of *N*-(2((dimethoxyphosphoryl)oxy)ethyl)-*N*,*N*-dimethylprop-2-yn-1-aminium (positively charged CP) is 236.1, which is consistent with the mass fragmentation shown in the spectrum, confirming that CP exists.

2.3.5 Chemistry and structure of HPG-Zwitterionic macromolecules

In this research study, the azido-carrying HPG was further modified with different numbers of cationic CP bearing terminal alkyne through a CuAAC "click" reaction. In order to avoid exposure of any free azido groups at the terminal site of HPG, an excess of CP components was added in the reaction to achieve a complete conversion into triazole. The feeding ratios of the cationic CP to the available azido group is commonly controlled around 5:1, which is also subject to the mass percentage of CP present in the product mixture obtained from the previous step. Copper^{I} bromide employed as the catalyst for the azide-alkyne cycloaddition was protected by the triamine ligand PMDETA due to the well-established efficiency of the CuBr/PMDETA system in polymerization processes. In order to insure rapid "click" reactions, it is necessary to adjust the ratio of methanol and DMF used as the solvent mixture to solubilize both the Cu^{I} catalyst and the substrates. This is essential because a homogeneous reaction environment is able to offer opportunity for the two reactive groups to "meet" and access each other in the solution medium to achieve an efficient conversion. Typically, DMF has been reported to be an optimal solvent for the CuBr catalyst.[65] The ultimate goal of this study is to manufacture a zwitterionic material carried by HPG, therefore the final step includes substitution of the methoxyl attached to the phosphorus center with hydroxyl which is negatively charged at physiological pH. Hydrolysis is known to take place rapidly and completely with presence of catalyst, and acetic acid is one of the most generally used catalysts to create mild acidic conditions.[68] A period of 4 h reaction time allows for the nucleophilic attack of water **O** carried out initially at the **P** center of the phosphotriester, while exposure to acidic aqueous conditions for a longer time could result in cleavage at the methylenic carbon next to the oxygen bridging the quaternary amine and phosphate. Dialysis in water was finally applied to remove any impurities remaining in crude CP or after the "click" reaction. During

the first day of dialysis, EDTA was added into water to form strong chelator with Cu^{II} outside of the regenerated cellulose tube in order to rapidly remove the remaining copper from the product mixture.

The complete synthesis signifies that all the terminal azido groups on HPG transform to triazole. According to Figure 2.14, FT-IR was employed and discovered that the band labeled as **a** at 2101 cm^{-1}, representing the stretches of N=N=N on HPG-N_3, disappeared when observing the band distribution of HPG-CP, which indicates the successful conjugation of alkyne head groups with peripheral azide. Other featured stretching bands are also assigned to the relevant functional groups on the spectra for structure reference.

As shown in Figure 2.15, by assigning featured peaks on ^{1}H NMR and comparing their integrated values, we are able to conclude if the "click" reaction successfully took place, and that the degree of conjugation reached 100%. Compared to the ^{1}H NMR of HPG-N_3, the new peak emerged at 8.38 ppm represents the only proton belonging to -C***H*** (indicated by *Italics*) on the triazole ring, indicating the azide-alkyne "click" reaction was carried out successfully; due to the deshielding effect of triazole, protons on the two methylene groups closest to the azide on the spacer, together shifted downfield by 0.26 ppm and ~1.35 ppm, labeled as **c** and **d** respectively. Due to the overlaps between protons on HPG backbone and choline phosphate between 3.5-4.5 ppm, only a few peaks are able to give reliable integration information for the determination of the conjugation degree. Therefore, we decided to select the proton signal of triazole located at 8.38 ppm, along with the methylene signal at 2.43 ppm (which originally appears at 2.48 ppm on ^{1}H NMR of HPG-N_3) to compare their integrations, and a ratio of 1:2 manifests that the full conversion from HPG-N_3 to HPG-CP is achieved.

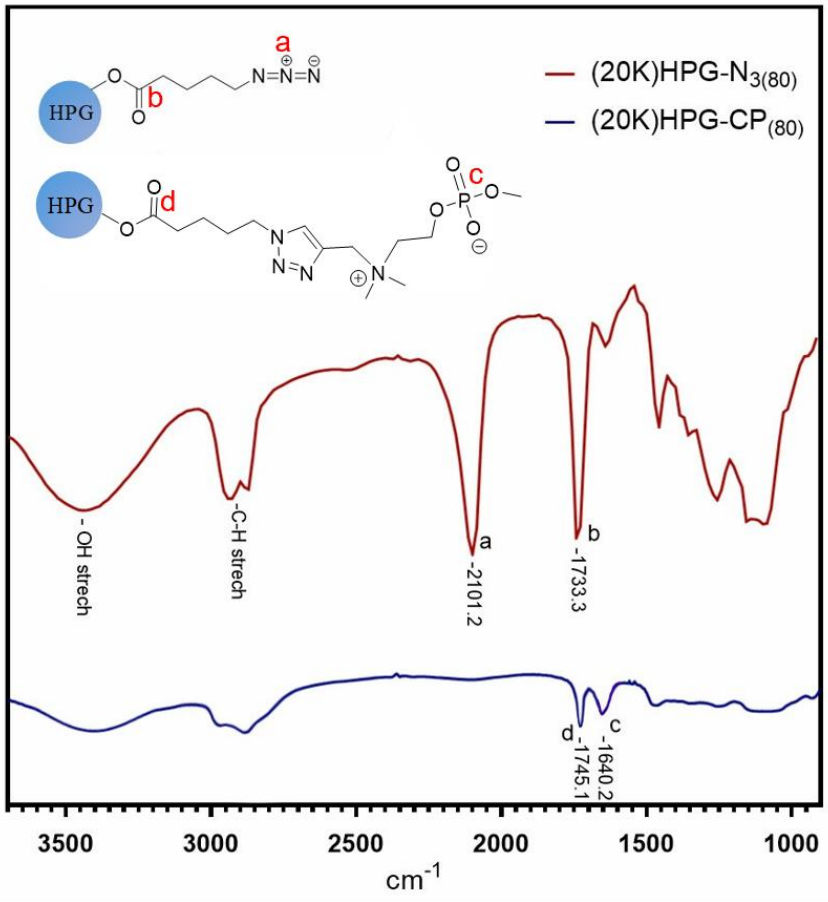

Figure 2.14. FT-IT spectrum of (20K)HPG-$N_{3(80)}$ and (20K)HPG-$CP_{(80)}$ in comparison. Both spectra were collected using KBr as background.

Figure 2.16 demonstrates the ^{13}C DEPT-135 NMR spectrum of (20K)HPG-$CP_{(80)}$, where CH_3 and CH show positive signals, and CH_2 groups display as negative peaks. Using the DEPT technique helps determine where the carbons of -***C***H_3 and -***C***H are located, which is more efficient, reliable and selective when assigning peaks for a macromolecule compared to other ^{13}C NMRs. Compared to the ^{13}C of HPG-N_3 (Figure 2.15), the carbon signal coming from HPG backbones and azido spacers remain around the same shift, and the newly introduced peaks of CP locate between 50-70 ppm. All peaks are assigned according to the carbons on the spectrum.

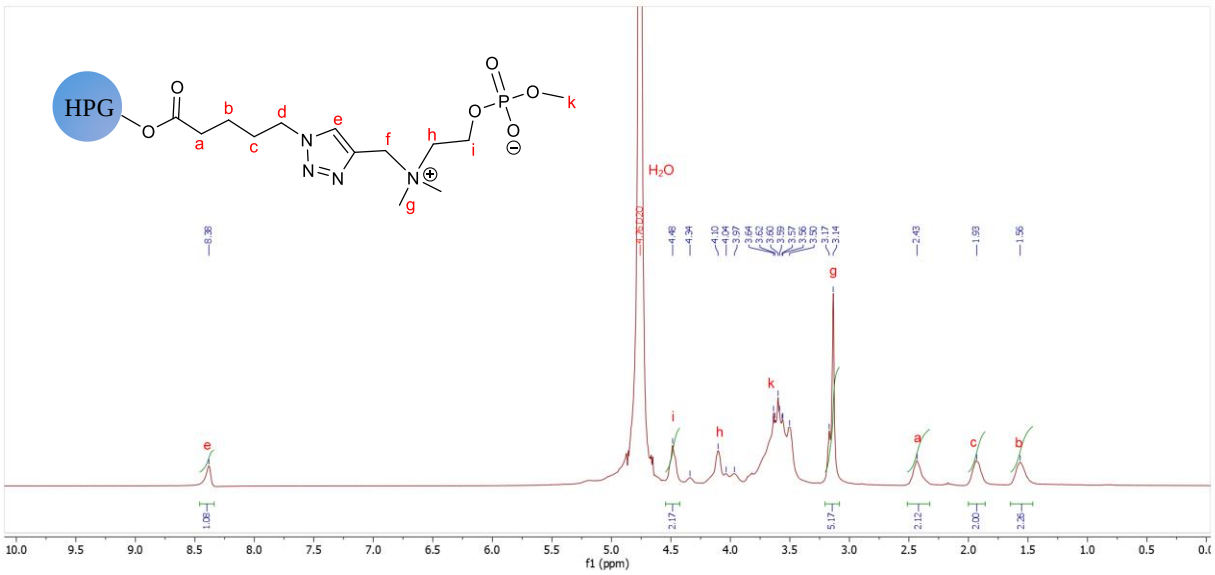

Figure 2.15. Representative ^{1}H NMR spectrum of zwitterionic HPG-CP in D_2O.

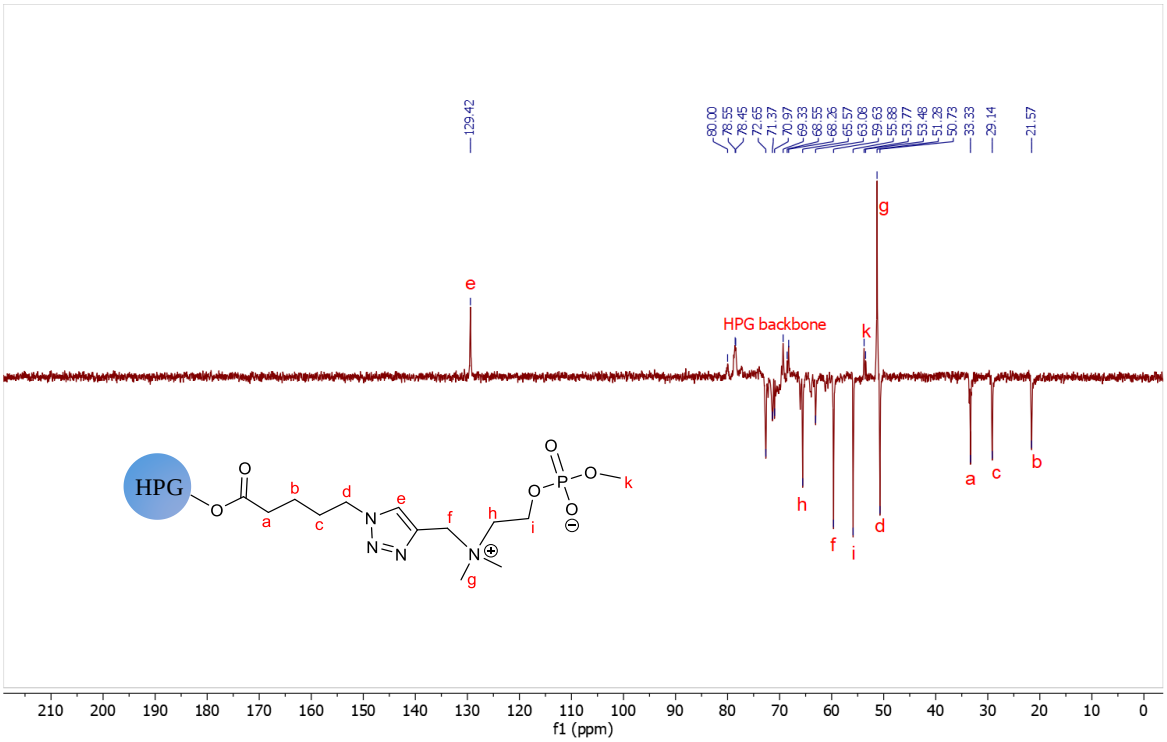

Figure 2.16. Representative ^{13}C NMR of Zwitterionic HPG-CP in D_2O.

Proton decoupled ^{31}P NMR (Figure 2.17) was applied to examine how many phosphorus centers existed in the final structure, which is directly affected by the degree of hydrolysis. The only peak appearing at 0.04 ppm indicates the reaction resulted in a singular phosphorus environment. Meanwhile, as shown in Figure 2.18, a ^{1}H-^{31}P HMBC NMR experiment was conducted to see if there exists any ^{1}H-^{31}P heteronuclear correlation, and where the proton signals locate on the ^{1}H NMR. The protons labeled as **k** and **i**, which are two bonds from ^{31}P are observed signals on the 2D spectrum, providing the structure information to confirm that pure zwitterionic HPG-CP formed as the result of hydrolysis.

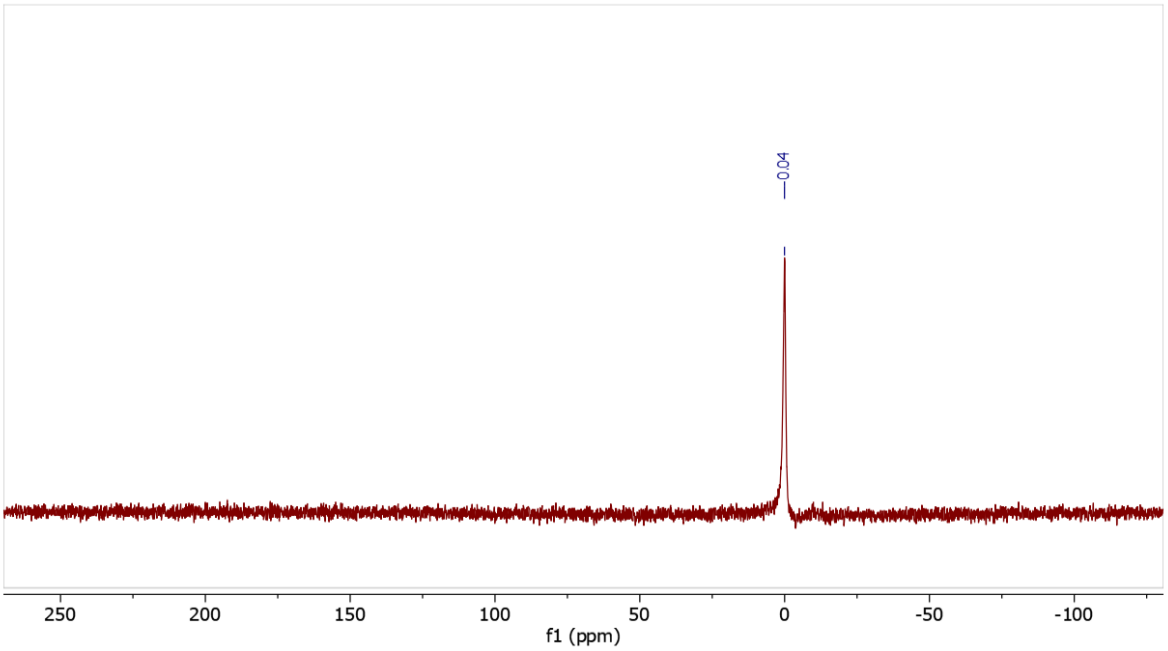

Figure 2.17. Representative ^{31}P NMR spectrum of zwitterionic HPG-CP in D_2O.

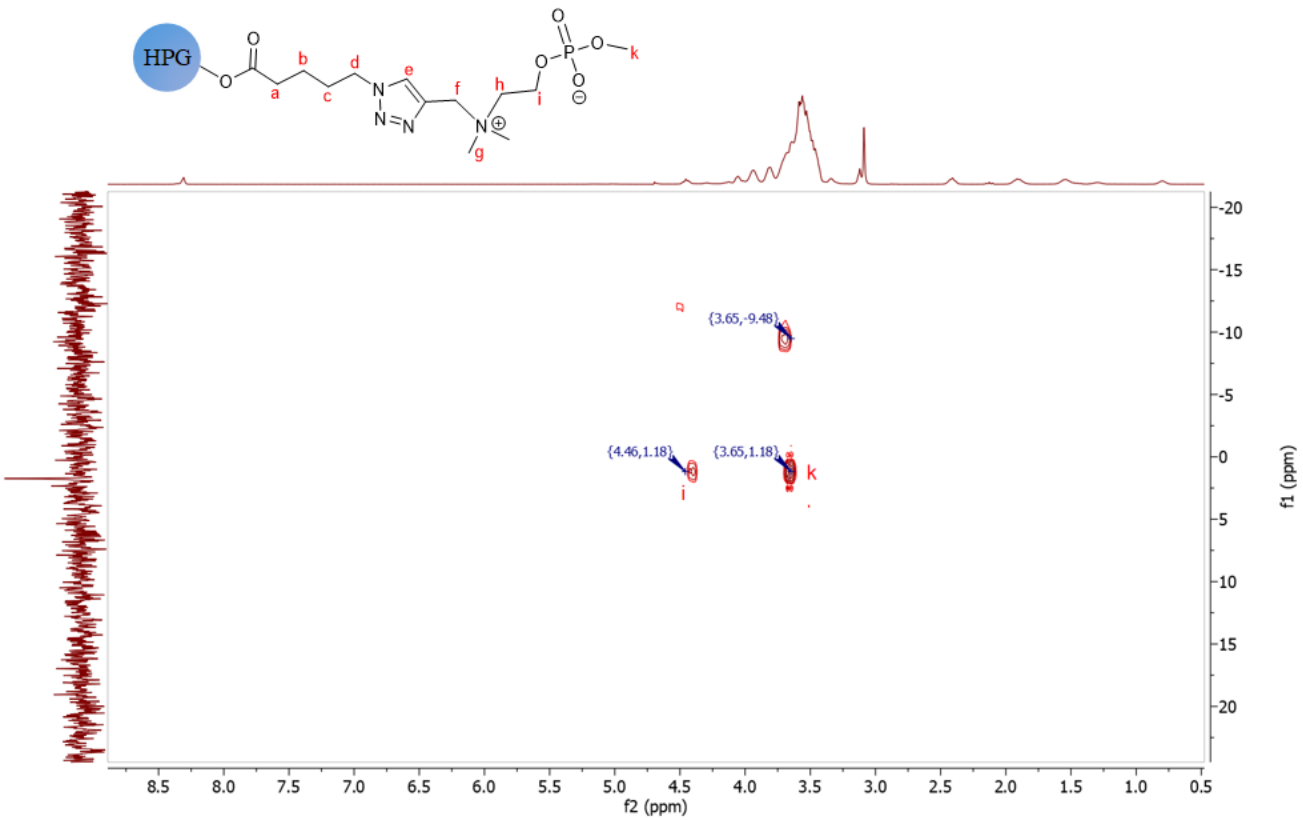

Figure 2.18. Representative ^{1}H-^{31}P HMBC NMR spectrum of zwitterionic HPG-CP in D_2O. f1 represents chemical shift of ^{31}P in ppm, f2 stands for the chemical shift of protons in ppm.

The GPC signals detected by light scattering (LS) of both native HPG and HPG-CP derivative were overlaid within a graph window to check if the molecular weight shifted, displayed as the shift in retention time. As demonstrated in figure 2.19, compared to the original HPG without any modification, CP decorated HPGs have shown decreased retention time, which signifies the increase in molecular weight. In terms of the two representative peak signals on graph, Mn of (20K)HPG-$CP_{(15)}$ was determined to be 29 kDa, after conjugating HPG (20 kDa) with 15 azido linkers and CP ligands. Molecular weight of other HPG derivatives were given in Table 2.1.

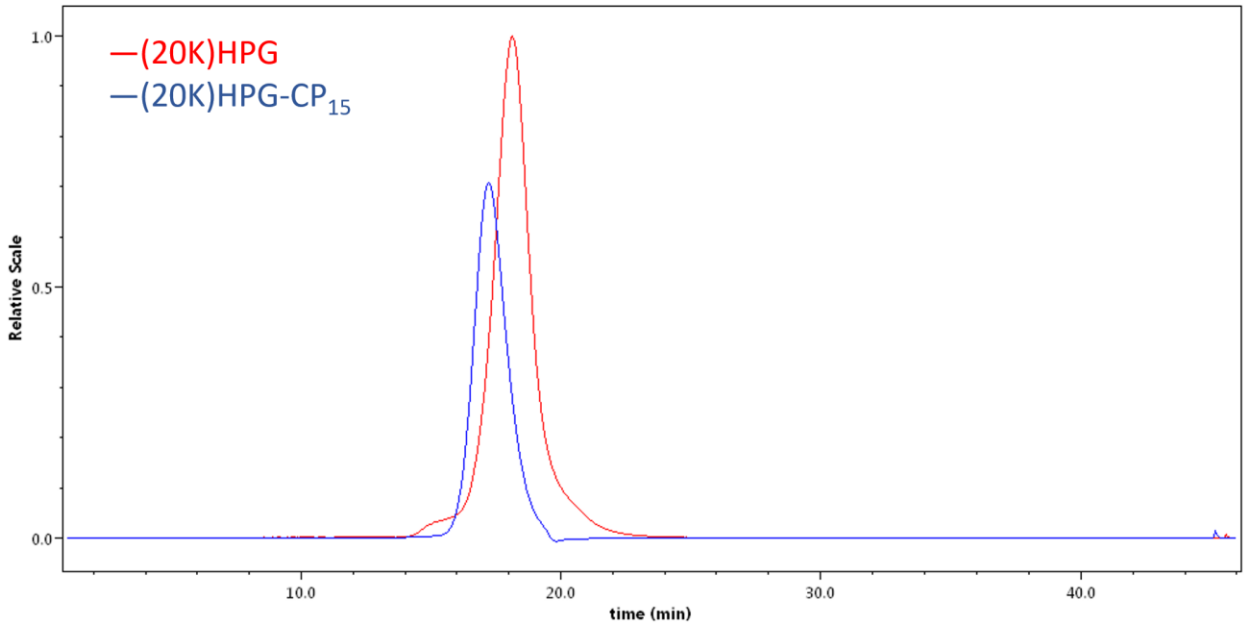

Figure 2.19. GPC of representative HPG (Mn = 2.0 × 10^4 Da, Đ = 1.2) and HPG-$CP_{(15)}$ (Mn = 2.9 × 10^4 Da, Đ = 1.2) macromolecule. Signal intensity in red was measured by light scattering (LS) at 90 degree.

The library consisting of 10 synthesized polymer structures was characterized and summarized in Table 2.1. The macromolecules are colloquially named as follows: (20K)HPG is the polymer which possesses a GPC based Mn around 20 kDa; HPG-$N_{3(15)}$ stands for the one that has 15 -OH groups converted to azido groups; HPG-$CP_{(15)}$ represents the HPG molecule holding 15 **C**holine **P**hosphate groups conjugated through the "click" reaction with the azide-containing linkers.

Table 2.1. Characteristics of HPGs and their derivatives.

Polymer	# CP [a]	Mw [a]	M_n [b]	Đ [b]	R_h (nm) [c]
(3K)HPG	NA	NA	3.2×10^3	1.2	1.4
(20K)HPG	NA	NA	2.0×10^4	1.2	2.7
(3K)HPG-$CP_{(3)}$	3	4.1×10^3	4.3×10^3	1.1	1.6
(20K)HPG-$CP_{(15)}$	15	2.5×10^4	2.9×10^4	1.2	3.1
(20K)HPG-$CP_{(30)}$	30	3.1×10^4	NA	NA	NA
(20K)HPG-$CP_{(50)}$	50	3.8×10^4	NA	NA	NA
(20K)HPG-$CP_{(80)}$	80	4.8×10^4	NA	NA	NA

[a] Calculated from ^{1}H NMR integration values

[b] Determined by GPC at 25 °C in 0.1N $NaNO_3$, not applicable to HPG conjugates over 30,000 Da.

[c] Obtained by dynamic light scattering (QELS) at 25 °C in 0.1N $NaNO_3$, not applicable to HPG conjugates over 30 kDa.

2.4 Summary

Through presenting a series of small-molecule synthesis and polymer modification, this section describes design of a novel HPG-based zwitterionic polymer conjugates. HPG with different molecular weights were made via an efficient one-pot reaction, followed by modification through esterification with freshly prepared 5-azidovaleric acid to achieve HPG-$N_{3(x)}$. This polymer containing different percentages of pendant azido linkers was then functionalized via a CuAAC "click" reaction with positively charged CP in excess. The critical zwitterionic structure was finalized by hydrolysis in acidic environment over controlled reaction time. The structure characterization of the library of polymer conjugates were analyzed and confirmed by variety of techniques, namely, GPC, 1D- and 2D-NMRs, FT-IR and LC-MS.

The synthesis template designed here particularly leads to the manufacture of CP decorated HPG. The decision to select a non-cyclic phosphate ester as starting material resulted in limited side reactions and improved yield (improved by ~30%) compared to previous studies. This zwitterionic polymer containing the “PC-inverse” headgroup is predicted to show bioadhesion and biocompatibility subject to the number density of CPs per macromolecule, which are further investigated and reported in Chapter 3.

Chapter 3: Physical property and *In Vitro* biological tests of functionalized HPG-CP material

3.1 Introduction

The synthesized HPG-CP macromolecules were expected to possess a hydrating property by binding water molecules, which is considered important for eliminating nonspecific protein adsorption to avoid biofouling.[69] Therefore, quantification of bound water on original and modified HPGs was determined by differential scanning calorimetry (DSC) to determine the average numbers of water bound to different functional groups. From the perspective of molecular architecture, CP-decorated HPGs perform effectively only when the net charge is neutral, and thus, zeta potential (ZP) tests estimating the surface potential, proportional to the surface charge at low potentials, were conducted in physiological saline to obtain a measure of the total charge distribution on the polymers. During ZP measurements, an electric filed is applied to the polymer solution accompanied by dynamic light scattering (DLS) to measure the sign and magnitude of the electrophoretic mobility (velocity per unit electric field strength) which provides a measure of the sign and magnitude of the surface charge on the polymer. A Malvern Zetasizer® which is able to join DLS and ZP detection, in combination with disposable polycarbonate cuvettes were used together as a popular option among members of our group to obtain the best ZP measurement results.[70]

HPG-CP is believed to achieve strong cell adhesion through CP-PC interactions applicable to all eukaryotic cells containing PC lipid head groups on the exterior of the cell membrane. Herein, the biomembrane adhesion properties of CP ligands were examined through analyzing the interaction with blood components including red blood cells (RBCs) and platelets. It is known that

blood aggregates can be observed under digital high-power light microscopy as a result of cell-cell interactions not produced by induced coagulation when CP carried by spherical HPG adsorbs to the erythrocytes at different sites in a bridging conformation (Figure 3.1). In this way, RBC aggregation, as well as activation and aggregation of platelets, were evaluated in the presence of native HPGs, azido linker attached HPGs and CP modified HPGs. It is assumed that HPGs and HPG-N_3 show low inherent binding to cells since they do not cause visible aggregation, while HPG-CP demonstrates interactions with RBC membranes which are capable of causing cell aggregation in a manner depending on concentration and number density of CP ligands.

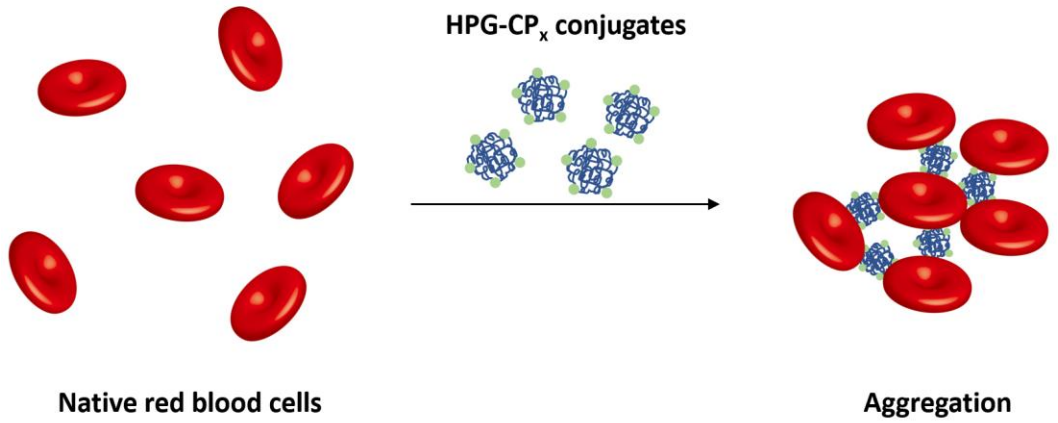

Figure 3.1. Illustration of cellular aggregation caused by zwitterionic HPG-CP$_x$ conjugates. The material acts as a bridge that adsorbs RBCs at different sites with CP ligands available.

In order to develop applications of HPG-CPs to broader biological fields, safety and feasibility of polymer conjugates for potential tissue engineering applications have to be considered. Hemolysis and cytotoxicity tests were selected to study if disruption of a cell moiety or lysis of RBC membranes occurs due to some unrecognized toxicity or bioincompatibility of the synthesized polymers.

Being established that the electrostatic force driving "PC-CP" adhesion is applicable to eukaryotic membrane rich in PC lipids, including red blood corpuscles which takes up 40% ~ 50% of blood's volume, HPG-CPs are considered as potential hemostatic agents which are able to strongly adhere to the cell surfaces, and physically create a barrier to hemorrhage. Compared to fibrin-derived hemostatic material and the positively charged agents developed in the absence of delicate charge neutralization, HPG bearing CP groups is here shown to be a readily synthesized, low-cost polymer which is expected to manifest low cytotoxicity through adjusting the binding affinity. Chapter 3 describes relevant experiments to investigate and analyze the properties of HPG-CPs.

3.2 Experimental section

3.2.1 Material

The HPG conjugates used for study were synthesized as described in Chapter 2. Freshly drawn venous blood samples from consenting healthy human donors (blood type was not controlled) were collected using plastic tubes containing sodium citrate, and applied for all blood related tests, following the policy and approval of the UBC Clinical Ethics Committee for work involving human blood. Phosphate buffered saline (PBS, 0.01M) used for mimicking human physical conditions, was prepared by dissolving one PBS tablet (ordered from Sigma-Aldrich, Oakville ON) in 200 mL double deionized water purified by a Milli-Q Plus water purification system (Millipore Corp., Bedford, MA). Physiological saline solution was made by dissolving NaCl in water to achieve a final concentration of 0.15 M. Platelet-rich plasma (PRP) was obtained by spinning citrated blood in an Algebra X-22R Centrifuge (Beckman Coulter) at 200 xg for 15 min at room temperature (22 °C) to sediment RBCs and white cells; the supernatant PRP was

removed by pipetting. Platelet-poor plasma (PPP) was prepared by centrifuging PRP in a Platelet Function Centrifuge (Bio/Data Corporation) for 10 min. ADP used was a lyophilized preparation of adenosine-5'-diphosphate with a concentration of 1.8×10^{-4} M. The system employed to measure aggregation was a Platelet Aggregation Profiler (Model PAP-8E) manufactured by Bio/Data Corporation. Human fibroblasts were ordered from Cedarlane Laboratories (Burlington, ON).

3.2.2 Zeta potential test

The density of surface charge was inferred by measuring zeta potentials of the HPG conjugates dispersed in 0.15 M saline solution at pH 7. HPGs with or without CP ligands attached were first prepared as 1mg/mL solutions, followed by loading 1 mL into the disposable folded capillary zeta cell (DTS 1070). The cassette was then placed in the zetameter (Zetasizer Nano ZS, Malvern Instruments, UK) which uses dynamic light scattering (DLS) combined with an applied electric field for the measurement of zeta potentials for macromolecules. Each test was run in triplicate for two trials to guarantee the centralized distribution of the data. The calculated average zeta potential values of each tested HPG polymer were reported.

3.2.3 Quantification of bound water of polymers

The hydration properties of polymeric materials were determined by measuring ice-water fusion enthalpy via a Q2100 differential scanning calorimeter (DSC) from TA Instruments (New Castle, DE). The polymers were all dissolved in deionized water and prepared as 5 (w/w) % concentrations. Twenty microlitres of each polymer was pipetted into a Tzero pan and weighed by difference using a balance from a thermogravimetric analysis (TGA) instrument (TGA Q500, TA

instrument, New Castle, DE). All the pans were equipped with Tzero hermetic lids and sealed by using a die set. An empty pan was used as the reference. The protocol followed was adapted from work published by our group.[71] Basically, the DSC was cooled down to -30 °C and left isothermally for 10 minutes. The temperature was gradually increased to -10 °C at a rate of 1 °C/min; the scanning was then conducted from -10 °C to 6 °C at 0.2 °C/min, and finally to 25 °C at 1°C/min. The fusion enthalpy (ΔH_p) was evaluated from the peak integral at negative temperatures around 0 °C from the TA Universal Analysis Software.

The number of water molecules bound to each polymer (*N*) was calculated from the equation as follows[20,88]:

$$N = \frac{\Delta H_0 \left(1 - C_p\right) - \Delta H_p}{M_{H_2O} \Delta H_0 C_P} \cdot Mw \qquad \text{(Eq. 3.1)}$$

where ΔH_0 is the fusion enthalpy of deionized water, C_p stands for the weight percentage of each tested polymer, ΔH_p is the fusion enthalpy of free water in the polymer solution, M_{H_2O} is the molecular weight of water and *Mw* represents the molecular weight of the polymer samples determined by ^{1}H-NMR.

3.2.4 Blood test

3.2.4.1 Red blood cell aggregation

The RBC aggregation test was conducted using both whole blood and washed erythrocytes freshly drawn from volunteers and stored in 3.8% sodium citrated tubes (BD Vacutainer™). The experimental method previously published by our lab[39] was followed for RBC aggregation tests in whole blood. Specifically, 10 µL of HPG/HPG-CP stock solution (50 mg/mL or 10 mg/mL) was

first transferred into a 1.5 mL Eppendorf tube, followed by transferring 90 µL of whole blood using a micropipette to achieve a final concentration of 5 mg/mL or 1 mg/mL polymer/blood mixture. PBS used as a negative control was mixed with whole blood following the same addition ratio. In order to homogenize the distribution of polymer material, up- and down-aspirations were performed using the same micropipette for blood transfer. The prepared sample mixtures were then incubated in a thermostatic water bath at 37 °C for 5 min. After incubation, polymer/plasma and RBCs were separated by centrifugation (Model 5415D, Eppendorf, Germany) at 8000 rpm for 3 min to obtain two layers. To observe the aggregation performance, 2 µL of the red blood cells (bottom layer) were resuspended and mixed with 6 µL of supernatant on a wet mounted slide, and examined by bright field light microscopy (Zeiss Axioskop 2plus) under 40x magnification, where the images were captured via a digital microscope camera (AxioCam ICc 1, Carl Zeiss Microimaging Inc) connected to a desktop computer.

The aggregation test was also conducted on washed red blood cells by treating stored citrated whole blood. Two milliliters of whole blood and 6 mL of PBS were added into a 15 mL polypropylene centrifuge tube and inverted gently to mix. The blood/buffer mixture was centrifuged at 1000g for 5 min. The washing process was repeated 3 times, replacing the supernatant with new PBS after each centrifuge cycle. One eighty microliter washed red blood cell aliquot was then mixed with 20 µL of polymer solution or PBS, and tested for aggregation following the same operating procedure applied to whole blood.

3.2.4.2 Hemolysis test

The hemolysis assay was used to determine the hemolytic effect of the manufactured polymers at different concentrations. The protocol carried out was based on and modified from

previous references[72], assessed as follows. Whole blood drawn into a 4.5 mL citrated tube was centrifuged at 1000 g for 5 min to remove the platelet and plasma. After the removal of supernatant, the hematocrit of the bottom layer was measured using a Sysmex XN-550 automated hematology analyzer (ON, CA) and diluted to 10% v/v using PBS.

A 360 µL aliquot of the resulting 10% v/v RBCs was added to 40 µL of stock polymer solution (both 50 mg/mL and 10 mg/mL) in 1.5 mL Eppendorf tube to make the final test material concentrations of 5 mg/mL and 1 mg/mL. Deionized water and PBS used as positive and negative controls were prepared in the same way. The RBC/polymer mixture was incubated at 37 °C for 1 h, and then centrifuged at 900 g for 10 min to settle RBCs. One hundred and fifty microliters of each supernatant was transferred into a 96-well plate, and the release of hemoglobin was measured with a spectrophotometer (SpectraMac190 Plate Reader CA, US) with wavelength setting at 540 nm. The hemocompatible nature of polymers was assessed by calculating the percent hemolysis based on the formula shown below:

$$Hemolysis\ \% = \frac{Abs_{540,test\ sample} - Abs_{540,PBS}}{Abs_{540,water} - Abs_{540,PBS}} \times 100\% \qquad \text{(Eq. 3.2)}$$

3.2.4.3 Platelet aggregation test

Aggregation of plasma-rich platelets was detected by light transmission using a platelet aggregometer (Platelet Aggregation Profiler PAP-8E, PA, US) set on “ADP” mode within 4 hours of specimen collection. A maximum of 8 test tubes equipped with stir bars were first prepared and placed into the incubation well. The blank sample was obtained by pipetting 0.250 mL platelet poor plasma (PPP) into a tube with no stir bar added. Each of the prewarmed test tubes was then filled with 0.225 mL of the sample platelet rich plasma (PRP), followed by incubation at 37 °C for

another 2 min. The 100% baseline was set via placing the blank (PPP) into the Test Well one by one ahead of running any PRP samples. Aliquots of 0.025 mL HPG/HPG conjugate material were directly added into the PRP, immediately followed by pressing the "inject" button to allow the test run for pre-set 10 min. Adenosine diphosphate (ADP) with a concentration of 2×10^{-5} M was used as a positive control. Primary Aggregation (PA) values representing the final aggregation in normal patterns were obtained from the program. Six synthesized HPG/HPG conjugates were finally prepared and tested at two concentrations, 5 mg/mL and 1 mg/mL.

3.2.4.4 Platelet activation test

The level of P-selectin or CD62P, a glycoprotein expressed on the surfaces of platelets upon activation, is used as a marker for the platelet activation. Specifically, the three tested concentrations (0.2 mg/mL, 0.5 mg/mL and 1 mg/mL) of each polymer sample were obtained by mixing 90 µL of PRP and 10 µL of HPG/HPG conjugate stock solutions which were prepared in 2 mg/mL, 5 mg/mL and 10 mg/mL respectively. The polymer/platelet mixtures were then incubated at 37 °C for 1 h, followed by transferring an aliquot of 5 µL from each sample into 45 µL PBS buffer with 5 µL of anti-CD62-PE added as fluorescent labeled antibodies. The final mixtures were further incubated for 20 min in the dark at room temperature. After the incubation was completed, another 300 µL of PBS buffer was added to each sample mixture. Meanwhile, a flow cytometer (model: BD FACSCanto II) was set up to measure the degree of platelet activation referred to their individual light scattering profile. The detected fluorescence of the marker CD62-PE was reported as the number of fluorescing platelets as a percentage of the total population determined from light scattering describe the degree of platelet activation. Data was obtained from two donors with each test being performed twice.

3.2.5 Cytotoxicity evaluation

Cell viability was assessed in BJ human fibroblasts using the (3-(4,5-dimethylthiazol-2-yl)-2,5-diphenyltetrazolium bromide) tetrazolium reduction (MTT) assay. Human fibroblasts were seeded at 30,000 cells/well on a 96 well flat bottom plate (Corning Inc, New York, US). After 24 hours of settling and adhering, the polymer samples were introduced into the well. Ten µL of each polymer stock solution was prepared in 90 µL of growth media to obtain final concentrations of 0.5 mg/mL, 1.0 mg/mL and 2.0 mg/mL. The fibroblast/polymer mixtures were then incubated for another 48 hours. Wells containing DMSO and media in equivalent volumes were applied as positive controls. Normal controls were prepared by adding saline and media in similar volumes to the wells containing polymer samples. After 48 hours of incubation, cells were washed with PBS buffer 3 times followed by adding 100 µL of fresh media and 10 µL of 12 mM MTT reagent (ATCC). After 4 hours, 100 µL of sodium dodecyl sulphate (SDS)-HCl was added to solubilize the generated formazan. After solubilization for 2 hours, absorbance at 570 nm was read on SpectraMax 190 microplate reader (Molecular Devices, California, US) and compared to saline controls. Measurements were conducted in quintuplicates with average values in percentage and standard deviation being reported.

3.3 Results and discussions

3.3.1 Zeta potential and surface charge of HPG materials

Zeta (ζ) potential analysis is a very useful technique for understanding the surface charge of nanoparticles through measuring the electrophoretic mobility in the presence of charge compensation by ions in aqueous solution.[73] In this study, we applied zeta potential analysis to determine if the surface modification of HPG molecules with zwitterionic CP had been

successfully conducted, where the resulting zeta potential values are expected to display values distributed around 0 mV, meaning a relatively neutral charge distribution was achieved. Repeated tests were performed where each sample underwent 3 measurements of 10 runs to guarantee the consistency of data.

As shown in Table 3.1, the averaged ζ potential of the synthesized HPG polymers were determined to be between –7 mV and +3 mV at pH 7. These results indicate that around physiological pH, HPGs modified with CP ligands present relatively neutral surface charge at a specific sodium chloride concentration (0.15 M) examined, indistinguishable from the core HPG itself.

Table 3.1 Zeta potential of HPGs and HPG conjugates in 0.15 M saline at pH 7.

	Number of CP moieties	Zeta potential (mV)
(3K)HPG Conjugates	0	-6.71 ± 0.71
	3	2.54 ± 0.59
(20K)HPG Conjugates	0	-4.93 ± 0.32
	15	-3.36 ± 0.27
	30	1.33 ± 0.18
	50	-6.13 ± 0.48

This finding is consistent with previous studies, where these works showed that polymer possessing zwitterionic structure demonstrated a ζ potential around 0 mV at physiological pH (pH 7.4) and proved antifouling abilities as well. For example, Schroeder *et al.* prepared an antifouling hydrogel bearing equal densities of positively charged [2-(acryloyloxy)ethyl] trimethyl ammonium and negatively charged 2-carboxyethyl acrylate, for which the ζ potential was

determined to be 3~9 mV at pH 7.4.[74] Similarly, according to Dobbins *et al.*, the hydrogel they manufactured combining equal amounts of [2-(methacryloyloxy)ethyl]-trimethylammonium chloride and negatively charged 3-sulfopropyl methacrylate potassium salt on the surface showed antifouling properties and demonstrated a ζ potential between –3 ~ +1 mV.[75]

3.3.2 Quantification of bound water of HPG polymers

HPG and its derivatives are hydrophilic materials capable of creating a hydration layer associated with the polymer branches, which efficiently acts as an entropic and structural blockade that can prevent bio-foulants from attaching to the materials. To demonstrate the interactions between water and HPG polymers, differential scanning calorimetry (DSC) was utilized to analyze the amount of bound water through enthalpy measurements. Generally, when dissolving polymers in water, three states of water exist, namely, free water, freezable bound water and non-freezing water. Among them, non-freezing water and freezable bound water can either interact strongly or weakly with hydrophilic sites of the polymer, while free water shows no interaction with polymers, and thus, only free water displays the same melting temperature as the bulk water.[76] During DSC heating, only free water is supposed to crystallize and melt around 0 °C (273 K), and this process solely contributes to the enthalpy change around zero that can be detected using DSC. By obtaining the enthalpy change of aqueous polymer solutions and pure water, the numbers of bound water molecules can be determined for each macromolecular species.

Table 3.2 DSC measured enthalpy change of free water in different HPG polymer aqueous solutions. The normal control used was pure water.

Polymer	C(g/g)	ΔH_p/(J/g)	N_{Total}	$N_{Glycerol\text{-}OH}$	N_{cp}
H_2O	NA	335	NA	NA	NA
(3K)HPG	0.048	287	322	7	NA
(20K)HPG	0.051	286	2000	7	NA
(20K)HPG-$CP_{(15)}$	0.048	287	2700	7	48
(20K)HPG-$CP_{(50)}$	0.043	282	4000	7	45
(20K)HPG-$CP_{(80)}$	0.052	286	4800	7	41

C(g/g): The polymer concentration in aqueous solution
ΔH_p/(J/g): The enthalpy changes of free water
N_{Total}: The total number of water molecules bound per HPG or HPG conjugate, calculating using Eq. 3.1
$N_{Glycerol\text{-}OH}$: The number of water molecules bound per glycerol-OH unit
N_{cp}: The number of water molecules bound per CP ligand

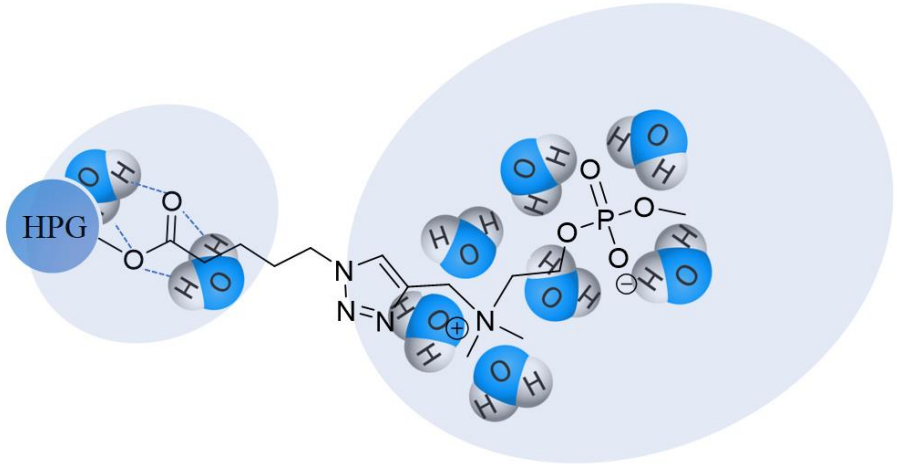

Figure 3.2 Two-dimensional illustration of possible interactions between water molecules and HPG-CP conjugates.

As shown in Table 3.2, as the CP density increases on the HPG backbone, the total number of waters bound per macromolecule calculated by applying Equation 3.1, also demonstrates an increasing trend. Since (3K)HPG and (20K)HPG were free of modifications, all the water molecules bound to polymers are due to their interaction with glycerol-hydroxy through hydrogen bonding, therefore, the amount of water bound per -OH group could be calculated. The result indicates that there are approximately 7 water molecules bound to each glycerol repeating unit by averaging the values obtained from the two native HPGs. The water molecules bound to one CP ligand were also calculated by subtracting the water molecules bound to just glycerol-OH from the total amount of water bound to each HPG conjugate, and then dividing by the number of CP groups present. The average number of water molecules bound per CP group determined from three (20K)HPG-CP derivatives is 44. CP functional groups comprise a cationic quaternary amine and an anionic phosphate ester, where water molecules can be bound to these charged moieties through electrostatic forces into a tight hydration layer (Figure 3.2).

3.3.3 Effects of synthesized polymers on the aggregation of red blood cells

As previously reported by our group[61], due to the inverse structure orientation, CP-polymers solely bearing a methyl phosphate group did not behave hydrophobically, and apparently caused binding to the phosphatidyl choline (PC) groups on the membrane of PC liposomes and eukaryotic cells including RBCs, inducing extreme RBC aggregation. In general macromolecules can cause cellular aggregation either by acting as a bridge to connect cells at the opposing facets[15,77,78] or by being excluded from the intercellular environment by the membrane glycocalyx, resulting in cells gathering together owing to the osmotic effect of the concentration difference between the bulk and surface regions.[79,80] In the case of HPG-CP radiolabeling of the polymers

and binding studies show strong binding of the polymers to RBC surfaces so the bridging model is the accepted mechanism.[61]

Figure 3.3 and 3.4 demonstrate representative images of RBC aggregation morphology when mixing whole blood with PBS or HPG macromolecules at 5 mg/mL. As shown in Figure 3.3A, B and C, no hemagglutination was observed in cases of PBS control, (20K)HPG as well as the click intermediate (20K)HPG-$N_{3(80)}$. As shown in Figure 3.3D, aggregation of RBC exposed to (20K)HPG-$CP_{(80)}$ was detected as the strongest, with almost no monodispersed cells being observed. During this process, RBCs underwent shape distortion as a result of dominating adhesive forces rather than the elasticity-driven shape recovery given by the membrane structure. As the percentage of CP groups decreased, fewer/smaller clumps of native blood tended to form, so that as demonstrated in Figure 3.3F where HPG-$CP_{(15)}$ data is presented, RBCs only stacked together in groups of 10-15 cells, showing a rouleaux effect. As the results indicated, the cellular binding affinity increases in relation to the increment of CP substitution degree while maintaining the molecular weight of HPG constant.

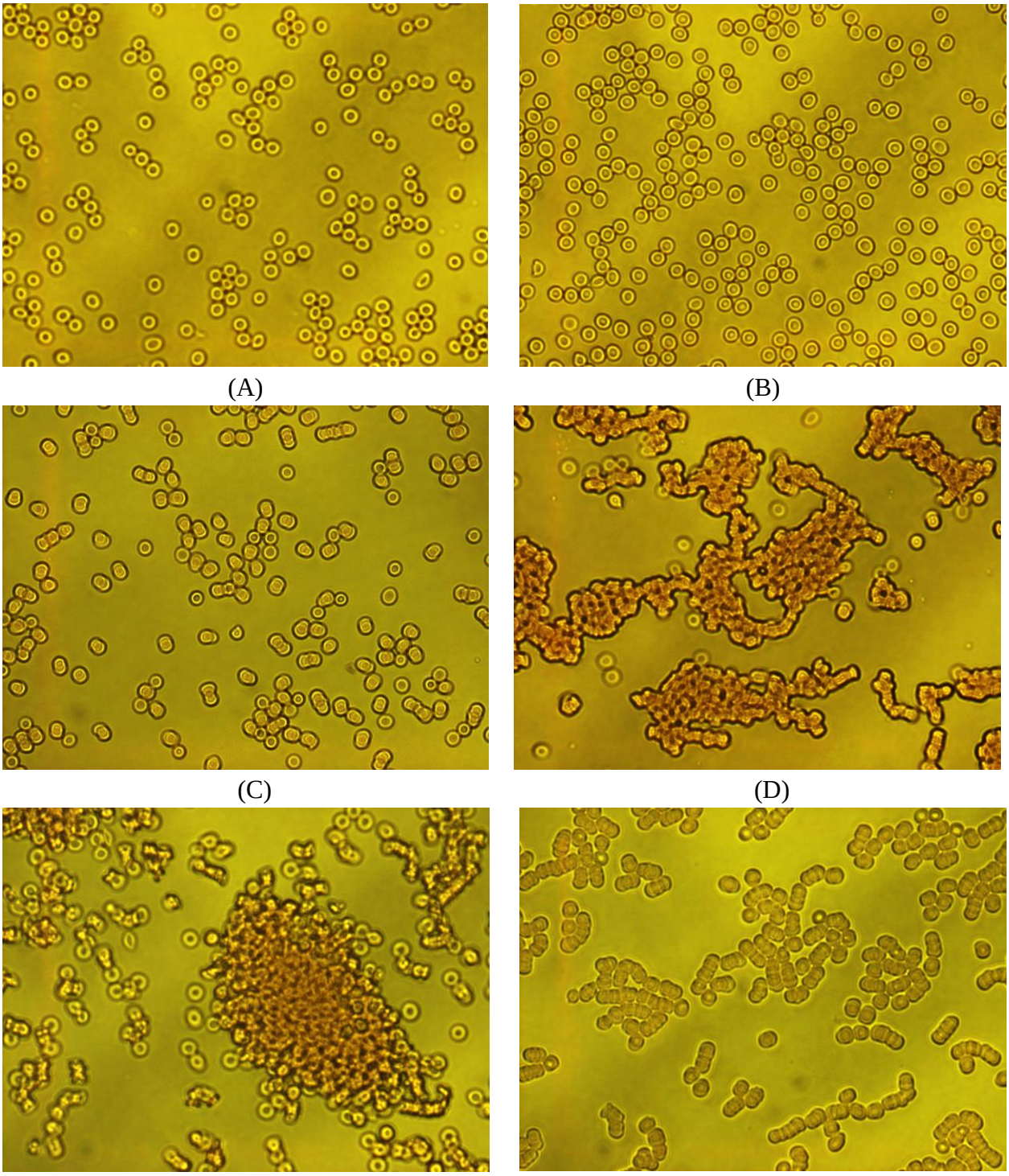

Figure 3.3 Optical microscopic images of whole blood aggregation effect in 5 mg/mL (20K)HPG polymers. All images are at 40× magnification. (A) PBS control, (B) (20K)HPG, (C) HPG-$N_{3(80)}$, (D) HPG-$CP_{(80)}$, (E) HPG-$CP_{(30)}$, (F) HPG-$CP_{(15)}$.

In order to investigate if the molecular weight of macromolecules can also be a factor that significantly affects the bound strength with RBCs, (3K)HPG and its conjugates were examined using the same concentration (5mg/mL) to compare with (20K)HPG derivatives, shown in Figure 3.4. According to *Yu et al.*, higher molecular weight polymers adsorbed less strongly to the cellular surface than lower molecular weight homologues due to repulsion between CP carrier and the RBC glycocalyx consisting of glycolipid chains and glycoprotein. This exclusion force has been demonstrated through a polymer brush model with different molecular weights impinged.[81] Therefore, when 5mg/mL (20K)HPG-$CP_{(15)}$ which carries about 6% -OH modified into CP groups was observed to produce only a weak aggregation effect on whole blood RBCs, (3K)HPG containing the same CP percentage (3 CP moieties) was selected to examine. As expected, the same percentage of CP coupled to HPG with lower Mn demonstrated stronger binding since increasing number and size of RBC clumps were observed in Figure 3.4B compared to Figure 3.4F.

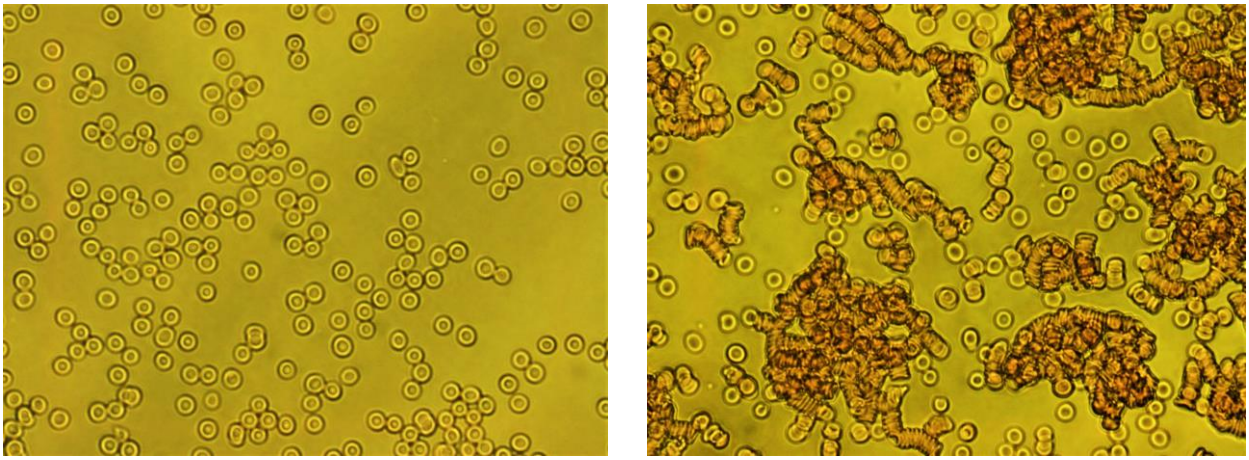

(A) (B)

Figure 3.4 Optical microscopic images taken at 40× magnification, showing whole blood cells incubated with 5 mg/mL (3K)HPG polymers. (A) (3K)HPG, (B) HPG-$CP_{(3)}$.

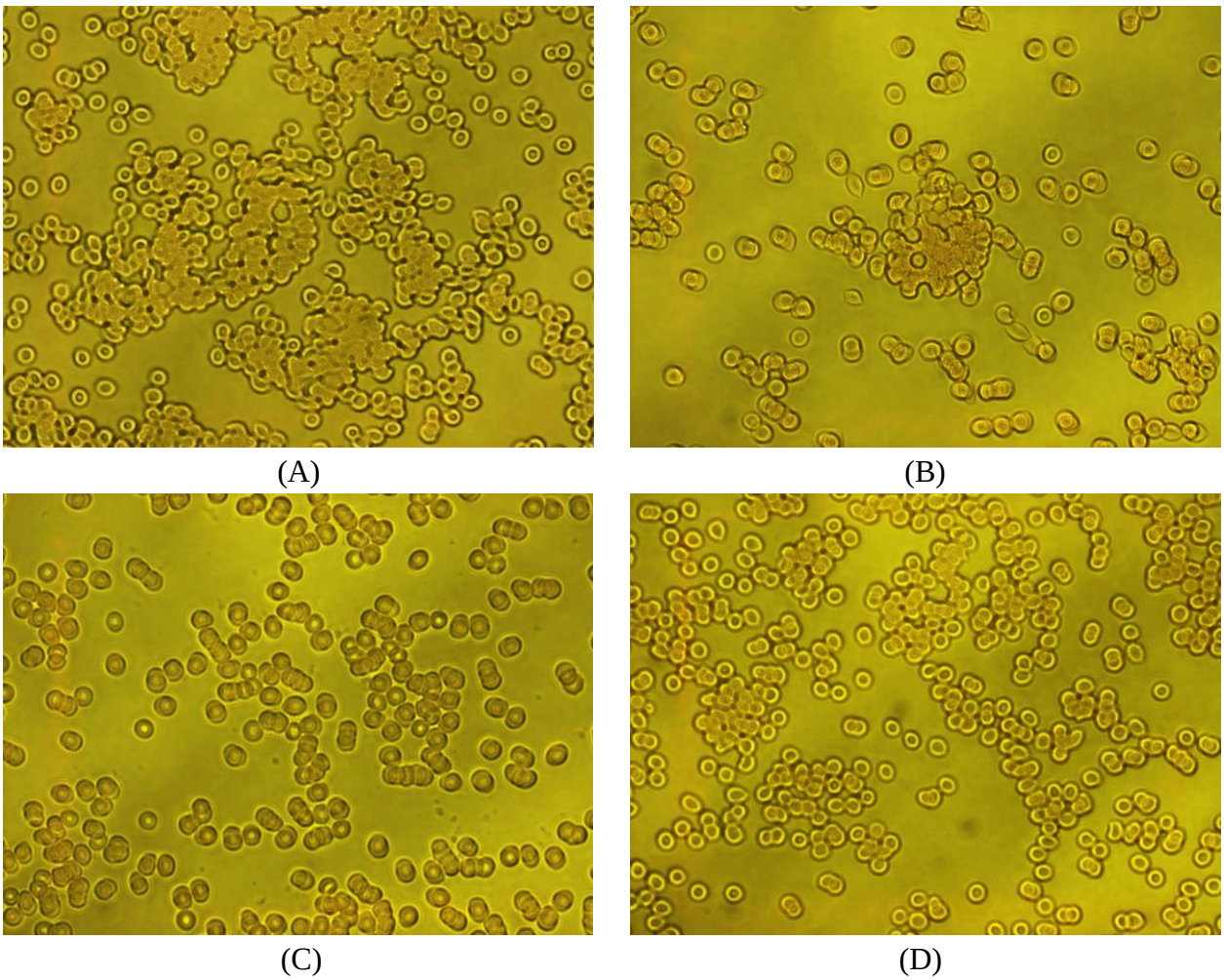

Figure 3.5 Optical microscopic images of whole blood cells incubated with 1mg/mL polymer materials. (A) (20K)HPG-CP$_{(80)}$, (B) (20K)HPG-CP$_{(30)}$, (C) (20K)HPG-CP$_{(15)}$, (D) (3K)HPG-CP$_{(3)}$.

When the concentration of HPG/HPG conjugates is reduced to 1 mg/mL, if visible aggregation is likely/unlikely to be observed depends on degree of CP substitution as well as molecular weight of HPG. As shown in Figure 3.5, in general, higher numbers of monodispersed RBCs and smaller size of clots were detected from the samples mixed with 1mg/mL polymer solution compared to 5 mg/mL, regardless of the size or CP density of the polymer. Specifically, only regional aggregations were observed when the number of CP moieties present were 80 and 30 for (20K)HPG, as manifested in Figure 3.5A and B; while for (20K)HPG-CP$_{(15)}$, RBCs behaved

similarly to those in the 5mg/mL sample. Figure 3.5D displays the morphology of RBCs incubated with 1mg/mL (3K)HPG-$CP_{(3)}$, where only weak affinity was detected, demonstrating sharp contrast to the agglutination in Figure 3.4B. The overall results showed that as the concentration of polymer increases, stronger binding and aggregation are exhibited, consistent with expectation based on binding behaviour observed previously.[61,82]

The aggregation effects on washed RBCs incubated with different HPG derivatives were also investigated, as shown in Figure 3.6. Interestingly, (20K)HPG-$CP_{(80)}$ incubated with erythrocytes at both concentrations shown in Figure 3.6D and E, demonstrate similar or slightly larger size of blood clots compared to those in Figure 3.3D and E, after removal of plasma. This result satisfied the expectation that the interaction only takes place between HPG material and the RBCs even if a more complicated matrix containing protein sources is present, namely blood plasma. As a macromolecule carrying a zwitterionic surface, HPG-CP is predicted to demonstrate a non-fouling effect through excluding nonspecific protein absorption in the plasma environment. According to Ladd *et al.*, it is believed that the nonspecific binding in a complex media can be prevented due to a "steric repulsion" and a surrounding hydration layer of hyperbranched glycerol-based poly-material.[83] Based on the fact that protein adsorption is considered as the first step contributing to an inflammatory response, which in turn, can lead to thrombosis and platelet adhesion[84-86], it is of interest to study the activation and aggregation in platelet-rich plasma. These studies are described and analyzed in the following section.

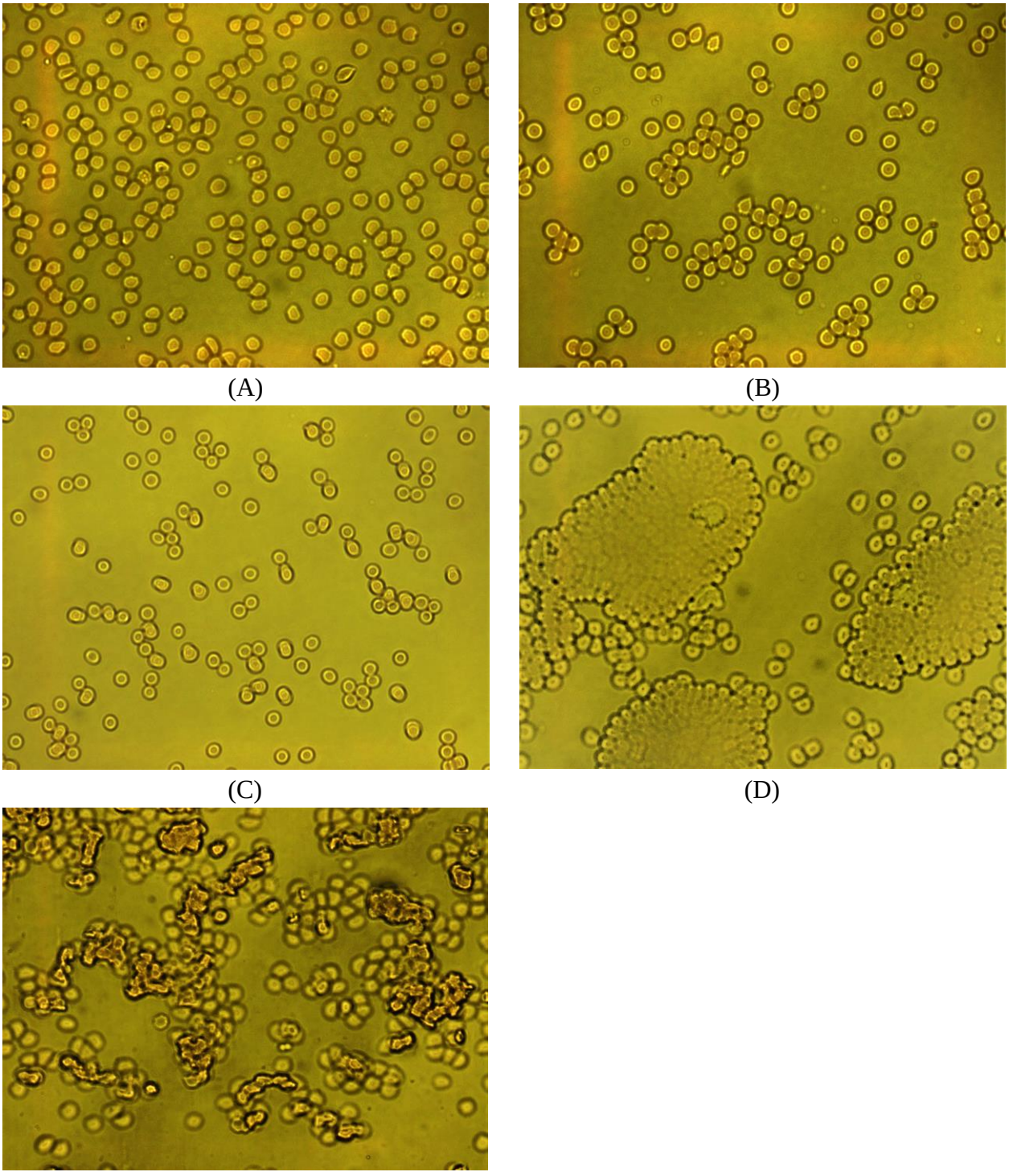

(A) (B)

(C) (D)

(E)

Figure 3.6 Aggregation effect of washed RBCs incubated with PBS or (20k)HPG polymers. (A) PBS control, (B) 5mg/mL HPG, (C) 5 mg/mL HPG-$N_{3(80)}$, (D) 5mg/mL HPG-$CP_{(80)}$, (E) 1mg/mL HPG-$CP_{(80)}$.

3.3.4 Interpretation of hemolysis activity

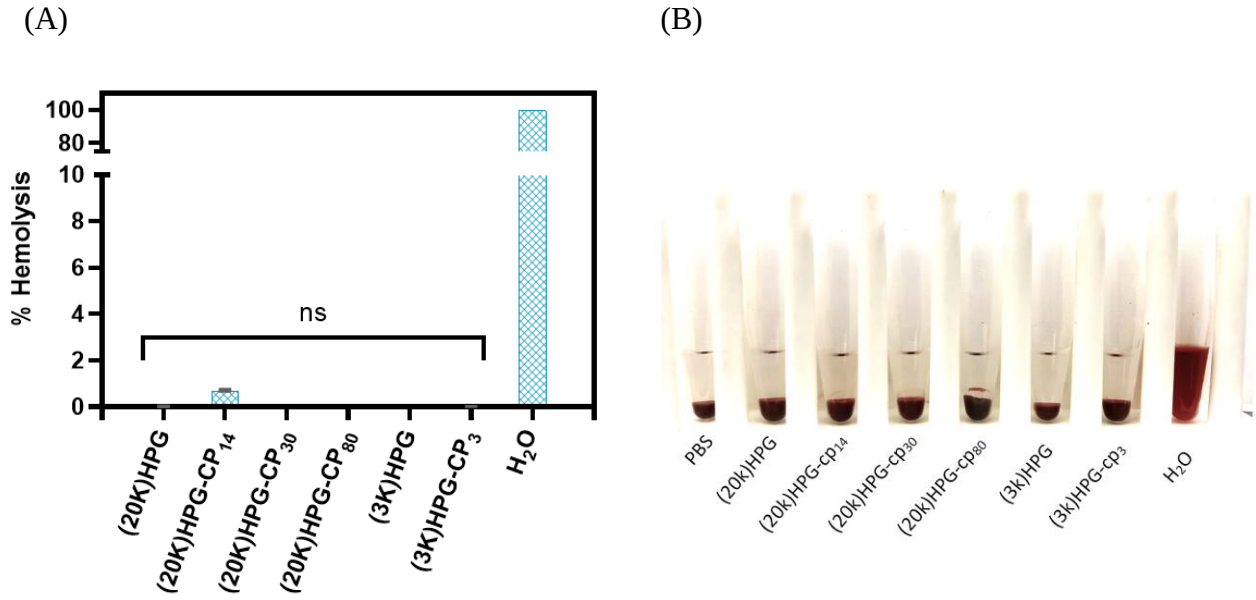

Figure 3.7 (A) Hemolysis test on HPG materials. The concentration of polymers is 5 mg/mL. The results are expressed in relative percentage compared to 0% hemolysis effect of PBS control and 100% for water/blood mixture. (B) RBCs incubated with different polymers or control samples at 5mg/mL.

After evaluating the RBC aggregation effect of the CP zwitterionic polymers, it is also of interest to test the extent of drug-induced hemolysis with a high concentration (5 mg/mL) of polymers present. The *in vitro* hemolysis assay is able to detect the degree of membrane breakage of RBCs which results in hemoglobin release into plasma. The occurrence of hemolysis will further lead to the study of the mechanisms behind it, which can be either due to the direct toxicity of the material or if the donor is pre-exposed to a related material it is possible there could be an immunological response to the polymer if plasma is present.[87]

In this study, a protocol modified based on previously published work by our group[21,88] was applied, where the hemolysis was evaluated and compared with PBS and water as negative and positive controls, respectively. As shown in Figure 3.7, even though HPG conjugates, namely

(20K)HPG-$CP_{(30)}$, (20K)HPG-$CP_{(80)}$ and (3K)HPG-$CP_{(3)}$ demonstrated strong binding affinity to RBCs, the hemolysis activity of these materials showed nonsignificant results which are entirely below 1%. This result was also a confirmation that zwitterionic ligands are stable in terms of bearing equal cation and anion groups under the physiological environment, instead of being hydrolyzed and chemically cleaved to keep only the cationic part. This conjecture was proposed since cationic ligands could cause severe hemolysis (~20%) as reported by previous group members, while zwitterionic structures possessing a hydration layer and neutral charge are able to bind water molecules near the polymer, thus generating a physical barrier to biofouling potentially created by adsorbing proteins. The demonstrated biocompatibility of the synthesized HPG conjugates suggests that *in vivo* applications can be performed using these polymers in future.

3.3.5 Effect of HPG conjugates on platelet activation and aggregation

As a sensitive component in blood cells, platelets can be activated as a result of exposure to foreign surfaces and drug materials; they play an important role in hemostasis where an early response when activated is usually platelet aggregation. Based on the results obtained from comparing our polymer effect on whole blood and washed blood cell aggregation, it is hypothesized that zwitterionic groups on the surface of HPG will not or just slightly disturb the plasma medium to trigger activation and aggregation of platelets. RBCs were predicted to form clumps only due to the binding interaction between their membrane and CP ligands so the question arises whether or not platelets will aggregate by the same mechanism or will they be activated to do so by their coagulation activity.

3.3.5.1 *In vitro* platelet aggregation

The on-going aggregation effects induced by HPG-$CP_{(x)}$ polymers of different concentrations (5 mg/mL and 1 mg/mL) were measured by transmitting light at 595 nm for 10 minutes through a stirred suspension. MA% values showing where the maximal aggregation occurs with respect to blank sample (PPP) were given, and a higher number indicates more light transmitting through the sample (less scattering) when platelet aggregates form due, for instance, to the presence of agonist. As the positive control, ADP has been employed as the stimulus for platelet aggregation in relevant studies due to its intrinsic interaction with ADP receptors on platelet membranes, resulting in platelet activation.[89] Figure 3.8A shows the percentage distribution of platelet aggregation triggered by HPG/HPG conjugates in platelet-rich plasma (PRP). The results clearly showed that none of the tested polymer materials caused significant platelet aggregation at either concentration (5 mg/mL and 1 mg/mL), in conspicuous contrast with the ADP control. As expected, HPGs bearing zwitterionic ligands were not capable of inducing strong aggregation of human platelets due to the neutral charge distribution on the polymer surface. This differs from studies that have demonstrated positively charged polymers tended to adhere to the negatively charged membrane of platelet, thereby forming connecting bridges between nearby platelets, which in turn, induced the platelet aggregation.[90] This result is also in accordance with the one drawn from HPG-SB-QA_x (a sulfobetiane- and quaternary amine- based HPG) aggregation studies conducted by two of our previous group members, who concluded that macromolecules only containing high concentrations of cationic ligands, not neutral or low density of positively charged groups, would induce platelet aggregation in human plasma.[91] On the other hand, in terms of design of zwitterionic structures, phosphobetaine-based polymers were considered to be more

fouling-resistant than sulfobetaine-based polymers[92], indicating a more advanced material was manufactured here compared to HPG-SB-QA_x produced in previous work in this group.

(A)

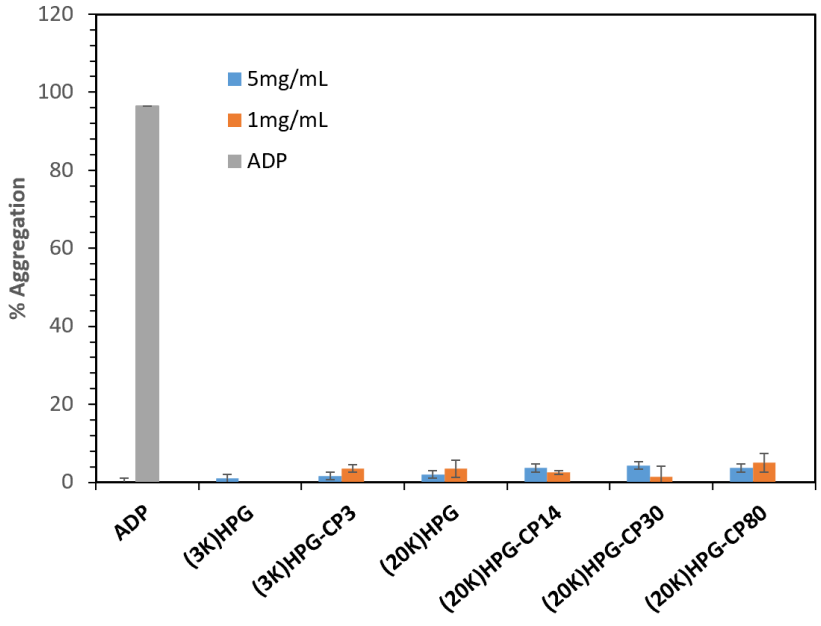

(B)

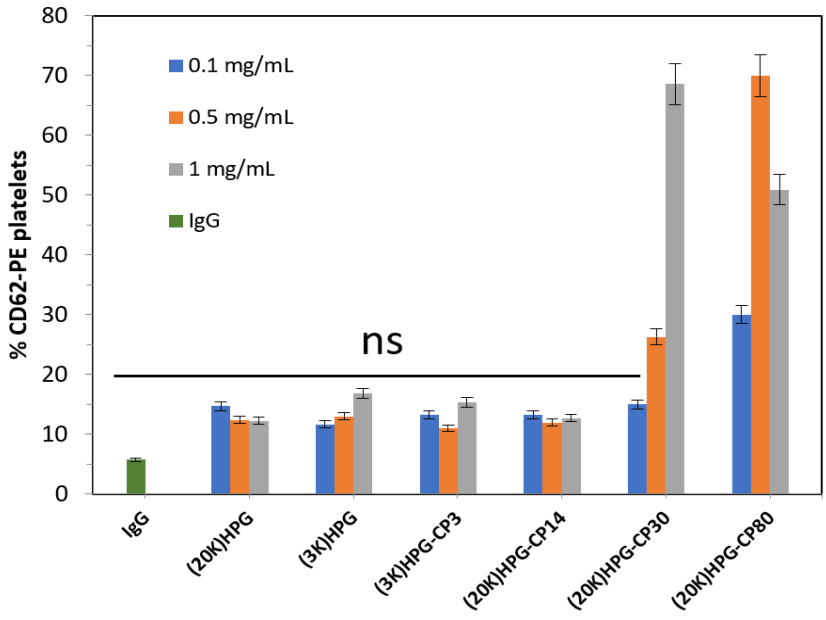

Figure 3.8 (A) Values represent the aggregation of PRP detected by light transmitting platelet aggregometer, ADP was shown as positive control; (B) Activation of platelet in PRP measured by flow cytometry, expressed by the marker CD62PE, IgG was employed as negative control.

3.3.5.2 *In vitro* platelet activation

Platelet activation is considered as an initial stage of the coagulation cascade, followed by a series of membrane-related events and platelet aggregation or adhesion to endothelial surfaces but interactions with the plasma matrix is the first step in the primary hemostatic effect. The expression of CD62 on the surface of platelets is an indicator of platelet degranulation and secretion, known as platelet activation. Herein, the level of platelet activation was measured and reported as a function of concentration and the density of CP groups on HPG polymers. The same materials were used to compare this behavior with results obtained from platelet aggregation test. As demonstrated in Figure 3.8B, the level showing activation of platelets in PRP was expressed as percentage of platelet carrying P-selectin (CD62P) on their surfaces and therefore marked with anti-CD62PE antibody which displayed fluorescence. Mouse immunoglobin G (IgG) antibody naturally created and released from plasma showed nonsignificant activation (~4%) as expected, according to Figure 3.8 (B). At three concentrations being measured, HPG macromolecules of both molecular weights, as well as low-density HPG-CP_x conjugates, namely, (3K)HPG-$CP_{(3)}$ and (20K)HPG-$CP_{(15)}$ did not show any significant activation effect (lower than 20%) in comparison with the control platelets incubated with buffer solution. As the number of CP moieties on the (20K)HPG core increased to 30 and 80, higher numbers of activated platelets were detected; and for individual HPG-CP_x polymers, the triggered platelet activity level also increased with concentration in most cases. The results show that HPG bearing higher than 15 CP groups can activate platelets depending on the concentration used, through the initial contacting interaction between platelet-rich plasma and CP functionalized HPG.

3.3.5.3 Relationship between activation and aggregation of platelets

Positive results in platelet activation are commonly considered to trigger an aggregation effect, while on the contrary in the present case, platelets did not demonstrate effective aggregation in human plasma after introducing polymers, as shown in Figure 3.8A. Possible explanations contributed to this finding might be: since the platelet-rich human plasma also contains over a hundred sources of proteins, it is possible that CP, as a zwitterionic ligand could interact with some types of protein other than fibrinogen[93], in such a way that the plasma medium was disturbed and induced the P-selectin (the platelet activation marker) expression. Another speculation suggested that HPG-CP conjugates might interact with or bind to the active compound, ADP, which would in turn impede the platelet aggregation. Although platelet activation was observed to be strong for higher-density CP functionalized HPGs, the coagulation cascade did not complete, perhaps due to a poor interaction between fibrinogen, thrombin and the activated platelets. This conjecture can be further tested by measuring activated partial thromboplastin time (aPTT) and prothrombin time (PT) to analyze the coagulation. Such measurements and further work to track down the reason for this interesting effect is beyond the scope of the current project however.

3.3.6 Cytotoxicity investigation on HPG polymers

The *in vitro* cytotoxicity test was carried out to detect if the synthesized HPG polymers were able to function as an adhesive material without sacrificing cell viabilities. MTT assays were applied to assess the metabolic activity of human cells based on colorimetry, where the NAD(P)H-dependent cellular oxidoreductase enzymes released from living cells are capable of reducing the yellow tetrazolium dye to the corresponding insoluble formazan, in order to display a purple color that can be detected by spectrophotometer at a certain wavelength between 500~600 nm. Human

fibroblasts were chosen as the object of study for the cytotoxicity investigation due to their critical function in forming the structural framework for human connective tissues as they synthesize the extracellular matrix and collagen. Based on these factors, fibroblasts are commonly known for involvement in healing wounds and recovering damaged tissues.

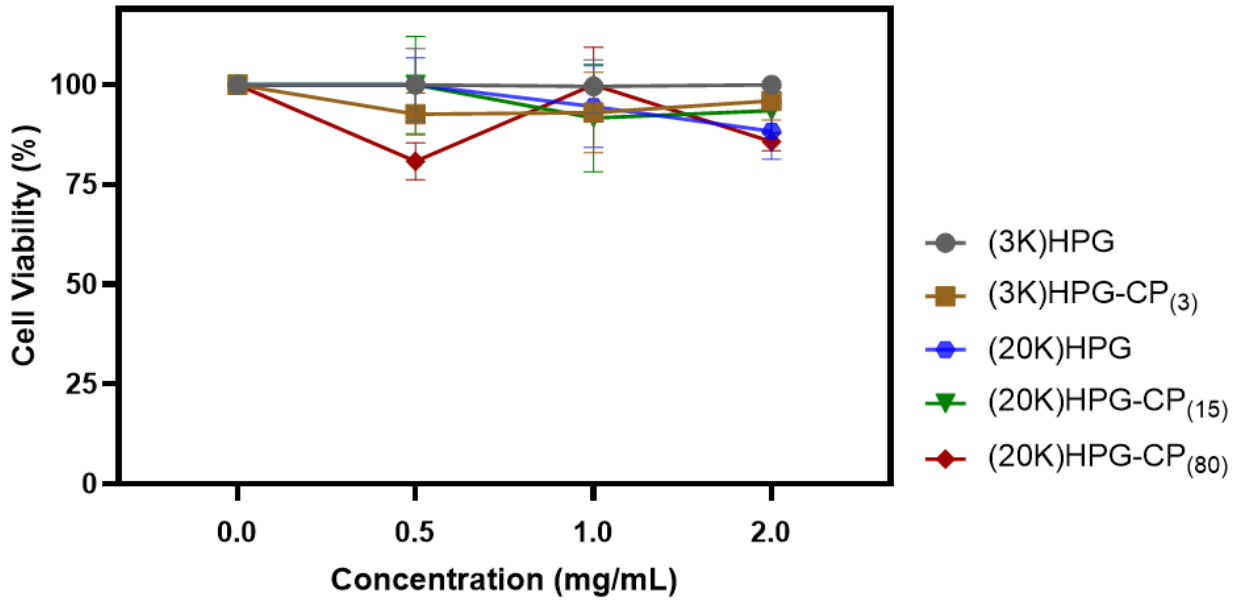

Figure 3.9. Dose-response curves for cell viability of human fibroblasts in percentage. Results are present with calculated means ± SD (n = 5).

The results are summarized in Figure 3.9, reporting the influence of synthetic HPG polymers on human fibroblasts at different concentrations. Compared to the positive control using DMSO which manifested an average cell viability of 13%, all the HPG and HPG conjugates demonstrated a relatively safe cytotoxicity level with at least 80% of the cell population maintaining viability even when the polymer concentration used was up to 2 mg/mL. No dependence of cell viability on polymer concentration was observed in the data. The outstanding

performance of maintaining cell activity and viability after introducing polymer materials could be explained by the structural benefit of hydroxyl-rich macromolecules and zwitterionic moieties, which are able to bind with water and form a protective hydration layer. The manufactured HPG-CP polymers were shown to successfully aggregate blood cells while not damaging fibroblasts.

3.4 Summary

In this chapter, after confirming the surface of the synthesized HPG polymers were relatively neutral while manifesting hydration properties, the proposed electrostatic interactions between zwitterionic CP ligands carried by HPG and cellular surfaces were evaluated via a series of blood tests. It has been found that the CP functionalized HPGs demonstrate hemostatic potential particularly through binding to red blood cells rather than by aggregating platelets via induction of the coagulation cascade, and meanwhile maintaining biocompatibility. According to the microscopic observations, when the number density of CP exceeds 3 on (3K)HPG and 30 on (20K)HPG, where the percentage of theses zwitterionic sites is over 15%, prominent RBC aggregations formed even at concentration as low as 1mg/mL. As both CP derivatization and polymer concentration increased, the binding affinity was shown to become stronger due to the higher CP content which is capable of linking erythrocytes together. Moreover, a further increase in both Mn of HPG and conjugated CP moieties resulted in nonsignificant or even decreasing adhesion effect, which was concluded by comparing (3K)HPG-$CP_{(3)}$ and (20K)HPG-$CP_{(15)}$, consistent with a cell exclusion force associated with larger sized HPG constructs potentially balancing off "CP-PC" interactions to some extent. Attribute to the zwitterionic structure, all the HPG derivatives showed an undetectable level of hemolytic activity, which effectively solved the lysis issue caused by cationic polymers used as traditional hemostatic agents. Although platelet

aggregation tests demonstrated negative results, (20K)HPG-$CP_{(30)}$ and (20K)HPG-$CP_{(80)}$ were observed to activate the platelets in human plasma at low concentrations, which runs counter to the platelet activation to inducing aggregation sequence. It seems possible that introducing HPG-CPs into the plasma medium disturbed the human plasma environment, which unexpectedly triggered platelet activation due to an unidentified complication. This resulted in the sequence of coagulation factors not being induced to complete the cascade, therefore no platelet aggregation was observed. This idea will be tested and verified in future by conducting PT, aPTT and thromboelastographic experiments.

CP-functionalized HPG acted as a glue material that aggregated red blood cells together through an electrostatic interaction, which is potentially able to be developed as a haemostatic and universal bioadhesive agents. All the tested materials demonstrated excellent biocompatibility during cytotoxicity and hemolysis tests by maintaining the cell viability and original shape.

Chapter 4: Conclusions and future work

4.1 Conclusions

In this project, a library of HPG polymers carrying different zwitterionic CP ligands was successfully developed using a new synthetic route. We conclude that CP-decorated HPG polymers are able to bind strongly to cell membranes through examining RBC aggregation caused by HPG-CPs. These polymer conjugates could potentially be used as a modern hemostatic material based on the results from blood tests, and we believe that a "PC-CP" binding mechanism may be applied in attaching related materials to any cell membrane containing phosphatidyl choline headgroups, realizing multiple bio-applications such us locally directed drug delivery and tissue seals. The zwitterionic structure of CP could not only provide cell attachment properties, but also create a hydration layer around the bound material to resist nonspecific protein adsorption.

Chapter 2 focuses on optimizing the synthetic pathways of manufacturing hyperbranched polyglycerol (HPG) carriers decorated with varied CP densities. Cu^{I}-catalyzed azide/alkyne cycloaddition (CuAAC) acts as a bridging step which conjugates the hydrating zwitterionic CP ligands on the azido-functionalized HPGs. The application of this "click" chemistry was tested by incorporating different mole percentages of CP ligands on the HPG backbone, and the structures as well as the composition of the resulting critical products from multi-step synthesis were characterized qualitatively and quantitatively by various tools and techniques. In this thesis work, we have successfully developed a family of hyperbranched polymers and their conjugates, namely, HPGs with molecular weights of 3 and 20 kDa, (3K)HPG-$CP_{(3)}$, (20K)HPG-$CP_{(15)}$, (20K)HPG-$CP_{(30)}$, (20K)HPG-$CP_{(50)}$ and (20K)HPG-$CP_{(80)}$.

In Chapter 3, the surface charge, water binding properties, *in vitro* bio-functionalities and biocompatibility of the manufactured polymers from Chapter 2 were evaluated and reported. Zeta

potential measurements showed that all the synthesized polymers were relatively neutral on the surface. According to the DSC results, the zwitterionic CP groups were found to enhance the water binding ability of the HPG core by holding more water molecules per ligand. In terms of biological tests, the manufactured polymers including (3K)HPG-$CP_{(3)}$, (20K)HPG-$CP_{(15)}$, (20K)HPG-$CP_{(30)}$ and (20K)HPG-$CP_{(80)}$ exhibited positive effects in erythrocyte aggregation without inducing platelets to aggregate. It is believed that HPG-CP acted as a bridge between red blood cells that hold them together in order to provide the energy needed to maintain blood cell aggregation of red cells but, interestingly, not for platelets. Finally, it was found that none of the synthesized polymers induced significant hemolysis or cytotoxicity of human fibroblasts, providing this material with an exciting future in biocompatible material applications.

4.2 Future works

The idea of creating CP functionalized polymers used as membrane-adhesive materials through "CP-PC" electrostatic interactions was first proposed by our group about 10 years ago. In 2012, in a published paper, the pilot study accomplished by our previous group members, foremost, revealed that CP decorated HPGs could bind strongly to lipid membranes containing phosphatidyl choline (PC) headgroups, inducing aggregation of red blood cells.[61] Subsequent work showed the synthetic route used originally was very inefficient, which was verified by other groups so the need to improve this was clearly recognized. In spite of several attempts by our group using different reaction pathways little progress was made and the yield of CP ligands remained low, frustrating our interest in attaching CP functional groups onto different polymer surfaces to create bio-adhesive products that could be utilized in diverse bio-applications. The ultimate goals of developing a series of CP-related projects are: first, realizing industrially directed manufacture by

optimizing reproducibility and reaction scalability in terms of the material science and engineering; moreover, further digging into the mechanism and investigating how the hemostasis is promoted by the therapeutic CP-biomolecules; last but not least, expanding the library of eukaryotic cells for bio-adhesion and bio-compatibility tests to examine the versatility of the CP materials. To this end, the future directions will be approached from three major aspects as discussed below.

In Chapter 2, the newly designed synthesis pathways of preparing CP ligands manifested a remarkable increase in yield compared to the previous works. However, impurities such as pyridinium salt and phosphate ester coexisted in the product before moving on to the next-step "click" reaction, suffering from limitations in separation methods. Although these impure compounds did not participate in CuAAC "click" reaction since they are structurally free of alkyne or azide functional groups, still, they might potentially affect the reaction rate or cause unwanted side reactions in a different Cu^{I}-catalyzed reaction system, resulting in low efficiency or incompletion of synthesis. Therefore, one area for future work could focus on developing a separation method through carefully using ion-exchange resins to replace the impurity ions. In addition, due to the fact that decreasing the length of the alkoxyl chain attached on the choline phosphate ester can increase the strength of cell adhesion[60], it has been predicted that CP bearing one hydroxyl group instead of a methoxyl group would show stronger binding affinity to cell surfaces, and thus, it is of interest to develop CP ligands with hydroxyl end-groups. Figure 4.1 illustrates the structural comparison between HPG-CP-OMe (synthesized in this project) and HPG-CP-OH. To achieve the structure of HPG-CP-OH, a more intense hydrolysis method could be employed, while the reaction condition should be adjusted in order to not cleave the phosphate

ester group off. Meanwhile, the pKa of the hydroxyl group has to be detected by titration to ensure the net charge of the HPG-CP derivative is neutral at physiological pH.

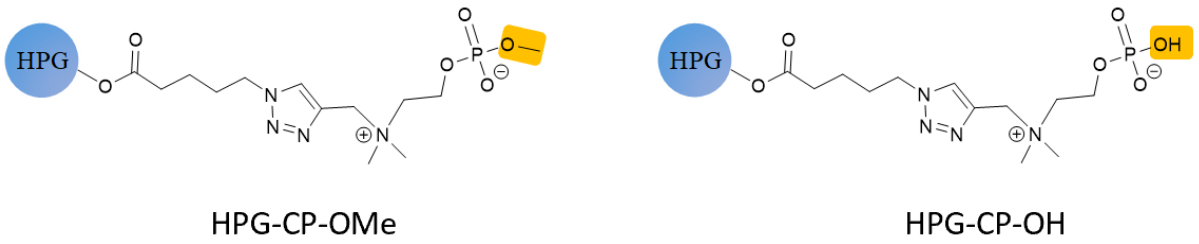

Figure 4.1 HPGs decorated with CP groups possessing methyl phosphate or hydroxyl phosphate. It has been predicted that HPG-CP-OH can bind to cell membrane more strongly than HPG-CP-OMe.

In terms of blood aggregation tests performed in this project, interestingly, it was found that HPG-CP conjugates did not cause platelet aggregation but induced platelet activation. To understand this phenomenon, future research work can be approached from two areas. One is that we can study mixtures of HPG conjugates with the positive control, ADP, prior to platelet aggregation tests in PRP to investigate ADP-CP interactions that could interfere with normal ADP binding to P2Y1 receptors, resulting in reduced or no platelet aggregation being initiated. Another direction that we can consider is to perform *in vitro* blood coagulation tests, which include measurements of prothrombin time (PT) and activated partial thromboplastin time (aPTT). In addition, in order to further understand the coagulation effect, thromboelastography (TEG) on appropriate mixtures can be utilized to evaluate the strength of human blood clots as a function of time in the presence of HPG-CPs.

The prediction of cytotoxicity of chemical materials is essential for minimizing expensive drug failures owing to toxicity during late-stage development or in clinical studies. In addition to

the human fibroblasts that were chosen for a cytotoxicity investigation in this project, more elaborate studies based on endothelial cell lines can be performed in future studies. Endothelial cells possess many specialized functions proven from *in vitro* investigations previously, for instance, forming non-thrombogenic surfaces for platelets and participating in the synthesis of fibronectin and collagen.[94] A useful system to use as a test material would be to measure cytotoxicity effects on human umbilical vein endothelial cells (HUVECs) by using the propidium iodide (PI) live cell staining assay to detect the membrane damage of HUVECs after introducing polymer materials.[21] The potential for understanding the effects associated with HPG-CP interactions with blood elements and blood contacting surfaces suggests it would be an excellent area for future study.

Bibliography

1. Singer, S. J.; Nicolson, G. L., The fluid mosaic model of the structure of cell membranes. *Science*. **1972**, *175*(4023), 720-731.
2. Li, J.; Wang, X.; Zhang, T.; Wang, C.; Huang, Z.; Luo, X.; Deng, Y., A review on phospholipids and their main applications in drug delivery systems. *Asian J Pharm Sci*. **2015,** *10*(2), 81-98.
3. Vance, D. E.; Li, Z.; Jacobs, R. L., Hepatic phosphatidylethanolamine N-methyltransferase, unexpected roles in animal biochemistry and physiology. *J Biol Chem*. **2007**, *282*(46), 33237–33241.
4. Vance, D. E., Physiological roles of phosphatidylethanolamine *N*-methyltransferase. *BBA*. **2013**, *1831* (3), 626–632.
5. Yeagle, P. L., *The structure of biological membranes*. CRC press: London, 2011; pp 61–62.
6. Sohlenkamp, C.; López-Lara, I. M.; Geiger, O., Biosynthesis of phosphatidylcholine in bacteria. *Prog Lipid Res*. **2003**, *42*(2), 115-162.
7. Doherty, G. J.; McMahon, H. T., Mediation, modulation, and consequences of membrane-cytoskeleton interactions. *Annu Rev Biophys*. **2008**, *37*, 65-95.
8. Goldfine, H., Bacterial membranes and lipid packing theory. *J Lipid Res*. **1984**, *25*, 1501-1507.
9. Peschel, A.; Jack, R.W.; Otto, M.; Collins, L. V.; Staubitz, P.; Nicholson, G.; Kalbacher, H.; Nieuwenhuizen, W. F.; Jung, G., Tarkowski, A. and Van Kessel, K. P., Staphylococcus aureus resistance to human defensins and evasion of neutrophil killing via the novel virulence factor MprF is based on modification of membrane lipids with l-lysine. *J Exp Med*. **2001**, *193*(9), 1067-1076.
10. Hazen, S. L.; Chisolm, G. M., Oxidized phosphatidylcholines: pattern recognition ligands for multiple pathways of the innate immune response. *Proc Natl Acad Sci*. **2002**, *99*(20), 12515-12517.
11. Kanno, K.; Wu, M. K.; Agate, D. S.; Fanelli, B. J.; Wagle, N.; Scapa, E. F.; Ukomadu, C.; Cohen, D. E., Interacting proteins dictate function of the minimal START domain phosphatidylcholine transfer protein/StarD2. *J Biol Chem*. **2007**, *282*(42), 30728-30736.
12. Steck, T. L., The organization of proteins in the human red blood cell membrane: a review. *J Cell Biol*. **1974**, *62*(1), 1.
13. Yoo, S. K.; Starnes, T. W.; Deng, Q.; Huttenlocher, A., Lyn is a redox sensor that mediates leukocyte wound attraction in vivo. *Nature*. **2011**, *480*(7375), 109.
14. Turgeon, M. L., *Clinical hematology: theory and procedures*. Lippincott Williams & Wilkins. 2005, p. 100.
15. Mohandas, N.; Gallagher, P. G., Red cell membrane: past, present, and future. *Blood*. **2008**, *112*(10), 3939-3948.
16. Brooks, D. E., Mechanism of Red Cell Aggregation. In *Blood Cells, Rheology, and Aging*, Platt, D., Ed. Springer Berlin Heidelberg: 1988; pp 158-162
17. Weiss, H. J.; Turitto, V. T.; Baumgartner, H. R., Platelet adhesion and thrombus formation on subendothelium in platelets deficient in glycoproteins IIb-IIIa, Ib, and storage granules. *Blood*. **1986,** *67* (2), 322-330.

18. Broos, K.; Feys, H. B.; De Meyer, S. F.; Vanhoorelbeke, K.; Deckmyn, H., Platelets at work in primary hemostasis. *Blood Rev.* **2011,** *25* (4), 155-167.
19. Bevers, E. M.; Comfurius, P.; Zwaal, R. F. A., Platelet procoagulant activity: physiological significance and mechanisiums of exposure. *Blood Rev.* **1991,** *5* (3), 146-154.
20. Wen, J. Y., The chemical modification of hyperbranched polyglycerols for improved bioadhesive and hemostatic properties. MSc Thesis, University of British Columbia, Vancouver, CA, 2015.
21. Kuhn, L. T., Chapter 5-Biomaterials. In *Introduction to Biomedical Engineering*, 3rd Ed. Academic Press: 2012; pp 221-223.
22. Woodley, J., Bioadhesion: new possibilities for drug administration. *Clin Pharmacokinet*. **2001**, *40*, 77-84.
23. Kumar, K.; Dhawan, N.; Sharma, H.; Vaidya, S. and Vaidya, B., Bioadhesive polymers: novel tool for drug delivery. *Artif Cells Nanomed Biotechnol*. **2014**, *42*(4), 274-283.
24. Williams, D. F., On the mechanisms of biocompatibility. *Biomaterials*. **2008**, *29*(20), 2941-2953.
25. Williams, D. F., *Dictionary of biomaterials*. Liverpool University Prees: 1999; p.42.
26. Saddow, S. E., Chapter 3 - Study of the Hemocompatibility of 3C–SiC and a-SiC Films Using ISO 10993-4. In *Silicon Carbide Biotechnology*, Second Edition. Elsevier: 2016; pp 63-84.
27. Mano, J. F.; Silva, G. A.; Azevedo, H. S.; Malafaya, P. B.; Sousa, R. A.; Silva, S. S.; Boesel, L. F.; Oliveira, J. M.; Santos, T. C.; Marques, A. P.; Neves, N. M.; Reis, R. L., Natural origin biodegradable systems in tissue engineering and regenerative medicine: present status and some moving trends. *J R Soc Interface.* **2007,** *4* (17), 999-1030.
28. Nanjwade, B. K.; Bechra, H. M.; Derkar, G. K.; Manvi, F. V.; Nanjwade, V. K., Dendrimers: emerging polymers for drug-delivery systems. *Eur J Pharm. Sci.* **2009,** *38* (3), 185-196.
29. Dufes, C.; Uchegbu, I. F.; Schatzlein, A. G., Dendrimers in gene delivery. *Adv Drug Deliv Rev.* **2005,** *57* (15), 2177-2202.
30. Duncan, R.; Izzo, L., Dendrimer biocompatibility and toxicity. *Adv Drug Deliv Rev.* **2005,** *57* (15), 2215-2237.
31. Kim, Y. H., Hyperbranched polymers 10 years after. *J Polym Sci A Polym Chem*. **1998**, *36*(11), 1685-1698.
32. Ihre, H.; Johansson, M.; MalmstroÈm, E.; Hult, A., In *Advances in dendritic macromolecules*, Newkome GR, Ed. JAI Press: 1996; p. 1.
33. Sunder, A.; Hanselmann, R.; Frey, H.; Mülhaupt, R., Controlled synthesis of hyperbranched polyglycerols by ring-opening multibranching polymerization. *Macromolecules.* **1999**, *32*, 4240–4246.
34. Kainthan, R. K.; Janzen, J.; Kizhakkedathu, J. N.; Devine, D. V.; Brooks, D. E., Hydrophobically derivatized hyperbranched polyglycerol as a human serum albumin substitute. *Biomaterials.* **200,** *29*(11), 1693-1704.
35. Kainthan, R. K.; Gnanamani, M.; Ganguli, M.; Ghosh, T.; Brooks, D. E.; Maiti. S., Blood compatibility of novel water soluble hyperbranched polyglycerol-based multivalent cationic polymers and their interaction with DNA. *Biomaterials*. **2006**, 27, 5377–5390.

36. Chapanian, R.; Constantinescu, I.; Brooks, D. E.; Scott, M. D.; Kizhakkedathu, J. N., *In vivo* circulation, clearance, and biodistribution of polyglycerol grafted functional red blood cells. *Biomaterials*. **2012**, *33*, 3047–57.
37. Rossi, N. A.; Constantinescu, I.; Kainthan, R. K.; Brooks, D. E.; Scott, M. D.; Kizhakkedathu, J. N., Red blood cell membrane grafting of multi-functional hyperbranched polyglycerols. *Biomaterials.* **2010**, *31*, 4167–78.
38. Kainthan, R. K.; Brooks, D. E., In vivo biological evaluation of high molecular weight hyperbranched polyglycerols. *Biomaterials*. **2007**, *28*(32), 4779-4787.
39. Ostuni, E.; Chapman, R. G.; Holmlin, R. E.; Takayama, S.; Whitesides, G. M., A survey of structure-property relationsgips of surfaces that resist the adsorption of protein. *Langmuir J* **2001,** *17* (18), 5606-5620.
40. Herrwerth, S.; Eck, W.; Reinhardt, S.; Grunze, M., Factors that determine the protein resistance of oligoether self-assembled monolayers - internal hydrophilicity, terminal hydrophilicity, and lateral packing density. *J Am Chem Soc.* **2003,** *125* (31), 9359-9366.
41. Knop, K.; Hoogenboom, R.; Fischer, D.; Schubert, U. S., Poly(ethylene glycol) in drug delivery: pros and cons as well as potential alternatives. *Angew Chem Int Ed.* **2010,** *49* (36), 6288-6308.
42. Ye, L.; Letchford, K.; Heller, M.; Liggins, R.; Guan, D.; Kizhakkedathu, J. N.; Brooks, D. E.; Jackson, J. K.; Burt, H. M., Synthesis and characterization of carboxylic acid conjugated, hydrophobically derivatezed, hyperbranched polyglycerols as nanoparticulate drug carriers for cisplatin. *Biomacromolecules.* **2011,** *12* (1), 145-155.
43. Mugabe, C.; Hadaschik, B. A.; Kainthan, R. K.; Brooks, D. E.; So, A. I.; Gleave, M. E.; Burt, H. M., Paclitaxel incorporated in hydrophobically derivatized hyperbranched polyglycerols for intravesical bladder cancer therapy. *BJU Int.* **2009,** *103* (7), 978-86.
44. Kumar, P.; Shenoi, R. A.; Lai, B. F.; Nguyen, M.; Kizhakkedathu, J. N.; Straus, S. K., Conjugation of aurein 2.2 to HPG yields an antimicrobial with better properties. *Biomacromolecules.* **2015,** *16* (3), 913-923.
45. Mendelson, A. A.; Guan, Q.; Chafeeva, I.; Da Roza, G.A.; Kizhakkedathu, J.N.; Du, C., Hyperbranched polyglycerol is an efficacious and biocompatible novel osmotic agent in a rodent model of peritoneal dialysis. *Perit Dial Int*. **2013**, *33*(1), 15-27.
46. Yang, W.; Xue, H.; Li, W.; Zhang, J.; Jiang, S., Pursuing "zero" protein adsorption of poly (carboxybetaine) from undiluted blood serum and plasma. *Langmuir*. **2009**, *25*(19), 11911-11916.
47. Keefe, A. J.; Jiang, S., Poly (zwitterionic) protein conjugates offer increased stability without sacrificing binding affinity or bioactivity. *Nat Chem*. **2012**, *4*(1), 59.
48. Shao, Q.; White, A. D.; Jiang, S., Difference of carboxybetaine and oligo (ethylene glycol) moieties in altering hydrophobic interactions: a molecular simulation study. *J Phys Chem. B.* **2013**, *118*(1), 189-194.
49. Ishihara, K.; Fukumoto, K.; Iwasaki, Y.; Nakabayashi, N., Modification of polysulfone with phospholipid polymer for improvement of the blood compatibility. Part 1. Surface characterization. *Biomaterials*. **1999**, *20*(17), 1545-1551.

50. Chen, S.; Zheng, J.; Li, L.; Jiang, S., Strong resistance of phosphorylcholine self-assembled monolayers to protein adsorption: insights into nonfouling properties of zwitterionic materials. *J Am Chem Soc*. **2005**, *127*(41), 14473-14478.
51. Jeon, S. I.; Lee, J. H.; Andrade, J. D.; De Gennes, P. G., Protein-surface interactions in the presence of polyethylene oxide I. simplified theory. *J. Colloid Interface Sci.* **1991,** *142* (1), 149-158.
52. Shao, Q.; Jiang, S., Molecular understanding and design of zwitterionic materials. *Adv Mater* **2015,** *27* (1), 15-26.
53. Jiang, S.; Cao, Z., Ultralow-fouling, functionalizable, and hydrolyzable zwitterionic materials and their derivatives for biological applications. *Adv Mater.* **2010**, *22*(9), 920-932.
54. Cao, Z.; Jiang, S., Super-hydrophilic zwitterionic poly (carboxybetaine) and amphiphilic non-ionic poly (ethylene glycol) for stealth nanoparticles. *Nano Today*. **2012**, *7*(5), 404-413.
55. Mi, L.; Jiang, S., Integrated antimicrobial and nonfouling zwitterionic polymers. *Angew Chem Int Ed Engl.* **2014**, *53*(7), 1746-1754.
56. Iwasaki, Y.; Ishihara, K., Cell membrane-inspired phospholipid polymers for developing medical devices with excellent biointerfaces. *Sci. Technol. Adv Mater.* ***2012***, *13*(6), 064101.
57. Ma, Y.; Tang, Y.; Billingham, N.C.; Armes, S.P.; Lewis, A.L.; Lloyd, A.W.; Salvage, J. P., Well-defined biocompatible block copolymers via atom transfer radical polymerization of 2-methacryloyloxyethyl phosphorylcholine in protic media. *Macromolecules.* **2003**, *36*(10), 3475-3484.
58. Bhuchar, N.; Deng, Z.; Ishihara, K.; Narain, R., Detailed study of the reversible addition–fragmentation chain transfer polymerization and co-polymerization of 2-methacryloyloxyethyl phosphorylcholine. *Polym. Chem.* **2001**, *2*(3), 632-639.
59. McRae Page, S.; Martorella, M.; Parelkar, S.; Kosif, I.; Emrick, T., Disulfide cross-linked phosphorylcholine micelles for triggered release of camptothecin. *Mol Pharm.* **2013**, *10*(7), 2684-2692.
60. Yu, X.; Liu, Z.; Janzen, J.; Chafeeva, I.; Horte, S.; Chen, W.; Kainthan, R. K.; Kizhakkedathu, J. N.; Brooks, D. E., Polyvalent choline phosphate as a universal biomembrane adhesive. *Nat Mater.* **2012,** *11* (5), 468-476.
61. Hu, G.; Parelkar, S. S.; Emerick, T., A Facile approach to Hydrophilic, Reverse Zwitterionic, Choline Phosphate Polymers. *Polym Chem.* **2015**, *6*, 525-530.
62. Kolb, H. C.; Finn, M. G.; Sharpless, K. B., Click chemistry: diverse chemical function from a few good reactions. *Angew Chem Int Ed*. **2001**, *40* (11), 2004-2021.
63. Tornøe, C.W.; Christensen, C.; Meldal, M., Peptidotriazoles on solid phase:[1, 2, 3]-triazoles by regiospecific copper (I)-catalyzed 1, 3-dipolar cycloadditions of terminal alkynes to azides. *J. Org. Chem*. **2002**, *67*, 3057.
64. Díez-González S., Well-defined copper (I) complexes for click azide–alkyne cycloaddition reactions: One click beyond. *Catal Sci Technol*. **2011**, *1*(2), 166-78.
65. Liang, L.; Astruc, D., The copper(I)-catalyzed alkyne-azide cycloaddition (CuAAC)"click" reaction and its applications. An overview. *Coord Chem Rev*. **2011**, *255* (23-24), 2933-2945.
66. Kainthan, R. K.; Janzen, J.; Levin, E.; Devine, D. V.; Brooks, D. E., Biocompatibility testing of branched and linear polyglycidol. *Biomacromolecules* **2006,** *7* (3), 703-709.

67. Neises, B.; Steglich, W., Simple Method for the Esterification of Carboxylic Acids. *Angew Chem Int Ed English.* **1978**, *17*, 522-524.
68. Brinker, C. J., Hydrolysis and Condensation of Silicates: Effects on Structure. *J Non Cryst Solids.* **1988**, *100*, 31-50.
69. Schlenoff, J. B., Zwitteration: coating surfaces with zwitterionic functionality to reduce nonspecific adsorption. *Langmuir*. **2014**, *30*(32), 9625-36.
70. Bhattacharjee, S., DLS and zeta potential–What they are and what they are not?. *J Control Release*. **2016**, *235*, 337-51.
71. Alizadeh Noghani, M.; Brooks, D. E. Progesterone Binding Nano-Carriers Based on Hydrophobically Modified Hyperbranched Polyglycerols. *Nanoscale* **2016**, *8* (9), 5189–5199.
72. Yu, T.; Malugin, A.; Ghandehari, H., Impact of silica nanoparticle design on cellular toxicity and hemolytic activity. *ACS Nano.* **2011,** *5* (7), 5717-5728.
73. Sze, A.; Erickson, D.; Ren, L.; Li, D., Zeta-potential measurement using the Smoluchowski equation and the slope of the current–time relationship in electroosmotic flow. *J. Colloid Interface Sci*. **2003**, *261*(2), 402-410.
74. Schroeder, M. E.; Zurick, K. M.; McGrath, D. E.; Bernards, M. T., Multifunctional polyampholyte hydrogels with fouling resistance and protein conjugation capacity. *Biomacromolecules*. **2013**, *14*(9), 3112-3122.
75. Dobbins, S. C.; McGrath, D. E.; Bernards, M. T., Nonfouling hydrogels formed from charged monomer subunits. *J Phys Chem B*. **2012**, *116*(49), 14346-14352.
76. Higuchi, A.; Iijima, T., DSC investigation of the states of water in poly(vinyl-alcohol) membranes. *Polymer*. **1985**, *26*, 1207-1211.
77. Neu, B.; Meiselman, H. J., Depletion-mediated red blood cell aggregation in polymer solutions. *Biophys J*. **2002**, *83*, 2482-2490.
78. Boynard, M.; Lelievre, J. C., Size determination of red blood cell aggregates induced by dextran using ultrasound backscattering phenomenon. *Biorheology*. **1990**, *27*(1), 39-46.
79. Chien, S.; Sung, L. A., Physicochemical basis and clinical implications of red cell aggregation. *Clin Hemorheol Microcirc*. **1987**, *7*(1), 71-91.
80. Nash, G. B.; Wenby, R. B.; Sowemimo-Coker, S. O.; Meiselman, H. J., Influence of cellular properties on red cell aggregation. *Clin Hemorheol Microcirc*. **1987**, *7*, 93-108.
81. Szleifer, I., Protein adsorption on surfaces with grafted polymers: a theoretical approach. *Biophys J*. **1997**, *72*, 595-612.
82. Yang, X.; Li, N.; Constantinesco, I.; Yu, K.; Kizhakkedathu, J. N.; Brooks, D. E., Choline phosphate functionalized cellulose membrane: A potential hemostatic dressing based on a unique bioadhesion mechanism. *Acta biomaterialia*. **2016**, *40*, 212-225.
83. Ladd, J.; Zhang, Z.; Chen, S.; Hower, JC.; Jiang, S., Zwitterionic polymers exhibiting high resistance to nonspecific protein adsorption from human serum and plasma. *Biomacromolecules*. **2008**, *9*(5), 1357-1361.
84. Brash, J. L., Exploiting the current paradigm of blood-material interactions for the rational design of blood-compatible materials. *J Biomater Sci Polym*. **2000**, *11* (11), 1135-1146.

85. Harris, J. M., In *Poly(Ethylene Glycol) Chemistry: Biotechnical and Biomedical Applications*; Harris, J. M., Ed.; Plenum Publishing Corporation: New York, NY, 1992; pp 1-14.
86. Shen, M. C.; Martinson, L.; Wagner, M. S.; Castner, D. G.; Ratner, B. D.; Horbett, T. A., PEO-like plasma polymerized tetraglyme surface interactions with leukocytes and proteins: in vitro and in vivo studies *J Biomater Sci., Polym. Ed.* **2002**, *13*, 367-390.
87. Dausset, J.; Contu, L. I., Drug-induced hemolysis. *Annu Rev Med*. **1967**, *18*, 55-70.
88. Liu, C., The synthesis and optimization of functionalized hyperbranched polyglycerols as potential topical hemostatic agents. MSc Thesis, University of British Columbia, Vancouver, CA, 2018.
89. Murugappa, S.; Kunapuli SP., The role of ADP receptors in platelet function. *Front Biosci*. **2006** ,*11*, 1977-1986.
90. Eika, C., On the mechanism of platelet aggregation induced by heparin, protamine and polybrene. *Scand J Gastroenterol*. **1972**, *9*(1-6), 248-57.
91. Wen, J.; Weinhart, M.; Lai, B.; Kizhakkedathu, J.; Brooks, D. E. Reversible Hemostatic Properties of Sulfabetaine/Quaternary Ammonium Modified Hyperbranched Polyglycerol. *Biomaterials.* **2016**, *86*, 42-55.
92. Liu, PS.; Chen, Q.; Wu, SS.; Shen J.; Lin, SC., Surface modification of cellulose membranes with zwitterionic polymers for resistance to protein adsorption and platelet adhesion. *J Membr Sci Technol*. **2010**, *350*(1-2), 387-394.
93. Adkins, JN.; Varnum, SM.; Auberry, KJ.; Moore, RJ.; Angell, NH.; Smith, RD.; Springer, DL.; Pounds, JG., Toward a human blood serum proteome analysis by multidimensional separation coupled with mass spectrometry. *Mol Cell Proteomics*. **2002**, *1*(12), 947-55.
94. Striker, G. E.; Harlan, J. M.; Schwartz, S. M., Human endothelial cells in vitro. In *Methods in Cell Biology*, Harris, C.C., Trump, B.F., Stoner, G.C., Eds.; Academic Press: New York, London, Toronto, Sydney, San Francisco, 1980; pp 135.